**SANDIA REPORT**

**FCRD-UFD-2013-000225**
**SAN2013-6048**
**Unlimited Release**
**July 2013**

# Preliminary Planning for Development of an Underground Laboratory in Shale

**W. Roggenthen, L. Stetler**
**Department of Geology and Geological Engineering**
**South Dakota School of Mines & Technology**
**501 East St. Joseph Street**
**Rapid City, SD 57703**

**J. Nopola, L. Roberts**
**RESPEC**
**P.O. Box 725**
**Rapid City, SD  57709**

**B. Cetin**
**Department of Civil and Environmental Engineering**
**South Dakota School of Mines & Technology**
**501 East St. Joseph Street**
**Rapid City, SD 57703**

**Prepared by South Dakota School of Mines & Technology and RESPEC under Contract No. 1252847**
**with Sandia National Laboratories, Albuquerque, New Mexico  87185**

**Printed July 2013**

Sandia National Laboratories is a multi-program laboratory managed and operated by Sandia Corporation, a wholly owned subsidiary of Lockheed Martin Corporation, for the U.S. Department of Energy's National Nuclear Security Administration under contract DE-AC04-94AL85000. This work is supported by DOE Nuclear Energy Used Fuel Disposition Program.

Unlimited Release
Printed July 2013

# Preliminary Planning for Development of an Underground Research Laboratory in Shale

William Roggenthen[1], Larry Stetler[1], Jay Nopola[2], Bora Cetin[3], and Lance Roberts[2]

[1]Dept. of Geology and Geological Engineering
South Dakota School of Mines and Technology
501 E. St. Joseph Street
Rapid City, SD 57701

[2]RESPEC
3824 Jet Drive
Rapid City, SD 57703

[3]Dept. of Civil and Environmental Engineering
South Dakota School of Mines and Technology
501 E. St. Joseph Street
Rapid City, SD 57701

## Abstract

Shale is one of the geologic environments that is under consideration for used nuclear fuel disposal. Disposal in shale has many favorable attributes that limit the possibility of communication to the environment, including low permeabilities and the potential for self-sealing, based on its ductility properties. Although current studies of shales and other fine-grained sedimentary materials are still at the generic stage, considering what will be necessary to move toward more definitive studies and concepts is important. In the United States (U.S.), defining shale behavior at depths and pressures likely to be encountered when constructing a working waste repository is a major consideration for an underground research laboratory (URL). Evaluating the justification for a U.S. URL begins with a summary of geological units classified as shale. Existing European URLs provide an invaluable resource for advancing understanding, but knowledge gaps still exist. The rationale for a U.S. URL in shale is based on its ability to fill these gaps.

Comparing experiments in individual shale units and other fine-grained-sedimentary rocks can be complicated by currently used classification systems. Fine-grained geological

units encompass a wide range of materials, but variations in the physical properties and physical environment contribute to the behaviors of individual units. A number of classification systems describe fine-grained geological units. A knowledge of these different systems can help researchers avoid misunderstandings when communicating between disciplines. A detailed, geological description is valuable for understanding differences in lithological structure that may affect behavior and are not obvious from a description of physical properties. This characterization is the basis for accurately describing empirical relationships that define behaviors and for assessing the transferability of concepts between dissimilar units and environments.

Fine-grained geological units encompass a wide range of materials. Many variations in the physical properties and physical environment contribute to the behavior of individual units. The Cretaceous-age Pierre Shale from the Midcontinent region of the U.S. was used as a representative shale formation to compare to the European shale-hosted URLs of Mont Terri, ANDRAS, and Bure (Mol). The greatest material differences for the European URLs are between the nonindurated Boom Clay and the more indurated formations (Callovo-Oxfordian and Opalinus). Properties of the Pierre Shale often fall between the Boom Clay and the more indurated formations. Poorly indurated formations, such as the Boom Clay, have relatively high porosity, high water content, low elastic properties, and low strength properties (cohesion and friction). By contract, the more indurated formations have lower porosity and, therefore, lower water content, higher elastic properties, and higher strength properties.

The numerical modeling of a preliminary design for a shale-hosted URL by using the properties of the Pierre Shale accentuates many of the existing knowledge gaps, which include:

- Understanding the development and sealing of fractures.
- Physical factors affecting radionuclide sorption and solubility.
- Relationships describing coupled THMC processes.
- Transferability of concepts between dissimilar materials.

The justification, design, and implementation of a shale-hosted URL in the U.S. must meet a number of major and minor milestones. The first major milestone is the general justification of a need for a U.S. URL, which depends on current knowledge gaps and the ability to fill those knowledge gaps through available means. If available means are considered insufficient and a U.S. URL in shale is considered justified, the second major milestone consists of general siting identification. This effort will define broad areas with qualifying conditions and omit areas with disqualifying conditions. Once broad areas have been defined, the effort of the third major milestone is the more specific classification and ranking of favorable and potentially unfavorable conditions. The more detailed classification of the third milestone includes physical properties, the physical system, and construction considerations.

# TABLE OF CONTENTS

## TABLE OF CONTENTS
**(Continued)**

# LIST OF TABLES

THIS PAGE INTENTIONALLY LEFT BLANK

# LIST OF FIGURES

# LIST OF FIGURES
## (Continued)

# 1. Introduction

The United States (U.S.) government's decision to withdraw the Yucca Mountain site in Nevada as a nuclear waste storage location accentuated the need for long-term storage of these materials. If all nuclear energy production had ceased in 2011, the U.S. would still have approximately 75,000 metric tons of spent nuclear fuel requiring disposal (Blue Ribbon Commission on America's Nuclear Future, 2011). If the existing nuclear power plants continue producing at their current rates and no new nuclear power plants are constructed, the U.S. will have amassed approximately 150,000 metric tons of spent nuclear fuel by 2050. The quantity of spent nuclear fuel will soon exceed the limit that could be legally placed at Yucca Mountain, even if policy changes allowed for construction and storage to proceed there. Spent nuclear fuel is currently stored in shielded concrete pools or in dry casks above ground at the nuclear power plant where it is generated. Nuclear waste can stay radioactive for thousands of years and these near-surface storage locations are more susceptible to catastrophic events (both environmental and human-induced) than isolated, long-term repositories. The need for long-term disposal of spent nuclear fuel is apparent, and deep, geological repositories in various geologic media are considered the most viable options, and one of these is shale (Blue Ribbon Commission on America's Nuclear Future, 2011).

## 1.1 Project Goals and Approaches

The project goals in this report include investigating of requirements and the path forward for an Underground Research Laboratory (URL) to be developed in a shale or other fine-grained geologic media. Because these geologic units have numerous favorable attributes, they are viewed as an option for such storage. If this medium will be used or investigated further, having a facility that provides access to the deep underground environment, which would allow the shales to be studied in situ, is necessary.

To gain the necessary insights into the potential design of a shale URL, a series of studies were initiated as part of this project and focused on the geomechanical behavior of shale and some preliminary consideration of the effects of thermal loading by nuclear waste packages. This provided information that allowed knowledge gaps concerning a shale URL.

## 1.2 Considering Shale as a Disposal Medium

Shales have unique properties that make them suitable candidates for hosting a nuclear waste storage facility. The benefits of fine-grained geological units for use as a nuclear repository identified by Boisson (2005) include the following:

- **Low permeability and low hydraulic gradients:** High permeability and high hydraulic gradients will both result in faster radionuclide transport. In porous materials with low permeability and low hydraulic gradients, the transport of radionuclides occurs through diffusion instead of advection, which produces a slower process. Fine-grained geological units typically possess small pore spaces with poor connectivity, which results in low permeability. Fine-grained geological units are deposited in low-energy environments in relatively flat-lying units. These flat-lying units generally maintain low hydraulic gradients if significant postdepositional structural events have not occurred.

- **Potential for deformation to close fractures**: The major mechanisms that allow for self-sealing in fine-grained units are increases in stress normal to the fracture, a viscoplastic response to deviatoric stress (creep), and swelling of the fracture wall materials (Bock et al., 2010). These mechanisms mostly depend on the physical properties of individual units (e.g., the amount and type of clay minerals).

- **Favorable geochemical characteristics to retard the migrations of radionuclides**: Fine-grained geological units typically include significant percentages of clay minerals. Clay minerals have a high, specific surface area on which radionuclides often are able to sorb. Many fine-grained geological units were deposited under reducing conditions, which is beneficial, because many radionuclides have lower solubility limits in reducing environments.

- **Geological units of suitable thickness and uniformity**: The previously described benefits of fine-grained geological units require the unit to be adequately thick and uniform to provide the necessary containment, dilution, and limited releases. Fine-grained geological units are abundant in the preserved geological record and represent over 50 percent of all sedimentary rocks (Boggs, 1995). The numerous fine-grained geological units indicate that many are capable of meeting the needed requirements for thickness and uniformity. In contrast, salt, which is also considered for a geological repository, represents a much smaller percentage of the preserved geological record and is often of insufficient thickness for repository use.

Even though these favorable attributes for shales as a disposal medium exist, other considerations need to be accounted for when contemplating a URL design. The following section describes the scope of the report in this regard. One of the more important considerations of fine-grained geologic units lies in the wide variability of material properties that compose different units. Although other evaporite minerals in addition to halite (NaCl) may be important in a stratigraphic section of salt (which is also considered as a potential repository host), massive salt deposits typically trend toward a predominantly monomineralic halite composition. Shale, by contrast, may vary in nonreactive mineral content (e.g., quartz), calcareous composition, clay mineral types, and porosity. The benefits of shale will vary between individual, fine-grained geological units that have differing physical properties and system states. Individual shale units, therefore, may constitute a complex system both mineralogically and mechanically.

Assessing the transferability of concepts developed to describe the behavior of fine-grained geological units first requires classifying the properties of fine-grained geological units. Understanding classification techniques allows for the comprehension of the wide range of materials that encompass fine-grained geological units. Knowledge of the different classification methods also prevents confusion and misunderstandings that may arise when working across different disciplines. An overview of the terminology used to describe fine-grained units and their textural and mineralogical compositions is provided in this report to emphasize the breadth of materials under consideration.

The overall effects of individual parameters and the extent to which they affect repository design require investigation. Most of this investigation can be accomplished through detailed laboratory testing and numerical modeling. However, analyzing complex, coupled processes and large-scale effects (such as the extent and characterization of the weathered zone, thermal stability, and development of a damaged zone) require in situ studies of rock behavior to determine effects that are from either an introduction of heat sources or excavations performed during development. Detailed material characterization and large-scale experiments conducted by the European shale-hosted URLs in Switzerland, France, and Belgium have been very useful. The U.S. effort is making considerable use its cooperation with European laboratories and is anticipated to glean information from these laboratories that will make the progression of experiments from surface laboratories to underground laboratories more efficient. A careful comparison of the European shales and those more typical in the U.S. is needed to determine which, if any, important factors might preclude a straightforward adaptation of the European experiences to issues relevant to U.S. shales. A comparison of the physical characteristics and behaviors of the formations that host European URLs with the Pierre Shale (a widespread and well-documented unit in the Midcontinent of the U.S.) is provided to identify dissimilarities.

Despite ongoing research and large-scale experiments, a number of knowledge gaps still exist. For example, the importance of particular properties (such as differences in clay composition) in predicting the behavior of fine-grained geological units has not been adequately quantified in many cases. A review of the current state-of-the-art methods, existing knowledge gaps, and limits of transferability is provided. A list of the topics that are considered to be highly important but do not have a sufficient current level of understanding indicates the need and direction of work to be performed in URLs.

A preliminary analysis of the Pierre Shale as a potential repository site emphasizes differences in the material properties between this unit and shale in European URLs. This analysis also accentuates the current knowledge gaps and areas that require further examination.

The design needs for developing a URL will encompass a wide variety of disposal issues relevant to shales and other fine-grained geological media. The physical, chemical, and mechanical behaviors of these media in such an environment must become an integral component of the design process. Given the breadth of physical properties included under the umbrella term of "shale," the current knowledge gaps, and the limits of transferability, consideration should be given to methods for studying shale in a U.S. URL. A preliminary design flow that illustrates the steps necessary to establish an underground research laboratory is provided. The scope of this list is limited to producing a conceptual framework that describes the process by which a URL could be designed and constructed in a shale-hosted environment. This work will assist in identifying critical activities and attributes that should be considered in designing such a laboratory, if it is ultimately determined that the shale option should be pursued. The investigators who work at the site will define the experimental requirements that inform the attributes, capabilities, and design of the URL. Many of the anticipated experiments will be directed toward the behavior of shale units under elevated lithostatic pressures that could be encountered from emplacing the URL below the weathering horizon and at depths where ductile properties of the shale dominate. Similarly, the geochemical and thermal properties of the shale are critical factors that determine the long-term functionality of the URL. All of these experiments are driven by the need for in situ information required for verifying and validating limited, laboratory and bench-scale results.

# 2. Basis for Classifying Fine-Grained Media

Nuclear waste disposal in the U.S. is considered in several geological environments: crystalline rock, salt, and shale. In this context "shale" is used as a generic term that represents a relatively wide range of geological materials and depositional conditions. In this report, the term "fine-grained geological units" is used to represent the full spectrum of geological units that fall under the generic "shale" term and are being considered for an URL.

Classifying and describing fine-grained geological units has been historically avoided, even though fine-grained geological units represent approximately 50 percent of the sedimentary rock record (Boggs, 1995). The small grain size of these units makes them difficult to classify and their low permeability makes them of little interest for petroleum and water development. Mineral resources in fine-grained geological units historically consisted of bentonite or kaolinite, which were most often exploited in open-pit mining operations that did not require a thorough understanding of their behavior. Technological advances in the last 50 years (e.g., x-ray diffraction, x-ray fluorescence, scanning electron microscopy, and CT scanning) have allowed for a more detailed characterization of fine-grained units, and the development of techniques to access mineral resources in fine-grained units (e.g., horizontal drilling and massive hydraulic fracturing) has resulted in an increased interest in their characterization.

Sedimentary rocks are classified using two parameters: texture and composition. Texture refers to relations between particles and includes grain size and shape factors. Composition refers to the mineralogy of the grains, such as quartz and mica, or some other chemical constituent. Composition is typically used as a name-modifier for the rock. Classification, in part, relies on intended use (i.e., whether the material is described geologically or defined for agricultural or engineering uses). In practice, texture, composition, and intended uses have all been used in separate classification schemes. These differences have resulted in multiple classification systems for fine-grained sedimentary rocks. Thus, there is some ambiguity in consistently classifying these units. For example, the term "shale" is often used as a generic term to represent any fine-grained geological unit. This may include unconsolidated clay, shale, mudstone, and argillite. However, the geological definition of shale is more specific: a laminated, indurated rock having greater than two-thirds clay-sized minerals (Jackson, 1997). Further complicating a clear depiction is the term "clay," which is used as both a particle-size classification and a mineralogical classification. The particle-size classification is further complicated by the presence of a variety of classification systems (Figure 2-1) where the particle-size breaks, used to differentiate between particle names, are different. Additionally, textural classification is not equivalent to mineralogical classification. Particles that are texturally classified as clay are often composed of clay minerals, but other minerals (e.g., silica or calcite) may also be clay-sized. Conversely, particles texturally classified as silt are often compositionally nonclay minerals but may consist of clay minerals.

| Classification Method | | | Classification System | | | | | | | |
|---|---|---|---|---|---|---|---|---|---|---|
| ϕ | mm | U.S. standard sieve size | Wentworth (1922) | | USDA | | AASHTO | | USCS | |
| -10.00 | 1024 | | Boulder | | Boulder | | Boulder | | Boulder | |
| -9.75 | 861 | | | | | | | | | |
| -9.50 | 724 | | | | | | | | | |
| -9.25 | 609 | | | | | | | | | |
| -9.00 | 512 | | | | | | | | | |
| -8.75 | 431 | | | | | | | | | |
| -8.50 | 362 | | | | | | | | | |
| -8.25 | 304 | | | | | | | | | |
| -8.00 | 256 | 12" | | | | | | | | |
| -7.75 | 215 | | Cobbles | | Cobbles | | Cobbles | | Cobbles | |
| -7.50 | 181 | | | | | | | | | |
| -7.25 | 152 | | | | | | | | | |
| -7.00 | 128 | | | | | | | | | |
| -6.75 | 108 | | | | | | | | | |
| -6.50 | 90.5 | | | | | | | | | |
| -6.25 | 76.1 | 3" | | | | | | | | |
| -6.00 | 64.0 | 2-1/2" | | | Gravel | | Gravel | coarse | Gravel | coarse |
| -5.75 | 53.8 | | Pebbles | very coarse | | | | | | |
| -5.50 | 45.3 | | | | | | | | | |
| -5.25 | 38.1 | | | | | | | | | |
| -5.00 | 32.0 | 1-1/4" | | | | | | | | |
| -4.75 | 26.9 | | | coarse | | | | | | |
| -4.67 | 25.4 | 1" | | | | | | | | |
| -4.50 | 22.6 | | | | | | | medium | | |
| -4.25 | 19.0 | 3/4" | | | | | | | | |
| -4.00 | 16.0 | 5/8" | | | | | | | | fine |
| -3.75 | 13.5 | | | medium | | | | | | |
| -3.50 | 11.3 | | | | | | | | | |
| -3.25 | 9.51 | 3/8" | | | | | | | | |
| -3.00 | 8.00 | 5/16" | | | | | | fine | | |
| -2.75 | 6.73 | | | fine | | | | | | |
| -2.50 | 5.66 | | | | | | | | | |
| -2.25 | 4.76 | 4 | | | | | | | | |
| -2.00 | 4.00 | 5 | | | | | | | Sand | coarse |
| -1.75 | 3.36 | 6 | Granules | | | | | | | |
| -1.50 | 2.83 | 7 | | | | | | | | |
| -1.25 | 2.38 | 8 | | | | | | | | |
| -1.00 | 2.00 | 10 | | | | | | | | |
| -0.75 | 1.68 | 12 | Sand | very coarse | Sand | very coarse | Sand | coarse | | medium |
| -0.50 | 1.41 | 14 | | | | | | | | |
| -0.25 | 1.19 | 16 | | | | | | | | |
| 0.00 | 1.00 | 18 | | | | | | | | |
| 0.25 | 0.841 | 20 | | coarse | | coarse | | | | |
| 0.50 | 0.707 | 25 | | | | | | | | |
| 0.75 | 0.595 | 30 | | | | | | | | |
| 1.00 | 0.500 | 35 | | | | | | | | |
| 1.25 | 0.420 | 40 | | medium | | medium | | | | |
| 1.50 | 0.354 | 45 | | | | | | fine | | fine |
| 1.75 | 0.297 | 50 | | | | | | | | |
| 2.00 | 0.250 | 60 | | | | | | | | |
| 2.25 | 0.210 | 70 | | fine | | fine | | | | |
| 2.50 | 0.177 | 80 | | | | | | | | |
| 2.75 | 0.149 | 100 | | | | | | | | |
| 3.00 | 0.125 | 120 | | | | | | | | |
| 3.25 | 0.105 | 140 | | very fine | | | | | | |
| 3.50 | 0.0884 | 170 | | | | very fine | | | | |
| 3.75 | 0.0743 | 200 | | | | | | | | |
| 4.00 | 0.0625 | 230 | | | | | Silt | | Silt | |
| 4.25 | 0.0526 | 270 | Silt | coarse | | | | | | |
| 4.32 | 0.0500 | | | | | | | | | |
| 4.50 | 0.0442 | 325 | | | Silt | coarse | | | | |
| 4.75 | 0.0372 | 400 | | | | | | | | |
| 5.00 | 0.0313 | | | | | | | | | |
| 5.25 | 0.0263 | | | medium | | | | | | |
| 5.50 | 0.0221 | | | | | | | | | |
| 5.75 | 0.0186 | | | | | fine | | | | |
| 6.00 | 0.0156 | | | | | | | | | |
| 6.25 | 0.0131 | | | fine | | | | | | |
| 6.50 | 0.0110 | | | | | | | | | |
| 6.75 | 0.0093 | | | | | | | | | |
| 7.00 | 0.0078 | | | | | | | | | |
| 7.25 | 0.0066 | | | very fine | | | | | | |
| 7.50 | 0.0055 | | | | | | | | | |
| 7.63 | 0.0050 | | | | | | | | | |
| 7.75 | 0.0046 | | | | | | Clay | | Clay | |
| 8.00 | 0.0039 | | | | | | | | | |
| 8.25 | 0.0033 | | Clay | | | | | | | |
| 8.50 | 0.0028 | | | | | | | | | |
| 8.75 | 0.0023 | | | | | | | | | |
| 9.00 | 0.0020 | | | | | | | | | |
| 9.25 | 0.0016 | | | | Clay | | | | | |
| 9.50 | 0.0014 | | | | | | | | | |
| 9.75 | 0.0012 | | | | | | | | | |
| 10.00 | 0.0010 | | | | | | | | | |

**Figure 2-1.** Comparison of Grain-Size Classification Systems for Sedimentary Rocks. The classification system is based on intended use for these materials as follows: Wentworth (geological), U.S. Department of Agriculture (agricultural), and American Association of State Highway and Transportation Officials and Unified Soil Classification System (engineering).

The existence of multiple classification systems warrants a review so that a thorough understanding of the range of materials considered for hosting a URL are more fully appreciated. The details of conventional, textural, and mineralogical classifications used in the physical classification of fine-grained geological units are presented in the following sections.

## 2.1 Textural-Based Classification

The foundation of a textural classification is the particle sizes that constitute the geological unit being analyzed. A number of disciplines (e.g., geologists, soil scientists, and geotechnical engineers) have developed particle-size classification systems based on intended use, and these systems are not always consistent (Figure 2-1). The second portion of a textural classification is assigning a rock name based on a series of adjectives that physically describe the unit; these include color, mineralogy, induration, and structure and arrangement of the grains.

### 2.1.1 *Particle-Size Classification*

Particle-size classification is based on describing the diameter of the individual particles that compose a geological unit and the proportion of each size class relative to the whole. Three common methods of classifying particle sizes are: (1) the phi ($\phi$) scale, (2) in millimeters (mm), and (3) by using standard U.S. sieve sizes. The phi scale was developed by Krumbein (1934) to describe small particles as successively larger positive numbers based on the following relationship

$$\phi = -\log_2 d \tag{2-1}$$

where $\phi$ is the phi scale and $d$ is the particle diameter in millimeters. A comparison of these particle-size classification methods is shown in Figure 2-1 where the particle definition varies according to the organization that developed the classification.

Nonindurated samples (e.g., soil) are classified using sieves for the coarse-grained fraction (sand-sized and larger) and a hydrometer for the fine-grained fraction (silt and clay). Particle-size distribution is described in terms of the percent passing or percent retained on selected sieves or size in millimeters. The results, either the percent passing or retained, are plotted semilogarithmically from which information on sorting (geological) or grading (engineering) can be obtained.

Well-indurated samples are not classified using sieves and hydrometers, because the individual particles cannot be easily separated. Classifying these rocks is based on a visual inspection that results in estimated proportions of each particle size and mineralogical composition. Difficulty arises using this approach when particle sizes are not readily discernible with a hand lens or microscope. Classifying indurated, fine-grained units is, therefore, more subjective and often based on estimating broad proportions between silt and clay.

A number of different particle-size classification systems have been developed for specific scientific disciplines. Knowledge of these different systems is important to prevent confusion when analyzing literature from different disciplines. The particle-size classification system typically used for geological descriptions is the Wentworth (1922) scale (Figure 2-1). Wentworth defines silt between 63 to 4 micrometers ($\mu m$) and clay as less than 4 $\mu m$. By comparison, the U.S. Department of Agriculture (USDA) system defines silt between 50 and 2 $\mu m$ and clay as less than 2 $\mu m$. Geotechnical engineers use either the American Association of State Highway and Transportation Officials (AASHTO) or the Unified Soil Classification System (USCS). Both AASHTO and the USCS define silt between 74 and 5 $\mu m$ and clay as less than 5 $\mu m$. In most instances, these classification systems retain the descriptive labels of Wentworth (e.g., sand and clay), but the particle diameters used to define terms are slightly different. Not possessing knowledge of these differences could yield inconsistent results for a project that relies on geological field data for engineering design.

### 2.1.2 *Descriptive Classification*

A descriptive classification is more subjective than a textural classification in that the sample is not typically disaggregated, and the particle size and mineralogy are based on visual inspection. Most of the existing classification systems for soils and sedimentary rocks (Folk, 1974; Shepard, 1954; Schlee, 1973) are based on ternary diagrams and the relative percentage of sand, silt, and clay (Figure 2-2 and Figure 2-3). The most widely used system for geological classification is Folk's (1974), which is based on the Wentworth classification. This classification system is used for both nonindurated (e.g., silt) or indurated (e.g., siltstone) units. The clastic portion of Folk's system is represented by the ternary diagrams in Figure 2-2. The left diagram is for coarser gravel materials and the right diagram is for finer sandy materials. In this system, the terms "gravel," "sand," "silt," and "clay" are used as both primary names and modifiers, such as :sand" or a "sandy" mud.

In Folk's classification system, fine-grained geological units are described as having silt and clay representing more than 50 percent of the unit (e.g., a sandy mudstone). This description of fine-grained geological units would include most of the Pleistocene glacial diamicton (till) in the Northern Plains. These tills resulting from the Keewatin ice sheet were derived largely from underlying Cretaceous shales, but also included significant portions of sand, gravel, and larger materials derived from crystalline rocks. Thus, the strict definition of "fine-grained" was satisfied, but these tills, although fine-grained, have not been consistently viewed as a member of the shale/clay bedrock inventory. A slightly stricter classification limit will be used in this report, where sand and coarser sediments are limited to no greater than 10 percent for classification as a fine-grained geological unit. This limit is based on Folk's classifications, which do not require a modifier (e.g., sandy). In addition, applying this limit will ensure the materials were deposited in a geologically quiet environment, such as the sea bottom.

The terms siltstone and claystone are rather broad and additional adjectives are useful for description. Most geological classification systems incorporate an estimation of the mineralogy as part of the description (e.g., quartzose sandstone); however, the visual identification of minerals in fine-grained geological materials is not often possible. Potter et al. (1980) expanded on Folk's classification of fine-grained geological units (Table 2-1) where the percentage of clay-sized constituents is determined by dividing clay-sized constituents by the sum of both silt and clay constituents (percentage of clay divided by the sum of the percentage of clay and the percentage of silt). For example, a bedded, indurated unit containing 20 percent sand, 60 percent silt, and 20 percent clay would classify as a bedded sandy siltstone, because the portion of the fine-grained fraction that is composed of clay is less than 33 percent. Silt-sized particles are distinguished by a gritty feel and are usually discernible with a hand lens. Clay-sized particles are not gritty and cannot be seen with a hand lens. A mixture of silt and clay may appear as clay but is gritty when cut with a knife or rubbed between teeth.

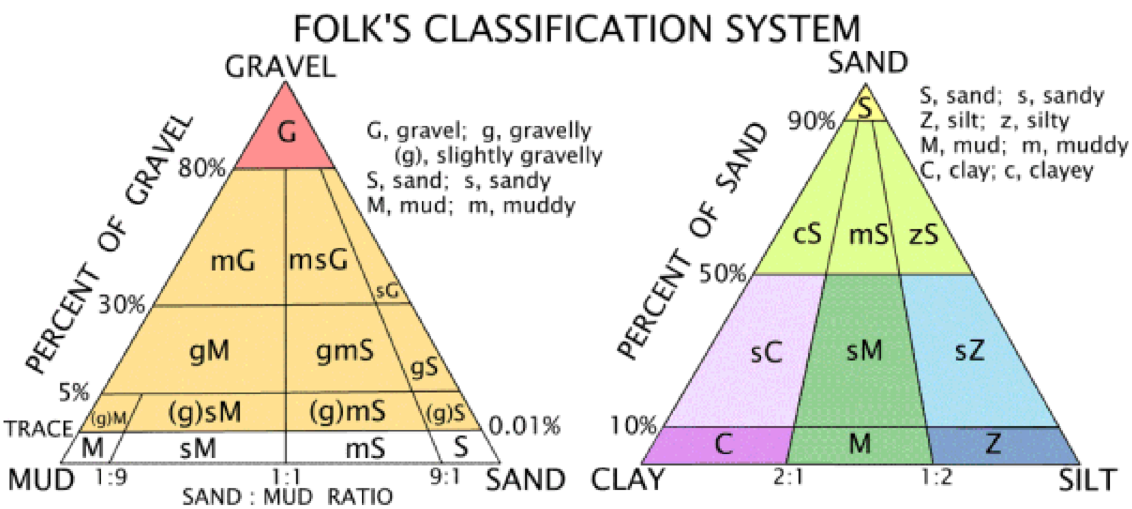


**Figure 2-2.** Folk's Sedimentary Classification System (From Poppe et al., 2003). The ternary diagrams are based on the proportions of gravel, sand, and mud, where mud is defined as all particles less than 63 μm which includes both silt and clay as defined by the Wentworth scale.

Numerous terms describe fine-grained units and many are specific to certain scientific disciplines. A complete list of all definitions pertaining to fine-grained units is not provided herein. An overview of often used terminology is provided to eliminate some ambiguity. Table 2-2 (Jackson, 1997) presents a simplified terminology that is generally applicable to fine-grained sedimentary materials. This terminology accounts for composition, texture, and diagenetic modifications. The terms sand, silt, and clay are widely used across disciplines to describe grain sizes. As noted in Figure 2-1, the actual particle size used to differentiate between these descriptive terms often varies between disciplines. Different disciplines often use their own terminology in describing fine-grained units. The ternary classification used by the USDA is shown in Figure 2-3. This diagram is intended for use with nonindurated soils and is based on a sieve analysis of a soil sample. In addition to sand, silt, and clay, the USDA system uses the term "loam" to describe a mixture of different-sized particles. These various systems will produce various names for the same material. For example, a material that has 55 percent sand, 30 percent silt, and 15 percent clay will be classified as a muddy sand in Folk's system and a sandy clay loam in the USDA system.

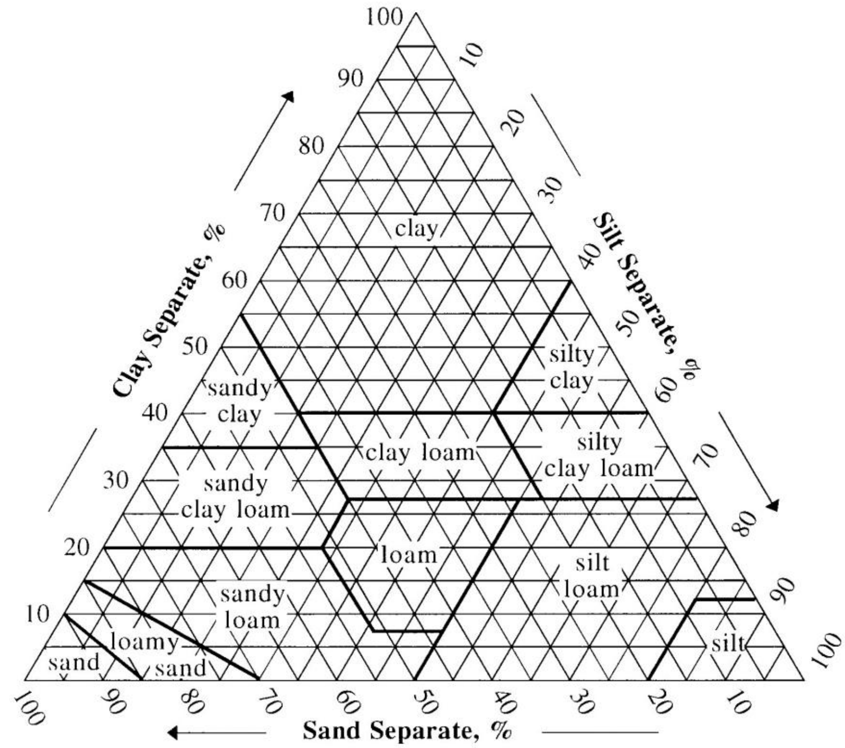


**Figure 2-3.** U.S. Department of Agriculture Soil Classification System (U.S. Department of Agriculture, Natural Resources Conservation Service, 2012).

**Table 2-1. Classification of Fine-Grained Geological Units (Modified From Potter et al., 1980)**

| Clay-Sized Constituents (%) | | 0–32 | 33–65 | 66–100 |
|---|---|---|---|---|
| Nonindurated | Beds (greater than 10 mm) | Bedded silt | Bedded mud | Bedded clay |
| | Laminae (less than 10 mm) | Laminated silt | Laminated mud | Laminated clay |
| Indurated | Beds (greater than 10 mm) | Bedded siltstone | Bedded mudstone | Bedded claystone |
| | Laminae (less than 10 mm) | Laminated siltstone | Mudshale | Clayshale |
| Metamorphosed | Low | Quartz argillite | Argillite | |
| | Medium | Quartz slate | Slate | |
| | High | Phyllite and/or schist | | |

**Table 2-2. Definitions of Fine-Grained Geologic Materials Derived From the Dictionary of Geological Terms (Jackson, 1997)**

| Material | Definition |
|---|---|
| Clay | plastic material mainly having particles < 0.074 mm |
| Claystone | indurated rock having > 67% clay-sized minerals |
| Shale | a laminated, indurated rock having > 67% clay-sized minerals |
| Mud | a slimy, sticky, or slippery mixture of water and silt- or clay-sized earth materials |
| Mudstone | an indurated mud having the texture and composition of shale but lacking fine laminations or fissility; a term only used when amounts of silt and clay are unknown or cannot be precisely identified |
| Argillite | a compact rock derived from mudstone or shale that has higher induration but is less clearly laminated and without fissility of shale (argillic—alteration of rock minerals into clay minerals, i.e., a weakly metamorphosed rock) |
| Marl | a term loosely applied to a variety of materials that occur as loose earth deposits of an intimate mixture of clay and calcium carbonate (35–65% clay – 65–35% carbonate) |

Geotechnical engineers classify fine-grained units based on engineering behavior (e.g., plasticity). A partial description of the USCS is shown in Figure 2-4. The Atterberg Limits test is used to determine the liquid limit and plastic limit of soils, which is used to classify silts and clays as "lean" or "fat." Fat clays are prone to volume change when subjected to changes in moisture content, whereas lean clays are generally not. An increase in the liquid limit and the plasticity index (i.e., the difference between the liquid limit and the plastic limit) generally corresponds to an increase in swelling clay minerals, which is discussed further in Section 2.2. It is worth noting that these geotechnical descriptive classifications do not address grain size. As an example, a late Pleistocene (Peoria) loess may contain 80 percent silt-sized particles and 20 percent clay-sized particles but have a USCS classification of lean clay because of the Atterberg Limits results.

An understanding of these different classifications systems is important. The broad classification systems mentioned above are useful for differentiating between significant changes in fine-grained units. However, a detailed, geological description of the unit is beneficial in identifying potential variations between two similar units. A comparison of two schematic geological units in Figure 2-5 can be used to illustrate this concept. Both units are indurated and composed of primarily clay with approximately 20 percent silt. Both units are laminated and would classify as clayshale in the classification system displayed in Table 2-1. A more detailed analysis of the structure of the two units shows that the silt-sized particles in Unit A are concentrated in laminae, and the silt in Unit B is disseminated throughout the unit. Even though these two samples have the same classification, their behaviors are not expected to be identical. For example, Unit A may exhibit greater anisotropy than Unit B. Unit A may also demonstrate greater hydraulic conductivity and reduced sorption along the silt laminae.

**Unified Soil Classification (USC) System (from ASTM D 2487)**

| Major Divisions | | Group Symbol | Typical Names |
|---|---|---|---|
| **Fine-Grained Soils** More than 50% passes the No. 200 sieve | **Silts and Clays** Liquid Limit 50% or less | ML | Inorganic silts, very fine sands, rock four, silty or clayey fine sands |
| | | CL | Inorganic clays of low to medium plasticity, gravelly/sandy/silty/lean clays |
| | | OL | Organic silts and organic silty clays of low plasticity |
| | **Silts and Clays** Liquid Limit greater than 50% | MH | Inorganic silts, micaceous or diatomaceous fine sands or silts, elastic silts |
| | | CH | Inorganic clays or high plasticity, fat clays |
| | | OH | Organic clays of medium to high plasticity |
| **Highly Organic Soils** | | PT | Peat, muck, and other highly organic soils |

Prefix: G = Gravel, S = Sand, M = Silt, C = Clay, O = Organic
Suffix: W = Well Graded, P = Poorly Graded, M = Silty, L = Clay, LL < 50%, H = Clay, LL > 50%

**Figure 2-4.** Portion of the Unified Soil Classification System for Fine-Grained Soils (ASTM D 2487-98, 1998).

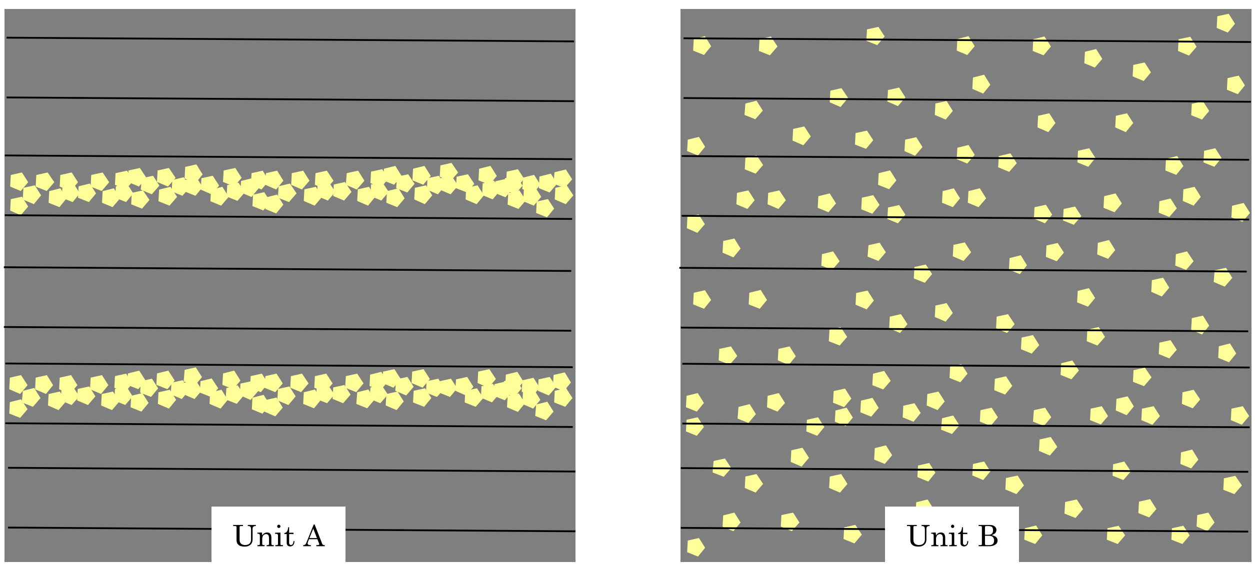


**Figure 2-5.** Comparison of Two Geological Units With Identical Grain-Size Distribution and Mineralogy but Different Structure.

## 2.2 Mineralogy

The mineralogy of fine-grained geological units is important, because it can be used to infer certain behaviors and assess transferability between units. Mineralogy does not explicitly provide information about grain sizes. Fine particles that are texturally classified as clay are most often composed of clay-sized particles, but not exclusively. Nonclay minerals, such as quartz, may be fine enough to be texturally classified as clay. Conversely, some clay aggregates may be large enough to classify texturally as silt (e.g., kaolinite). A brief description of typical minerals present in fine-grained units, and their importance, is provided in this section.

### 2.2.1 *Clay Minerals*

Most fine-grained geological units are characterized by the presence of clay. Clay minerals are phyllosillicates, or sheet-silicates, defined by tetrahedral and octahedral sheets. Tetrahedral sheets and octahedral sheets are stacked to form either 1:1 layers (one tetrahedral to one octahedral) or 2:1 layers (two tetrahedral to one octahedral). Individual clay minerals are defined by their tetrahedral:octahedral structure and the interlayer bond that holds the sheets together. Different clay minerals exhibit different behaviors. A summary of selected properties of common clay minerals is provided in Table 2-3. Kaolinite is a clay mineral with 1:1 layers and a strong interlayer bond (hydrogen bond of oxygen to hydroxyl). The strong interlayer bond prevents kaolinite from swelling, and, as a consequence, kaolinite has a low cation exchange capacity (CEC) and low specific area compared to other clays. By contrast, smectite is composed of 2:1 layers and has a weak interlayer bond. Water and ions can be absorbed into the interlayer space between clay sheets which allows smectite to expand. In addition to the uniform clay minerals, mixed layer clays composed of different 2:1 layer clay minerals are also common (e.g., smectite-illite or smectite-chlorite).

Clay minerals are grouped into clay aggregates that consist of multiple sheets of clay minerals. A conceptual example of the composition of a fine-grained geological unit is shown in Figure 2-7. In clay minerals, such as kaolinite or illite, the strong interlayer bonds cause the clay aggregates to be aligned in parallel and form a book. Books of parallel clay sheets are less common in smectite, because the interlayer bonds are weak.

The fractions of clay minerals present are important to know because they can be used to infer a number of behaviors. Processes that can be attributed to clay minerals, at least in part (Mazurek et al., 2008), include:

- Clay minerals with a high CEC and specific surface area (e.g., smectites) will sorb more solutes than clays with a lower CEC and specific surface.
- Swelling clays (e.g., smectites) are prone to volume change as the saturation changes. This can be beneficial in closing fractures, but they can also shrink when desaturated and create desiccation cracks.
- Anisotropic properties are related to the preferential alignment of clay aggregates.
- Elastic, plastic, and viscoplastic geomechanical properties are connected to the amount of clay minerals.
- Effective porosity depends on the amount of water that is chemically bound to clay minerals.

**Table 2-3. Characteristics of Select Clay Minerals (Modified From Mitchell, 1976)**

| Mineral | Tetrahedral: Octahedral Structure | Schematic | Interlayer Bond | Basal Spacing (Å) | Cation Exchange Capacity (meq/100 g) | Specific Surface Area ($m^2/g$) |
|---|---|---|---|---|---|---|
| Kaolinite | 1:1 | 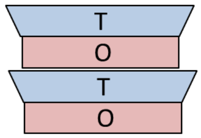 | Hydrogen (strong) | 7.2 | 3 to 15 | 10 to 20 |
| Illite | 2:1 | 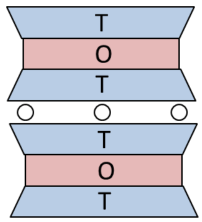 | $K^+$ ions (strong) | 10 | 10 to 40 | 65 to 100 |
| Chlorite | 2:1 | 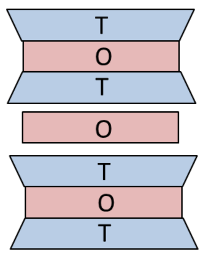 | Hydrogen (strong) | 14 | 10 to 40 | 70 to 150 |
| Smectite | 2:1 | 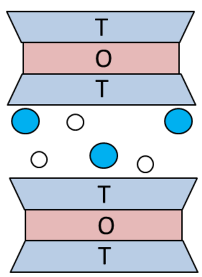 | Various ions and water molecules (weak) | 9.6 to complete separation | 80 to 150 | 50 to 120 (primary)<br>700 to 840 (including interlayer surfaces) |

T– tetrahedral layer

O – octahedral layer

### 2.2.2 *Other Minerals*

Fine-grained geological units are rarely composed entirely of clay minerals. Nonclay minerals may exist as detritus that was deposited at the same time as the clay minerals (e.g., quartz or feldspar) or may have formed diagenetically, which is discussed in Section 2.2. The proportion and mineralogy of nonclay minerals is important in assessing their effects on geochemistry and geomechanical properties. Many fine-grained units are deposited under reducing conditions, and as a consequence, organics are preserved. The presence of organic matter can act as a complexing agent that may enhance radionuclide transport. Several radionuclides have an affinity for carbon, and, as long as the carbon is stable, radionuclide transport is diminished or prohibited. Carbonates in a fine-grained geological unit can originate as primary minerals during deposition or secondarily from diagenesis or the subsequent geochemical alteration of primary minerals. In reducing conditions, these minerals and radionuclides attached to them are stable, but exhibit mobility in oxidizing conditions. The existence of other minerals may act as catalysts for increasing mobility. For example, pyrite ($FeS_2$) often forms under reducing conditions and is stable while iron oxides form under oxidizing environments. These other minerals also affect strength properties of rock. Carbonate minerals forming diagenetic cements can increase the strength of rock and potentially result in brittle behavior. However, the presence of carbonates does not necessarily ensure that the carbonates are diagenetic or that they have increased the rock strength; carbonates may be detrital or may be confined to seams or layers. Thus, the structural and geochemical conditions of each particular unit will dictate both the chemical and mechanical responses of the material under stress.

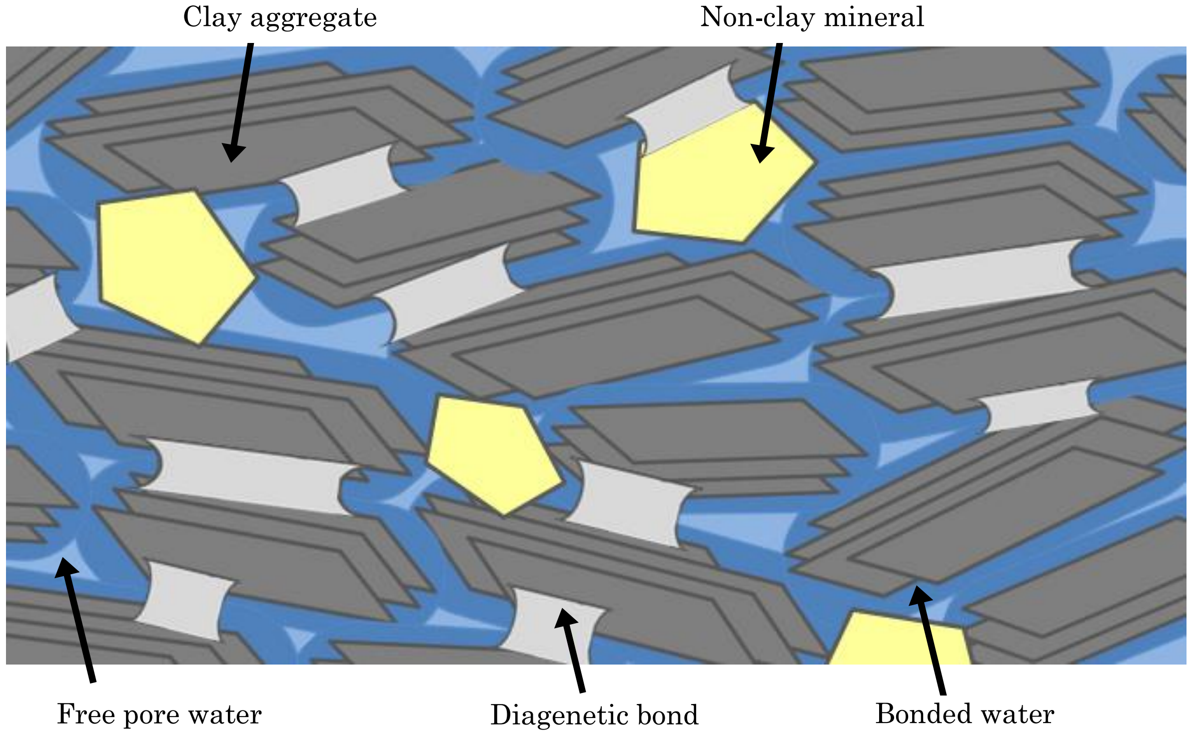


**Figure 2-6.** Schematic Representation of the Structure of Fine-Grained Geological Units on the Micrometer Scale (Nopola, 2013).

## 2.3 Induration/Diagenesis

The diagenetic history of a unit has a significant effect on its physical properties. A relatively uniform geological unit can have considerably different physical properties, if different portions of the unit have been subjected to different diagenetic conditions. Diagenetic processes may begin almost immediately after deposition by bioturbation, which can alter sedimentary structures. The resulting porosity and permeability are closely related to compaction and cementation. These values are important, because they will control radionuclide transport through advection and dispersion. Increasing the burial depth leads to compaction, which reduces porosity and permeability and increases density. A reduction in porosity may also occur from diagenetic cementation (e.g., filling voids with calcareous or siliceous material). The degree of compaction, or induration, will have an effect on geomechanical behavior. Increased induration will create brittle behavior compared to the ductile behavior in nonindurated units. This geomechanical response is important when considering the self-sealing potential of the unit.

## 2.4 Classifying the Physical System

The preceding sections focus on describing geological units and some of the effects that physical properties may have on behavior. However, physical environment will also have an effect on important processes. Even if the physical properties at the time of deposition are identical at two different locations, differences in the system can affect the behavior of the unit. A number of components of the physical system require important consideration, and include the following:

- **Hydraulic gradient:** The hydraulic gradient depend on the hydrogeological system surrounding a potential site. Lithologically, similar formations with different hydraulic gradients will have different predicted transport times. A greater hydraulic gradient will increase the rate of transport, and, therefore, low hydraulic gradients are considered beneficial.

- **Geological structure and fracture density:** Structural geological features, such as anticlines and faulted areas, are associated with a higher density of fractures than regions without structural features. Fractures can also be associated with more-indurated formations that exhibit a more brittle response than less-indurated formations. Fractures are order –of magnitude more conductive than the micro-structure of fine-grained geological units (Freeze and Cherry, 1979). The presence of fractures limits the transferability of processes that are based on correlations of intact rock.

- **State of stress:** The direction and magnitude of the principal stress field will affect the host rock's response to excavations. The orientation and extent of the Excavation Damaged Zone (EDZ) will be different in an isotropic stress field than in an area with significant differences in horizontal stress. Dissimilar in situ horizontal stresses may contribute to the anisotropic behavior of geomechanical and transport properties.

- **Porewater geochemistry:** The porewater geochemistry of the host rock can effect processes. Porewater geochemistry can influence radionuclide solubility and sorption. Porewater geochemistry may also impact the rate of degradation of engineered barrier systems.

## 2.5 Summary

Fine-grained geological units encompass a wide range of materials. Many variations in the physical properties and physical environment contribute to the behavior of individual units. A number of classification systems exist to describe fine-grained geological units. Knowledge of these different systems can help researchers avoid misunderstandings when communicating between disciplines. Mineralogical analyses are necessary to define the distribution of minerals that have an effect on behavior. The definitions of the physical properties provide a basis for assessing the transferability of concepts. A detailed, geological description is valuable in understanding differences in lithological structure that may affect behavior and are not obvious from a description of physical properties. This characterization is the basis for accurately describing empirical relationships that define behaviors and for assessing the transferability of concepts between dissimilar units and environments.

**THIS PAGE INTENTIONALLY LEFT BLANK**

# 3. Purpose of Underground Research Laboratories

The overriding purpose of URLs that dispose of nuclear waste is the ability to demonstrate sufficient understanding of all applicable technical considerations to satisfy the scientific community, stakeholders, and general public. Some of the specific technical considerations that are addressed in URLs include:

- Determining the dependability of site characterization by various surface-based and underground methods.
- Measuring the response of the system to the presence of the excavation.
- Developing and refining numerical models that describe observed behaviors.
- Developing and refining excavation methods and ground-support techniques.
- Simulating long-term experiments that represent repository conditions.

Three URLs have been constructed in fine-grained units in Europe. These URLs are the Centre de Meuse—Haute Marne near Bure, France; the Mont Terri Project in Switzerland; and the high-activity disposal experimental site (HADES) near Mol, Belgium. These facilities have, in some cases, been operational for decades and the large-scale tests performed in these URLs have greatly contributed to the current understanding of the behaviors of fine-grained geological units. The advances in knowledge that accompany these experiments instill confidence in the suitability of the design. Generic URLs are used to further the general understanding of processes in complex geological environments. The Mont Terri research facility and the HADES are generic URLs that are not proposed to be nuclear repository sites. The storage of nuclear waste is, however, proposed within the geological formations that host these URLs. Site-specific URLs may eventually be used for nuclear waste storage; the Bure facility in France may be transitioned into nuclear waste storage.

This section briefly describes attributes of the fine-grained units and the physical system that the three existing shale URLs are constructed in. Physical properties of the Pierre Shale are also provided to demonstrate physical differences.

## 3.1 HADES, Mol, Belgium

The HADES is a URL located near Mol, Belgium. The first shaft of the HADES was sunk in the early 1980s, and experiments have been performed in the URL since that time (Li et al., 2010). The HADES is located in the Boom Clay, a nonindurated clay of Tertiary age. The formation is approximately 100 m thick and is rather flat-lying (dip of 1 to 2 degrees) (Delecaut, 2004). Physical properties of the Boom Clay are presented in Figure 3-1 and Table 3-1. The Boom Clay is bedded mud that displays rhythmic layering of clay and silt, with the clay content ranging from 30 to 70 percent (Delecaut, 2004). The clay minerals of smectite, mixed layer smectite-illite, and illite are the most prevalent. Being poorly indurated, the Boom Clay has relatively high porosity, high water content, low elastic

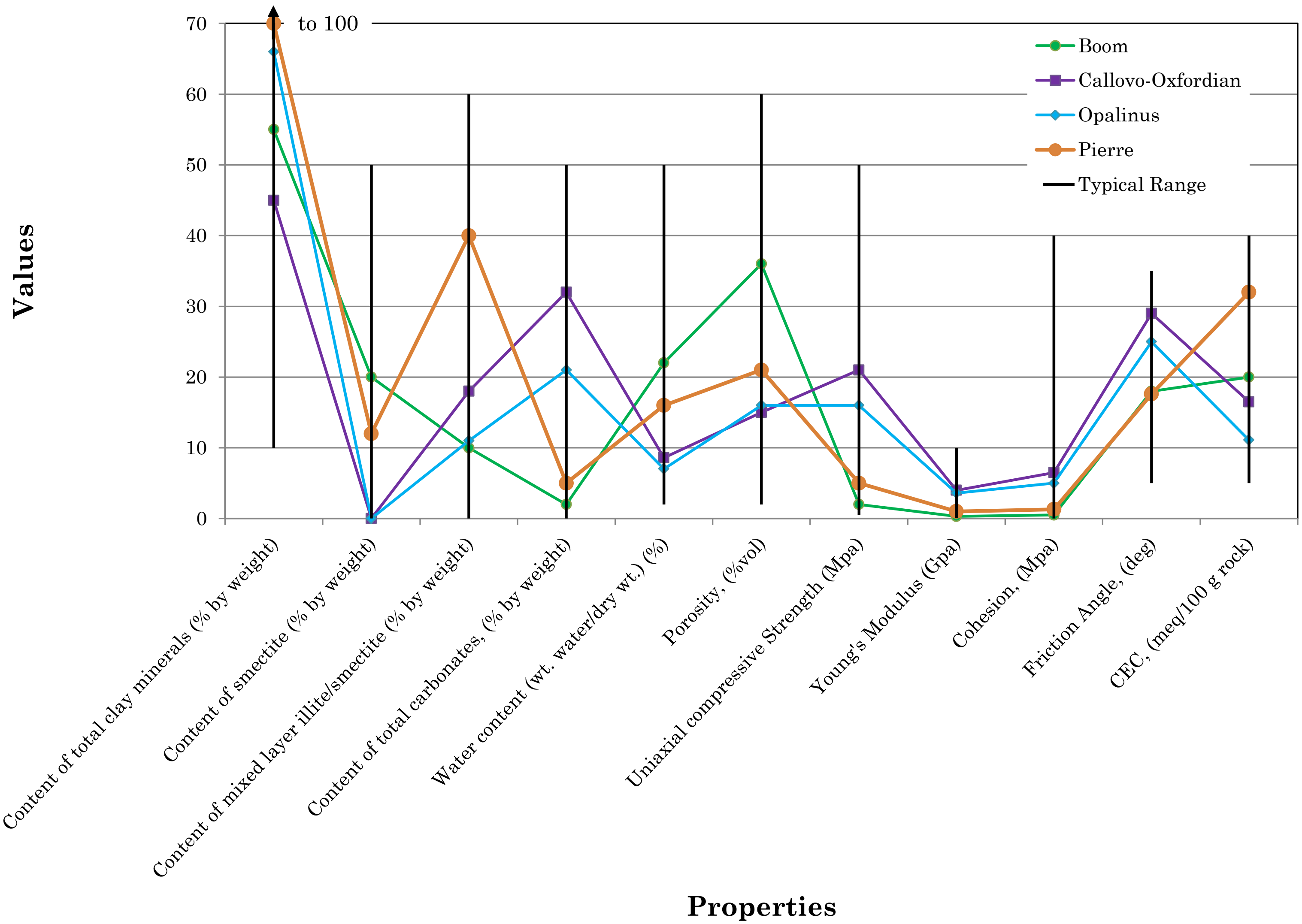


**Figure 3-1.** Values of Selected Properties for Geological Units at Existing Underground Research Laboratories and the Pierre Shale, and a Range of Typical Values of Fine-Grained Geological Units (Boisson, 2005; Kopp, 1986).

parameters, and low strength properties. These trends can been viewed graphically in Figure 3-1, which displays the properties of the Boom Clay within a typical range of fine-grained geological units (Boisson, 2005; Kopp, 1986).

**Table 3-1. Typical Properties of Selected Fine-Grained Geological Units, Results Expressed in Range (Best Estimate) (Boisson, 2005; Kopp, 1986; Delage et al., 2010; Hansen et al., 2010; Schultz et al., 1980)**

| Geological unit | Rock classification | Mineralogy | | | | Organic content (%) | Total porosity (%) | Unconfined Compressive Strength (MPa) |
|---|---|---|---|---|---|---|---|---|
| | | Content of all clay minerals (%) | Content of smectite (%) | Content of mixed layer smectite/ illite (%) | Content of carbonates (%) | | | |
| Boom | Bedded mud | 30–70 (40) | 10–30 (20) | 5–50 (10) | 0–5 (3) | 1–3 | >30 | 2 |
| Callovo-Oxfordian | Bedded mudstone | 25–60 (45) | 0 (0) | 15–33 (18) | 15–75 (35) | <3 | <13 | 20–30 (21) |
| Opalinus | Laminated clayshale | 25–90 (65) | 0 (0) | 5–20 (11) | 10–60 (20) | 0.5 | 13.5–17.9 | 4–22 (16) |
| Pierre | Bedded clayshale | 35–80 (75) | 0–60 (11) | 5–60 (40) | 0–90 (5) | 0.5–13 | 10–40 | 0.5–17 (5) |

The HADES is approximately 225 m deep, and the vertical total stress is approximately 4.5 MPa (Li et al., 2010). The Boom Clay is considered to be largely isotropic with both horizontal stresses estimated to be approximately 0.8 to 0.9 times the vertical stress (Horseman et al., 1987; 1993). The porewater salinity is 1,302 milligrams per liter (mg/L) and is composed primarily of $HCO_3$ and Na (Delecaut, 2004; Boisson, 2005).

## 3.2 Bure Underground Research Laboratory, France

The Bure URL was constructed in 2000 at the boundary between the Meuse and Haute-Marne departments in eastern France, near the town of Bure. The geological formation that hosts the Bure URL is the Callovo-Oxfordian Argillite, which classifies as a bedded mudstone. The Callovo-Oxfordian is a Jurassic age unit that is approximately 130 m thick and flat-lying (dip of 1 to 2 degrees) (Agence nationale pour la gestion des dechets radio, 2005a). The Callovo-Oxfordian is an indurated unit that has experienced diagenetic carbonate cementation (Mazurek et al., 2008), as illustrated by the carbonate content displayed in Figure 3-1 and Table 3-1. The cementation results in an increase in elastic and strength properties and a reduction in porosity. Clay minerals compose approximately 45 percent of the Callovo-Oxfordian and are composed mostly of mixed layer illite-smectite and illite.

The Bure URL is at a depth of approximately 490 m. The vertical stress is 12.7 MPa and the horizontal stresses are 12.4 MPa and 14.8 MPa (Fracture Systems Ltd., 2011). The porewater salinity is 6,530 mg/L and consists of mostly Na, Cl, and $SO_4$ (Mazurek et al., 2008).

## 3.3 Mont Terri Underground Research Laboratory, Switzerland

The Mont Terri URL is located in a dedicated branch off of a vehicle tunnel through the Jura Mountains in Northwestern Switzerland. The URL is located in an anticlinal portion of a thrust fault. The formation dip, therefore, varies throughout the URL. The tectonic history of the site has caused faults and fractures throughout the region, including the Opalinus Clay, which is the focus of the URL. The Opalinus is a 160-m-thick, heterogeneous, laminated mudstone of Jurassic age. Numerous quartz silt lenses, siderite concretions, and bioclasts are present within the clay matrix (Wenk et al., 2008). Clay minerals constitute approximately 66 percent of the Opalinus and are mostly illite, kaolinite, and mixed layer illite and smectite (Mazurek et al., 2008). The Opalinus is not cemented aside from the silt lenses and siderite concretions. However, the porosity is relatively low, because the Opalinus is overconsolidated. Compaction (instead of cementation) is the primary cause of induration in the Opalinus. Induration results in an increase in elastic and strength properties and a reduction in porosity.

The Mont Terri URL is approximately 250 m deep, but the maximum burial depth of the Opalinus is approximately 1,350 m. The maximum in situ stress is approximately vertical with stress roughly equivalent to the overburden, approximately 6 to 7 MPa (Heitzmann and Tripet, 2003). The intermediate compressive stress is approximately 4 to 5 MPa and is oriented horizontal and parallel to the tunnel. The least compressive stress is also horizontal, perpendicular to the tunnel, and approximately 2 to 3 MPa. The salinity in the porewater is 18,296 mg/L and consists of primarily of Na, Cl, and $SO_4$ (Mazurek et al., 2008; Boisson, 2005).

## 3.4 Pierre Shale, United States

The Pierre Shale is one of the most widespread lithological units in the Northern Plains of the U.S. (Gries and Martin, 1985). The Pierre Shale conforms to many of the desirable features for a potential repository site. In many locations within the Northern Plains, the top of the Pierre Shale is less than 500 m below the surface and has a total thickness between 200 m and 800 m (Shurr, 1977).

The following stratigraphic overview is an introduction to the variations present in the Pierre Shale; a detailed description of all the stratigraphic and the lateral variations is not provided. The dominant lithology of the Pierre Shale is dark gray, marine shale, but a number of variations exist both in the vertical stratigraphy of the Pierre Shale and in lateral lithological variation across its aerial extent (Schultz et al., 1980). Examples of some of the variations include the Ardmore Bentonite Bed where numerous bentonite layers are present; the Red Bird Silty Member, silty shale present in the Black Hills area of South Dakota; and the Crow Creek Member, a siltstone present in central South Dakota. The cross-section of the Pierre Shale extending from eastern Wyoming to eastern South Dakota shown in Figure 1-5 (Schultz et al., 1980) displays some of the stratigraphic and lateral variations. The Pierre Shale has recently been elevated to Group status (Martin and Parris, 2007), and many of the individual members have been raised to formational rank. However, many publications do not differentiate between any of the lithological variations. This study is focused on a preliminary analysis of the suitability of the Pierre Shale. In this task, typical properties representative of the dominant marine shale lithology of the Pierre Shale are used for analysis.

Figure 3-1 and Table 3-1 provide a comparison between the rock properties at European URLs and the Pierre Shale in the U.S. In general, the table indicates that the average clay mineral, organic, and smectite content of the Pierre Shale is greater than the European URLs. The organic content of the Pierre Shale has the greatest variability of the listed properties and is caused by the spatial variability in paleoenvironmental conditions during deposition.

Figure 3-2 is a representative stratigraphic profile of the Pierre Shale from Wyoming into South Dakota. Not only is the shale section variable vertically, it also shows significant lateral facies and petrologic changes laterally.

## 3.5 Summary

The summary of properties in Figure 3-1 shows that the existing URLs represent only a fraction of the typical range of properties of shale units. Furthermore, the properties of the Callovo-Oxfordian and Opalinus Formations are very similar to each other. Existing URLs do not provide information about high clay contents (specifically high smectite content), low clay contents, moderately indurated formations, and very well indurated formations.

The greatest difference between the summarized properties in Figure 3-1 and Table 3-1 is between the nonindurated Boom Clay and the more indurated formations (Callovo-Oxfordian and Opalinus). Properties of the Pierre Shale often fall between the Boom Clay and the more indurated formations. Some general correlations can be made from the displayed trends of properties. Poorly indurated formations, such as the Boom Clay, have relatively high porosity, high water content, low elastic properties, and low strength properties (cohesion and friction). The more indurated formations, by contrast, have lower porosity and, therefore, lower water content, higher elastic properties and higher strength properties. However, the diagenetic history that led to these properties is different between the Callovo-Oxfordian and the Opalinus Formations. Low porosity in the Callovo-Oxfordian Formation is attributed to carbonate cementation throughout the unit, which makes up approximately 30 percent of the formation by weight. The Opalinus Formation also has a significant portion of carbonates (approximately 20 percent). However, carbonates in the Opalinus Formation are primarily concretions. The low porosity in the Opalinus Formation is related to a higher level of compaction than was experienced by the Callovo-Oxfordian Formation.

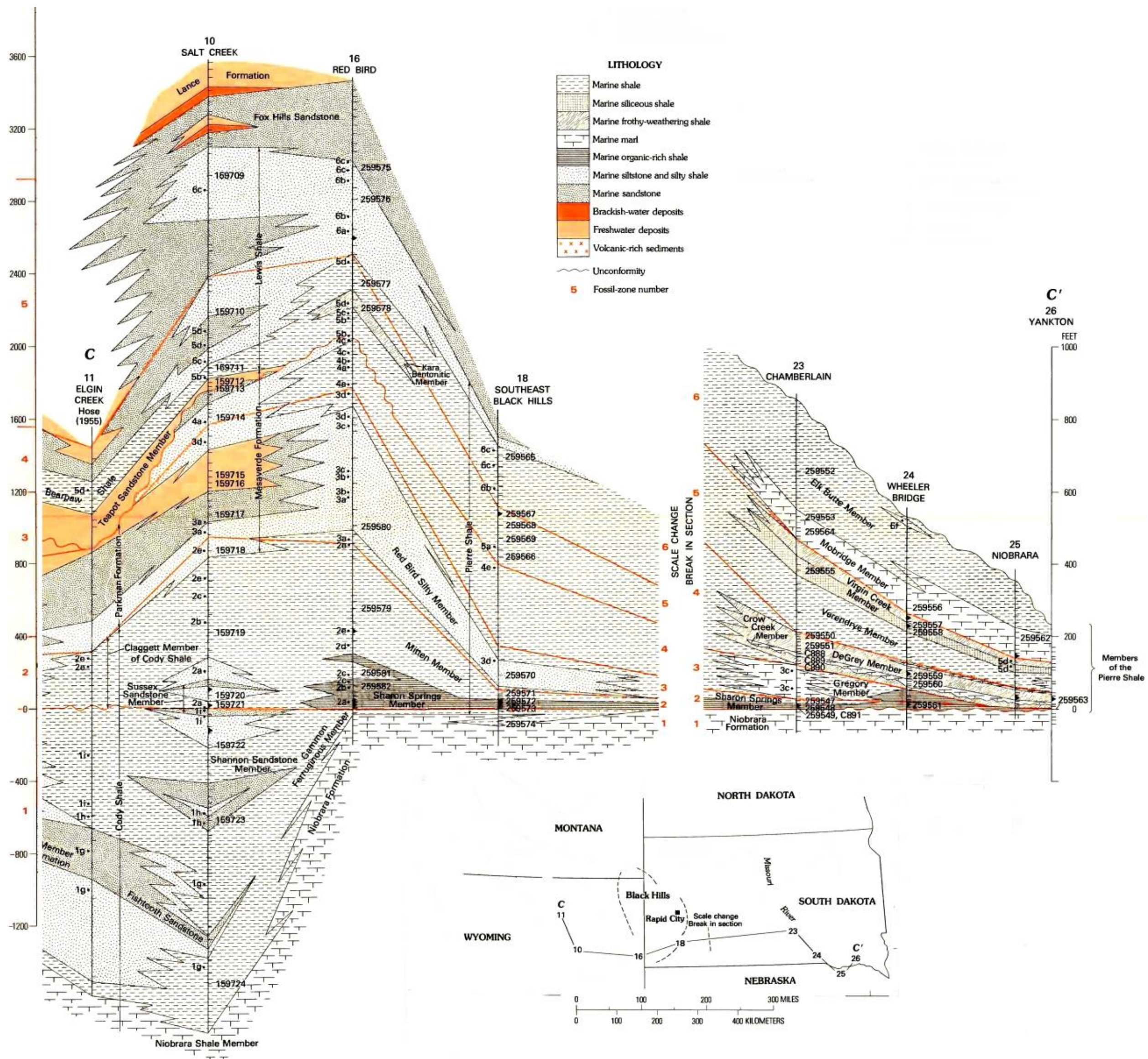

**Figure 3-2.** Stratigraphic Profile of the Pierre Shale Showing an Example of the Variations in Rock Type Found Within a Shale Formation in the Midcontinent Region (After Schultz et al., 1980).

Other general correlations can be made, such as an increasing porosity corresponding to increasing hydraulic conductivity and an increasing effective diffusion coefficient (the latter two properties are not explicitly listed). Another correlation that can be made is an increase in clay content (specifically smectite) that corresponds with a higher CEC.

# 4. Knowledge Gaps

The current understanding of the complex behavior of fine-grained geological units has advanced considerably through laboratory testing, numerical modeling, and experiments in URLs. However, a number of authors (Hansen et al., 2010; Bock et al., 2010; Argonne National Laboratory, 2011; Tsang et al., 2012) have indicated topics where significant knowledge gaps still exist.

Argonne National Laboratory (2011) prepared a Used Fuel Disposition Campaign Disposal Research and Development Roadmap. It includes issues identified as having a high overall importance for conducting research and development in clay or shale media where the available information in not sufficient. Argonne National Laboratory (2011) highlights the EDZ as a topic with insufficient information. Specific issues regarding the EDZ that require further understanding include the following:

- Improved methods for representing the complex coupling of processes, including engineered and natural systems
- Improved methods for representing near- and far-field interface chemistry
- Quantifying gas generation and potential impacts
- Evaluating the effects of excavation- and ventilation-induced fracturing
- A better understanding of fracture initiation and healing
- An improved understanding of anisotropy and heterogeneity in EDZ
- Evaluating the potential for fast transport pathways that could bypass the natural or engineered systems
- A better understanding of coupling between rock mechanics and hydrology
- An evaluation of thermal limits with respect to the EDZ
- Quantifying the geochemical environment in the EDZ.

Argonne National Laboratory (2011) also indicates the following topics where the available information is only partially sufficient:

- Host rock characterization
- Flow and transport pathways
- Mechanical processes
- Hydrologic processes
- Chemical processes/chemistry
- Thermal processes.

Of these broad topics, the following specific issues, which require a greater understanding, are identified by multiple authors (Hansen et al., 2010; Bock et al., 2010; Argonne National Laboratory, 2011; Tsang et al., 2012):

- **Development and sealing of fractures**
    - Sealing capability of rocks with less than 40 percent clay
    - Sealing capability of highly indurated rocks
    - Contribution of creep to fracture sealing
    - Contribution of clay swelling to fracture sealing
    - Evolution of hydraulic conductivity as fractures develop and seal
    - Effects of anisotropy and heterogeneity on fracture development
- **Radionuclide sorption and solubility**
    - Heterogeneity in host rock
    - Effects of pH, surface complexation, and reducing-oxidizing conditions
    - Effect on an environment with multiple radionuclides
    - Colloid-facilitated transport
    - Effect of groundwater geochemistry
- **Coupled Thermal-Hydrological-Mechanical-Chemical (THMC) processes**
    - Testing to better understand coupled effects
    - Developing constitutive models that describe these behaviors.

When concepts to describe aspects of the current knowledge gaps are developed, the transferability of concepts derived under specific conditions (such as at an existing URL) to different conditions is an important consideration. Mazurek et al. (2008) suggest that the basis for transferability depends on: (1) relevant formation properties, and (2) the state of the system. Transferability requires an understanding of all variables that affect the process being transferred. If the process can be shown to depend on only a few properties, the transferability of concepts may be warranted. Confidence in any empirical relationship will depend on the quantity of data points supporting the correlation and the breadth of other variables that are included.

Certain relationships are complex and developing simple transferable relationships is not possible. An example of such a relationship is radionuclide sorption and solubility, which depends on multiple physical properties of the host rock and conditions of the larger system. The relationship between porosity and the effective diffusion coefficient of tritium is an example of an empirical relationship that has been proven to be transferable between a number of different, fine-grained units (Mazurek et al., 2008). This relationship is valid, because tritium is not prone to adsorption. The transferability of this relationship to the effective diffusion coefficient of an element likely to adsorb (e.g., plutonium) may not be warranted. Another example of an empirical relationship that has been transferred between a variety of fine-grained units is the correlation between porosity and hydraulic conductivity documented by Neuzil (1994). This relationship is valid as long as flow is not fracture controlled. Highly indurated formations with very low porosity may contain open fractures that do not seal (e.g., the Boda Clay Formation in Hungary) (Mazurek et al. 2008), which creates higher hydraulic conductivity than expected from Neuzil's relationship. These examples demonstrate that transferability of even well-established relationships must be examined to verify that the inherent assumptions are still valid.

The Transferability of concepts is considered most suitable when the applicable material properties and state of the systems are similar. Even though the Opalinus Formation at the Mont Terri URL and the Callovo-Oxfordian Formation at the Bure URL have different lithological structures and diagenetic histories, many of their physical properties are similar. When differences in the system (e.g., the stress field and pore water salinity) are accounted for, the transferability of a number of concepts has been successful. Transferring concepts between these more indurated formations and the nonindurated Boom Clay is more difficult because of the numerous differences of physical characteristics. As an example, sealing fractures has been documented in both the Boom Clay and the more indurated units. However, the duration required for sealing to occur is much shorter for the plastic Boom Clay than the indurated units. Furthermore, the mechanisms suspected of controlling fracture sealing are thought to be different between the formations. Fracture sealing is attributed to plastic or viscoplastic (i.e., creep) processes in the Boom Clay, and the swelling of clay minerals is thought to play a large part in sealing fractures in more indurated formations (Volckaert et al., 2004).

Multiple levels of effort are needed to begin to fill the current knowledge gaps. Laboratory tests are necessary to characterize the behavior of fine-grained units under various controlled conditions. Tests on formations with different physical properties and under different conditions are needed to establish the transferability of concepts. Numerical modeling uses the constitutive models developed through laboratory testing to simulate the performance of a repository. URLs are necessary to validate the effectiveness of the constitutive relationships and numerical modeling software.

THIS PAGE INTENTIONALLY LEFT BLANK

# 5. Sample Evaluation

The Pierre Shale is a widespread formation distributed throughout the central U.S. As was described in Section 3.4, the Pierre Shale has a number of properties that are dissimilar to formations where European URLs exist. A preliminary modeling of the physical, hydrological, and thermal properties of the Pierre Shale was conducted by J. R. Nopola as part of his master's thesis at the South Dakota School of Mines and Technology (Nopola, 2013). The material in this section is derived from that thesis. This analysis was performed to investigate the potential similarities and differences between the predicted behaviors of the Pierre Shale compared to behaviors observed in URLs. This analysis provides insights into the transferability of certain concepts and emphasizes some of the current knowledge gaps.

## 5.1 Technical Approach

The suitability of the Pierre Shale to host a nuclear repository is herein evaluated in terms of defined parameters that are based on predicted behavior. These parameters include the effect of permeability with depth, the extent of the EDZ, and the potential for fractures to self-heal through rheological processes. Numerical modeling programs and analytical solutions are used to determine a potential repository design and predict the behavior of the Pierre Shale at different repository depths.

### 5.1.1 *Evaluation Topics*

The major design requirements of a nuclear repository in a natural system (Birkholzer et al., 2011) include the following:

- Containment
- Limited releases
- Dispersion and dilution
- Defense in depth.

These requirements depend on the transport properties (e.g., hydraulic conductivity, effective diffusion coefficient, and adsorption capabilities) of the intact rock. Transport through fractures may be orders-of-magnitude faster than transport through intact rock (Freeze and Cherry, 1979) and the capability of excavation-induced fractures to self-heal is important in defining radionuclide transport. Evaluating these topics will require developing a general repository design that includes necessary ground-support considerations. The evaluation topics used for assessing the suitability of the Pierre Shale as a potential host for a nuclear waste repository in this study included the following:

- Basic repository design and the effects of thermal limitations (i.e., the maximum allowable temperature) on repository design, such as drift spacing
- Potential for plastic failure in excavations

- Expected methods of ground support
- Extent of the EDZ
- Potential for healing the EDZ
- Effect of depth on hydraulic conductivity
- Approximate radionuclide transport time.

Some of these topics need to be evaluated in a specific order. For example, the basic design characteristics of the potential repository must be determined before additional evaluations can be performed. The basic design considerations of a potential repository include the drift diameter and the spacing between drifts. These dimensions will be determined in large part by thermal limitations. Thermal conditions within the Pierre Shale are analyzed to assess acceptable dimensions for repository design, which is used for further analyses.

The plastic behavior of fine-grained geological units is often perceived as a benefit (Hansen et al., 2010) when considering the healing of fractures. The counterpart of this plastic behavior is that the material is weak and prone to plastic failure. Methods of ground support (e.g., rock bolts and concrete liner) may be necessary to provide a safe working environment within the proposed repository site. If ground support is necessary, it should be included in the numerical modeling. This study addresses the potential for plastic failure in the repository and assesses the types of ground support that are likely needed.

Damage is expected to occur around the mined repository excavation in an area that has been termed the EDZ. The EDZ will be more heavily fractured than the surrounding rock mass; therefore, hydraulic conductivity and radionuclide transport are expected to increase locally. Fine-grained geological units are expected to behave viscoplastically and allow the EDZ fractures to heal after the repository is sealed. This study assesses the extent of the EDZ and evaluates expected time-frames for EDZ fractures to heal.

One of the benefits of fine-grained geological units is low hydraulic conductivity. Hydraulic conductivity exists in two basic forms: inherent and secondary. The former is controlled by the permeability of the intact rock and the latter is controlled by the existence, abundance, and aperture of fractures. The hydraulic conductivity of the rock mass and fractures will both have an effect on radionuclide transport and are included in this analysis.

### 5.1.2 *Evaluation Methods*

Numerical modeling programs are used to evaluate the suitability of the Pierre Shale for a nuclear repository. The two-dimensional, finite element, heat transfer numerical modeling program **SPECTROM-41** (Svalstad, 1983) is used to calculate the thermal effect of Used Nuclear Fuel (UNF) in the Pierre Shale. The program is part of the **SPECTROM** (**S**pecial **P**urpose **E**ngineering **C**odes for **T**hermal **Ro**ck **M**echanics) group developed by RESPEC to analyze thermal conditions related to nuclear waste disposal. **SPECTROM-41** contains models for conductive and convective heat transport, and includes the capability to model anisotropic thermal conductivity, heat generation, and heat decay. **SPECTROM-41** is used to determine a general repository design based on thermal limitations.

The three-dimensional, finite difference program, **FLAC3D** (Itasca Consulting Group, 2009), is used to perform numerical modeling of repository designs. **FLAC3D** (Version 4.00.84) was developed primarily for geotechnical applications and, therefore, embodies features to accurately represent the mechanical behavior of geologic materials. Constitutive models are mathematical relationships developed to describe observed behaviors under certain conditions and then predict behavior under different conditions. **FLAC3D** has several built-in material models ranging from the "null" model, which represents excavations in the grid, to the shear- and volumetric-yielding models, which include strain-hardening and -softening behavior, nonlinear shear failure, and compaction. The **FLAC3D** built-in constitutive model that is used for the numerical modeling is the "cpower" model. This model is selected because it incorporates linear elastic behavior (Hooke's Law), perfectly plastic failure (Mohr-Coulomb), and viscoplastic behavior (Norton Power Law).

**FLAC3D** also includes an internal programming code called **FISH**. When applicable constitutive models are not available, new code is written using the **FISH** programming. The modifications programmed through **FISH** include strain-softening behavior and changes to porosity, permeability, and density based on the calculated mean stress and swelling stresses related to changes in moisture content.

Materials are represented within the **FLAC3D** model as polyhedral elements, which form a three-dimensional grid that can be adjusted to fit the shape of the object being modeled. Each element behaves according to a prescribed linear or nonlinear stress-strain law (constitutive model) in response to the applied forces or boundary restraints. If the stresses (or stress gradients) are high enough to cause the material to yield, the grid is able to deform and move with the material represented in the model. **FLAC3D** is based on a "Lagrangian" calculation scheme that is well suited for modeling large distortions (Itasca Consulting Group, 2009).

Evaluating the Pierre Shale as a potential host formation for a nuclear repository requires describing the expected mechanical and hydrological behavior of the formation under different conditions. The **FLAC3D** numerical evaluation developed for this study accounts for the following behaviors of fine-grained geological units:

- Elastic
- Plastic
- Viscoplastic
- Hydrologic
- Poroelastic
- Shrink/swell.

Finally, radionuclide transport is investigated using an analytical solution. The one-dimensional relationship accounts for transport by advection and diffusion and includes sorption and decay

## 5.2 Material Properties and Processes

The calculations used by the numerical models and analytical solutions are presented in this section. Modifications and additions to the internal **FLAC$^{3D}$** calculations by using the programming code, **FISH**, are also provided in this section.

Material parameters (e.g., mechanical properties and hydrological characteristics) for the constitutive and numerical models were acquired from published literature. Lithological variations are present within the Pierre Shale and some publications (Hansen and Vogt, 1987) indicate the individual formation or member of the Pierre Shale that was tested. However, many publications (Boisson, 2005) do not differentiate units. Therefore, typical properties of the dominant marine shale lithology are used. Similarly, sufficient information is not available on anisotropy of the Pierre Shale, which results in an isotropic model for both hydrological and mechanical properties.

### 5.2.1 *Physical Properties*

Physical properties include mineralogy, density, porosity, and water content. The response of a geological unit to processes depends on the physical properties of that unit. For example, the potential for shrink and swell depends on the smectite content, and the permeability through intact rock is reliant on the porosity and density of the unit. Physical properties provide a means of comparing geological units and correlating expected behaviors, such as plastic deformation, and the potential for shrink and swell. The physical properties obtained for the analysis are derived from the dominant marine shale facies of the Pierre Shale.

The mineralogy of the Pierre Shale was acquired from a number of sources (Schultz et al., 1980; Boisson, 2005; Hansen and Vogt, 1987; Al-Bazali et al., 2008). The most extensive mineralogical analysis obtained is provided in Schultz et al. (1980), which includes mineralogical analyses on over 1,000 samples of the Pierre Shale and equivalent formations. A wide range of mineralogical properties are reported in this extensive database of samples and originate from the presence of lithological variations, such as bentonite layers and sandstone beds. Representative values for the marine shale facies are selected based on typical values from the studies analyzed and are shown in Table 5-1. The typical mineralogy of the marine shale facies contains a high percentage of clay (70 percent), and most of it is either smectite or mixed-layer smectite and illite. The low percentage of carbonates (5 percent) is also notable. These mineralogical properties contrast the properties of the indurated units in existing URLs (i.e., Opalinus and Callovo-Oxfordian Formations), as shown in Table 3-1.

Physical properties of the Pierre Shale including density, porosity, and water content are listed in Table 5-2. These physical properties display a significant variability that is likely caused, in part, by differences in lithology as a result of facies changes in a dynamic marine environment. However, depth variations also affect the mean stresses and are expected to have a significant influence on material properties. Variations in density and porosity based on mean stress are described in greater detail in Section 5.2.6.

**Table 5-1. Mineralogical Composition of the Marine Shale Facies of the Pierre Shale (Modified From Schultz et al., 1980; Boisson, 2005; Hansen and Vogt, 1987; Al-Bazali et al., 2008)**

| X-Ray Diffraction Analysis Percent by Weight | Best Estimate for Marine Shale | Minimum | Maximum |
|---|---|---|---|
| Total clay | 70 | 65 | 85 |
| Smectite | 12 | 0 | 60 |
| Mixed-layer smectite and illite | 40 | 5 | 60 |
| Illite | 11 | 0 | 30 |
| Chlorite | 3 | 0 | 5 |
| Kaolinite | 4 | 0 | 12 |
| Quartz | 20 | 10 | 35 |
| Feldspars | 4 | 0 | 10 |
| Carbonates | 5 | 0 | 10 |
| Accessory minerals (pyrite, gypsum, zeolite, organic carbon) | 1 | 0 | 5 |

**Table 5-2. Physical Properties of the Pierre Shale (Modified From Boisson, 2005; Kopp, 1986; Nichols and Collins, 1986; Schultz et al., 1980)**

| Property | Best Estimate | Minimum | Maximum |
|---|---|---|---|
| Bulk density, $\rho_b$ (kg/m$^3$) | 2,060 | 1,710 | 2,330 |
| Dry density, $\rho_d$ (kg/m$^3$) | 1,740 | 1,210 | 2,000 |
| Average grain density, $\rho_g$ (kg/m$^3$) | 2,600 | 2,440 | 2,670 |
| Porosity, $\phi$ (%) | 20.8 | 9.3 | 33.0 |
| Water content, $w$ (%) | 16 | 12 | 38 |

### 5.2.2 *Thermal Properties*

Thermal properties of the Pierre Shale were acquired from Gilliam and Morgan (1987), Hansen and Vogt (1987), and Sass and Galanis (1983). The reported results were averaged, and those used in the analysis are presented in Table 5-3. An analysis performed by

Hansen et al. (2010) indicated that the thermal conductivity had a greater influence on heat transport than heat capacity did. The thermal conductivity of the Pierre Shale is 0.96 W/m·°C. This is less than other indurated, fine-grained units where URLs exist (approximately 1.25 to 2.70 W/m·°C) (Hansen et al., 2010), and it is much less than that of salt (approximately 3.09 to 4.70 W/m °C) (Hardin et al., 2011), another geological unit under consideration for use as a nuclear repository.

**Table 5-3. Thermal Properties of the Pierre Shale (Gilliam and Morgan, 1987; Hansen and Vogt, 1987; Sass and Galanis, 1983)**

| Property | Best Estimate | Minimum | Maximum |
|---|---|---|---|
| Thermal conductivity, $K^T$ (W/m·°C) | 0.96 | 0.63 | 1.49 |
| Heat capacity, $C_v$ (J/kg·°C) | 1,297 | 963 | 1,465 |

The **SPECTROM-41** one-dimensional model for temperature as a function of time and radial distance from an infinite line decaying heat source is given as:

$$T(r,t) = \frac{(Q_L)}{4\pi K^T} \int_0^t \frac{\left(e^{\lambda t}\right) e^{\frac{-r^2}{4\kappa t}}}{t} dt \tag{5-1}$$

where:

$T$ = temperature

$r$ = distance from heat source

$Q_L$ = line load power

$\lambda$ = decay constant

$t$ = time

$K^T$ = thermal conductivity

$\kappa$ = thermal diffusivity

### 5.2.3 *Elastic Properties*

Materials subjected to stresses that do not exceed their strength will strain elastically. The elastic behavior of materials is modeled in **FLAC3D** by using Hooke's law, a linear and reversible elastic relationship:

$$\Delta\sigma_1 = \left(K + \frac{4}{3}G\right)\Delta\varepsilon_1^e + \left(K + \frac{2}{3}G\right)\left(\Delta\varepsilon_2^e + \Delta\varepsilon_3^e\right)$$

$$\Delta\sigma_2 = \left(K + \frac{4}{3}G\right)\Delta\varepsilon_2^e + \left(K + \frac{2}{3}G\right)\left(\Delta\varepsilon_1^e + \Delta\varepsilon_3^e\right) \quad (5\text{-}2)$$

$$\Delta\sigma_3 = \left(K + \frac{4}{3}G\right)\Delta\varepsilon_3^e + \left(K + \frac{2}{3}G\right)\left(\Delta\varepsilon_1^e + \Delta\varepsilon_2^e\right)$$

where:

$\sigma_1$, $\sigma_2$, $\sigma_3$ = maximum, intermediate, and minimum principal stresses where $\sigma_1 \geq \sigma_2 \geq \sigma_3$

$\varepsilon_1^e$, $\varepsilon_2^e$, $\varepsilon_3^e$ = maximum, intermediate, and minimum principal elastic strains

$K$ = bulk modulus

$G$ = shear modulus.

The elastic parameters of Poisson's ratio and Young's modulus are related to the bulk modulus and shear modulus through the following relationships:

$$K = \frac{E}{3(1-2\nu)}$$

$$G = \frac{E}{2(1+\nu)} \quad (5\text{-}3)$$

where:

$E$ = Young's modulus

$\nu$ = Poisson's ratio.

Elastic parameters for the Pierre Shale were obtained from a number of sources (Kopp, 1986; Hansen and Vogt, 1987; Nataraj, 1991; Nichols and Collins, 1986; Botts, 1986), and a best estimate was determined based on the most common values reported and are provided in Table 5-4.

### 5.2.4 *Plastic Properties*

Materials will strain elastically until they reach their strength limit when irreversible plastic strain will occur. Numerous failure criteria have been developed to describe the plastic behavior of geomaterials. These criteria include linear relationships, such as the relationship described by the Mohr-Coulomb criterion, and nonlinear relationships, such as the Hoek-Brown or Cam-Clay criterion. Although the Mohr-Coulomb criterion is a simple model, it is widely used and has a large presence in existing literature (Kopp, 1986; Hansen and Vogt, 1987; Nataraj, 1991; Nichols and Collins, 1986; Botts, 1986; Al-Bazali et al., 2008; Stark et al., 2005). For these reasons, plastic failure of the Pierre Shale was modeled using this model and is represented in **FLAC3D** as follows:

**Table 5-4. Elastic Properties of the Pierre Shale (Kopp, 1986; Hansen and Vogt, 1987; Nataraj, 1991; Nichols and Collins, 1986; Botts, 1986)**

| Property | Best Estimate | Minimum | Maximum |
|---|---|---|---|
| Young's modulus, $E$ (MPa) | 1,000 | 100 | 1,800 |
| Poisson's ratio, $\nu$ | 0.20 | 0.10 | 0.33 |
| Bulk modulus, $K$ (MPa) | 556 | — | — |
| Shear modulus, $G$ (MPa) | 417 | — | — |

$$f^s = \sigma_1 - \sigma_3 + \left(\frac{1+\sin\varphi}{1-\sin\varphi}\right) + 2c_o\sqrt{\left(\frac{1+\sin\varphi}{1-\sin\varphi}\right)} \tag{5-4}$$

where:

$f^s$ = Mohr-Coulomb shear failure criterion

$\varphi$ = friction angle

$c_o$ = cohesion.

A tensile cutoff is used in conjunction with the Mohr-Coulomb criterion and is described as:

$$f^t = \sigma_3 - \sigma^t \tag{5-5}$$

where:

$f^t$ = tensile failure criterion

$\sigma^t$ = tensile strength.

Numerous sources were reviewed to provide Mohr-Coulomb parameters for the analysis (Kopp, 1986; Hansen and Vogt, 1987; Nataraj, 1991; Nichols and Collins, 1986; Botts, 1986; Al-Bazali et al., 2008; Stark et al., 2005). The reviewed data included compression tests where the ultimate axial stress, $\sigma^a$, was recorded at a variety of confining stresses, $\sigma^r$. The uniaxial and triaxial compression test data were used to determine a least-sum-of-squared-errors fit to a Mohr-Coulomb failure criterion on a *p-q* diagram, where:

$$p = \frac{\sigma^a + \sigma^r}{2}$$
$$q = \frac{\sigma^a - \sigma^r}{2} \tag{5-6}$$

The *p-q* diagram in Figure 5-1 includes the test data and a best-fit regression line. Variability existed in the test data at low confining stresses, and limited information was available from high-confining stresses. Additional test data that identifies stratigraphic variations may indicate if a parabolic or bilinear failure criterion model would provide a better representation of the data. Values of cohesion and the friction angle obtained through the *p-q* diagram are listed in Table 5-5 and are within the range of published values obtained for the Pierre Shale. The tensile strength used in the analysis was chosen from an average of available test data (i.e., Brazilian indirect tension test) and is also provided in Table 5-5 (Hansen and Vogt, 1987).

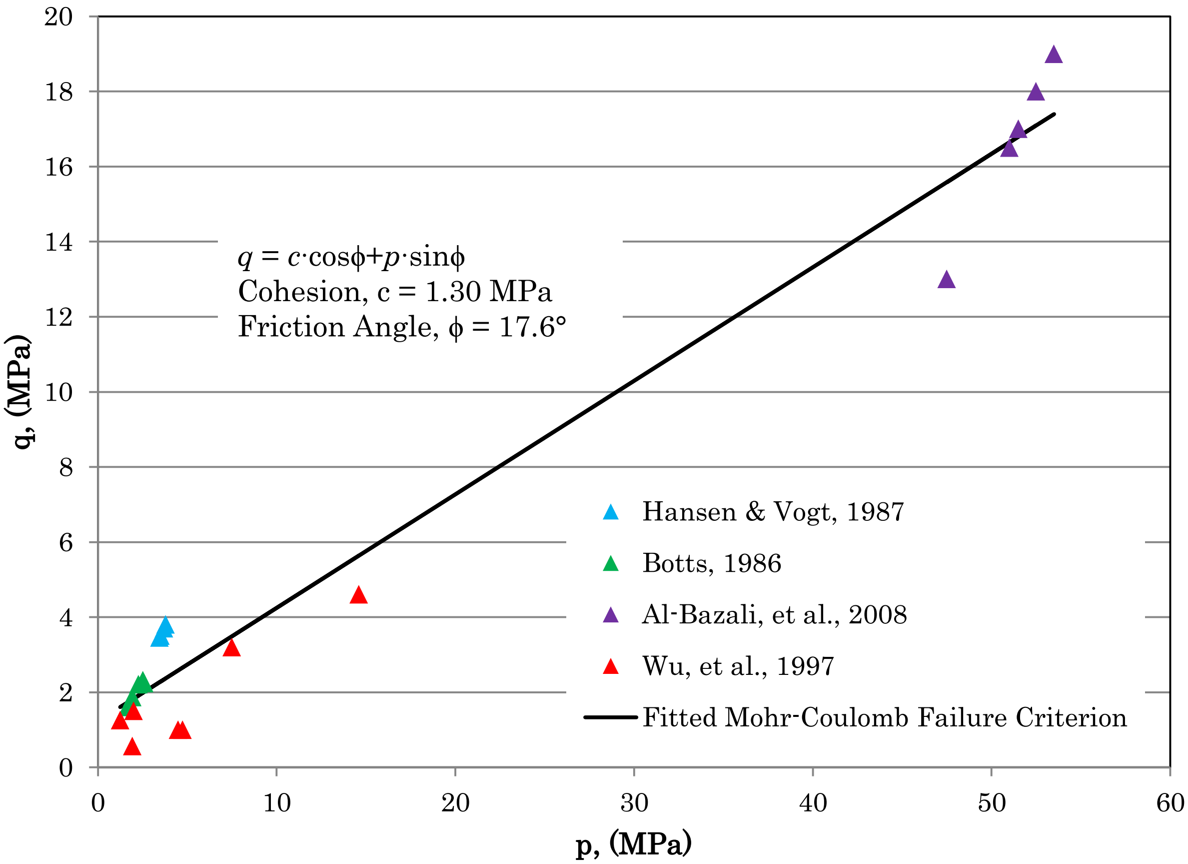


**Figure 5-1.** Pierre Shale Compression Test Data That Has Been Plotted on a *p-q* Diagram, Including the Equation for the Mohr-Coulomb Failure Criterion.

A material that fails plastically will often experience an increase in volume (dilation) as porosity increases along the plane of failure. The dilation angle, $\psi_d$, describes the amount of volume increase associated with plastic failure. Published data on the dilation angle of the

Pierre Shale was not available and was estimated using the following relationship for low-strength rocks (Rocscience Inc., 2013):

$$\psi_d \approx \frac{1}{3}\varphi_p \tag{5-7}$$

**Table 5-5. Peak Plastic Properties of the Pierre Shale Used in the Analysis, Including Minimum and Maximum Values Obtained From Published Sources (Botts, 1986; Kopp, 1986; Nichols and Collins, 1986; Hansen and Vogt, 1987; Nataraj, 1991; Wu et al., 1997; Stark et al., 2005; Al-Bazali et al., 2008) and the Best Estimate Determined Through the *p-q* Line Fitting**

| Property | Best Estimate | Minimum | Maximum |
|---|---|---|---|
| Internal friction angle, $\varphi_p$ (°) | 17.6 | 5.3 | 43.8 |
| Cohesion, $c_o$ (MPa) | 1.30 | 0.02 | 1.4 |
| Tensile strength , $\sigma^t$ (MPa) | 0.53 | 0.31 | 0.83 |
| Dilation angle, $\psi_d$ (°) | 5.0 | — | — |

When a material reaches its peak strength and begins to deform plastically, the residual Mohr-Coulomb properties often do not remain at peak values but also may not immediately drop to zero. Published stress-strain curves from triaxial compression tests were used to estimate the amount of postpeak shear strain that occurred when the Mohr-Coulomb properties reached residual values. Residual strains were identified by a constant strain rate at a constant stress. Residual strains were observed when the postpeak strains exceeded an average of approximately 0.013 m/m (Botts, 1986). The residual values of cohesion and tension were reduced to zero when the postpeak strain exceeded 0.013 m/m.

The work of Stark et al. (2005) was used to estimate the residual friction angle for the Pierre Shale. They analyzed dozens of landslides (including many in the Pierre Shale and equivalent formations) to establish a relationship between the residual friction, liquid limit, clay fraction (defined as particles less than 2 μm in diameter), and normal stress. This relationship is shown in Figure 5-2. The average liquid limit of the Pierre Shale was estimated at 80 percent (Kopp, 1986; Schultz et al., 1980). Based on the liquid limit, a clay fraction greater than 50 percent, and an effective normal stress between 100 to 700 kPa, the residual friction angle for the Pierre Shale was estimated to be between 7 to 12 degrees. A residual friction angle of 8 degrees was used for the analysis. Residual values for the Mohr-Coulomb strength criterion with a tension cutoff are provided in Table 5-6. Reductions in Mohr-Coulomb parameters were calculated in **FLAC^3D^** by a **FISH** program that determined the magnitude of postpeak strain.

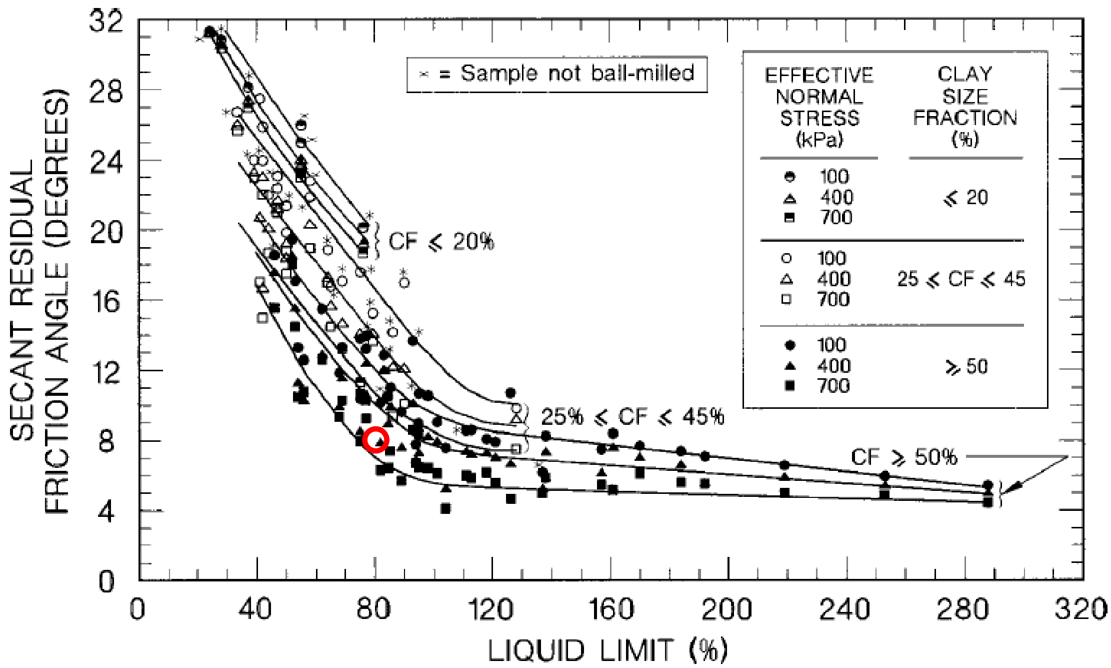


**Figure 5-2.** Residual Friction Angle Based on Liquid Limit, Clay Fraction, and Normal Stress (Stark et al., 2005).

**Table 5-6. Residual Mohr-Coulomb Strength Criterion**

| Postpeak Shear Strain | Friction Angle $\varphi$ (°) | Cohesion $c_o$ (MPa) | Tensile Strength $\sigma^t$ (MPa) |
|---|---|---|---|
| 0 | 17.6 | 1.30 | 0.53 |
| 0.013 | 8.0 | 0.00 | 0.00 |

### 5.2.5 *Viscoplastic Properties*

Under certain temperature and pressure conditions, materials will deform viscoplastically (creep) when subjected to deviatoric (shear) stress. Creep can be broadly grouped into three regions: transient, steady-state, and accelerated. These three regions are displayed in Figure 5-3. Transient creep is a period of rapid deformation immediately after a stress difference is applied. The rate of transient creep decreases with increasing time until the region of steady-state creep is reached. During steady-state creep, the relationship between strain and time is approximately linear. The final region is accelerated creep, where the damage in the rock accumulates more quickly than it can be repaired. Accelerated creep is often the precursor to plastic failure.

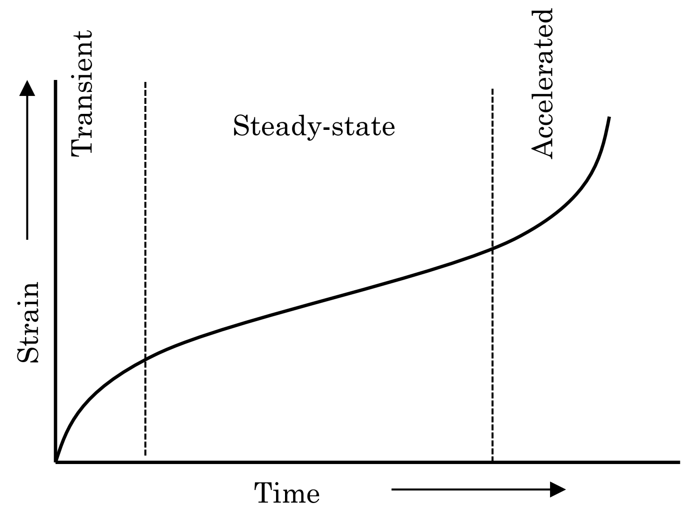


**Figure 5-3.** The Three Regions of a Creep Curve Under Constant Stress Difference.

Most laboratory tests on fine-grained geological units are conducted for hours instead of days, and the steady-state creep rate is often not reached within this duration. A few recent studies (Zhang and Rothfuchs, 2004; Bock et al., 2010; Nopola and Roberts, 2013) have subjected fine-grained geological units to shear stress for over 1 month and have shown that these units deform continuously (steady-state creep) throughout this period. At relatively low stress differences some fine-grained geological units creep at rates comparable to salt under similar stress differences (Nopola and Roberts, 2013). Information related to the creep rate of fine-grained geological units is not widespread, and specific examples related to the creep rate of the Pierre Shale are unavailable. In the absence of formation-specific information, the creep behavior of other fine-grained geological units is used as an analog.

For this analysis, the Pierre Shale was considered to be a time-dependent creeping material modeled by the Norton-type creep law (Norton, 1929). This simple creep law only accounts for steady-state creep; transient and accelerated creep were not considered. Accelerated creep is not well recognized or understood within the limited information available for fine-grained geological units. Transient creep may account for a significant portion of creep deformation during short durations, but steady-state creep will account for an increasing percentage of the total creep deformation over longer time periods. Defining these relationships will require additional and prolonged creep testing. The rate of creep is also depends on the deviatoric stress and increases as a power function of the deviatoric stress magnitude. Deviatoric stress was defined as the von Mises stress, which is based on the second deviatoric stress invariant, $J_2$. Using the Norton-type creep law, the creep strain $\varepsilon^{cr}$ was written as:

$$\varepsilon^{cr} = A\left(\sigma_v\right)^n t^m \tag{5-8}$$

where:

$$\sigma_v = \text{von Mises stress}$$

$$\sigma_v = \sqrt{3J_2}$$

$$J_2 = \frac{1}{6}\left[\left(\sigma_1 - \sigma_2\right)^2 + \left(\sigma_1 - \sigma_3\right)^2 + \left(\sigma_2 - \sigma_3\right)^2\right]$$

$$t = \text{time}$$

$$A = \text{creep factor}$$

$$n = \text{stress exponent}$$

$$m = \text{time exponent.}$$

If the material constant, $m$, is assumed to be 1, (which is the case in the internal **FLAC3D** calculation) the steady-state creep law can be expressed in terms of the creep rate, $\dot{\varepsilon}^{cr}$ :

$$\dot{\varepsilon}^{cr} = A\left(\sigma_v\right)^n \tag{5-9}$$

The Norton-type creep model has two parameters ($A$ and $n$) that must be determined for each material. Available information suggests that the steady-state creep rate of fine-grained geological units generally lies between approximately $5 \times 10^{-12}$ and $5 \times 10^{-10}$ $\Delta\varepsilon$ $s^{-1}$ (Zhang and Rothfuchs, 2004; Bock et al., 2010). Existing laboratory data indicate that creep rate has little dependence on stress difference and shows a linear increase with increasing deviatoric stress. The creep material properties used in the analysis are provided in Table 5-7.

**Table 5-7. Viscoplastic Properties Used in the Analysis of the Pierre Shale (Zhang and Rothfuchs, 2004; Bock et al., 2010; Nopola and Roberts, 2013)**

| Property | Best Estimate |
|---|---|
| $A$, ($MPa^{-n} \cdot s^{-1}$) | $1 \times 10^{-11}$ |
| $n$ | 1.0 |

### 5.2.6 *Hydrological Properties*

**FLAC3D** is capable of modeling the single-phase flow of fluid through a permeable medium. Unless it is coupled with mass transport programs, such as **TOUGH** (Rutqvist and Tsang, 2003), **FLAC3D** is unable to model two-phase flow of gas and liquid phases and does not include capillary action. Fluid transport in **FLAC3D** is portrayed through Darcy's law, which is described as:

$$q = -k_f \cdot \hat{k}(s)\left(\nabla p - \rho_f x g\right) \qquad (5\text{-}10)$$

where:

$q =$ specific discharge

$k_f =$ **FLAC$^{3D}$** permeability coefficient

$k_f = \dfrac{K^H}{\rho_f g} = \dfrac{k}{\mu}$

$\rho_f =$ fluid density, 1,000 kg/m$^3$

$g =$ gravitational acceleration, 9.81 m/s$^2$

$k =$ intrinsic permeability

$K^H =$ hydraulic conductivity

$\mu =$ dynamic viscocity, $10^{-3}$ Pa $\cdot$ s

$\hat{k}(s) =$ mobility coefficient

$\hat{k}(s) = s^2\left(3 - 2s\right)$

$s =$ saturation

$\nabla p =$ pore pressure gradient

$x =$ unit vector in the vertical direction.

The coupling of hydrological and mechanical process is described through the relationship of poroelasticity. The poroelastic relationship in **FLAC3D** is described as:

$$\frac{1}{M}\frac{\partial p}{\partial t} + \frac{\phi}{s}\frac{\partial s}{\partial t} = \frac{1}{s}\left(-q + q_v\right) - \alpha\frac{\partial \varepsilon^v}{\partial t} \qquad (5\text{-}11)$$

where:

$M =$ Biot modulus, 2 GPa

$\phi =$ porosity

$q_v =$ volumetric fluid source intensity

$\alpha =$ Biot coefficient, 1.0

$\varepsilon^v =$ mechanical volumetric strain.

The internal programing of **FLAC^3D** holds parameters such as porosity, permeability, and density at constant values. In reality, these values change according to depth, and more specifically, on mean stress. Neuzil (1986) summarized dozens of consolidation and transient flow laboratory tests that measured the hydraulic conductivity of Pierre Shale samples at different effective mean stresses. Jiang et al. (2010) used the data of Neuzil to develop empirical equations that related permeability and porosity to depth. Figure 5-4 shows the predicted relationship between permeability and depth and includes the test data of Neuzil. These data indicate that permeability decreases by up to 4 orders-of-magnitude from the surface to thousands of meters in depth. Hydraulic conductivities (in meters per second [m/s]) measured by Neuzil were converted to intrinsic permeabilities (in $m^2$) by assuming $\mu/\rho_f\, g = 10^{-7}$ m·s. The effective mean stress was converted to depth by assuming that the effective mean stress increased at approximately $1.3 \times 10^4$ Pa/m, which implied a bulk density of approximately 2,300 $kg/m^3$.

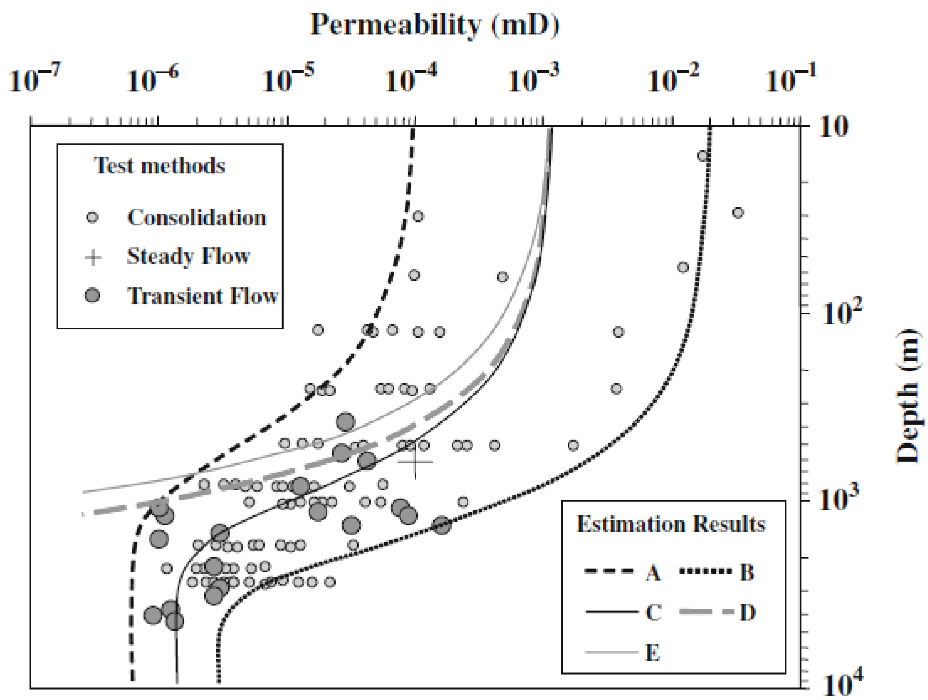


**Figure 5-4.** Predicted Relationship Between Permeability and Depth in Pierre Shale. Data points are from Neuzil (1986) and empirical relationships are from Jiang et al. (2010), whose estimation results refer to different sets of variables used to populate the empirical relationship. Estimation line "C" is used in this study.

The equation developed to describe the relationship between mean stress and porosity (Jiang et al. 2010) is:

$$\phi = \phi_r + \frac{(\phi_0 - \phi_r)(1 + \phi_r)}{(\phi_0 - \phi_r) + (1 + 2\phi_r - \phi_0)\exp\left(\sigma'_m (1 + \phi_r)\eta\right)} \tag{5-12}$$

where:

$$\phi = \text{porosity}$$

$$\phi_r = \text{minimum, residual porosity, 0.073}$$

$$\phi_0 = \text{surficial, initial porosity, 0.4}$$

$$\sigma'_m = \text{effective mean stress}$$

$$\sigma'_m = \frac{\sigma_1 + \sigma_2 + \sigma_3}{3} - \alpha p$$

$$\alpha = \text{Biot's coefficient, 1.0}$$

$$p = \text{pore pressure}$$

$$\eta = \text{fitting variable, } 2.0 \times 10^{-7}.$$

and the relationship developed between permeability and mean stress was:

$$k = k_0 \left( \frac{\phi_r}{\phi_0} + \frac{\left(\phi_0 - \phi_r\right)\dfrac{\left(1+\phi_r\right)}{\phi_0}}{\left(\phi_0 - \phi_r\right) + \left(1 + 2\phi_r - \phi_0\right)\exp\left(\sigma'_m\left(1+\phi_r\right)\eta\right)} \right)^{n^H} \tag{5-13}$$

where:

$$k = \text{permeability}$$

$$k_0 = \text{surficial, initial permeability, } 10^{-18}\text{m}^2 \ \left(10^{-3}\text{mD}\right)$$

$$n^H = \text{fitting variable, 4.}$$

These equations assume that permeability and porosity vary between maximum values at the surface (where the mean stress approaches zero), and minimum, or residual, values at depth. An initial surficial porosity of 0.4 was used based on the deformation characteristics reported by Neuzil (1993). The fitting variables were those determined for the estimation line "C" in Figure 5-4. These relationships of permeability and porosity were programmed using **FISH** to allow variations based on mean stress. Changes in density were also calculated from changes in porosity. A relationship between porosity and density was programmed using **FISH**, as follows:

$$\rho_b = \rho_g\left(1-\phi\right) + \rho_s \cdot \phi \cdot s \tag{5-14}$$

where:

$$\rho_b = \text{bulk density of rock}$$

$$\rho_g = \text{average grain density, 2,600 kg/m}^3$$

$$s = \text{saturation.}$$

### 5.2.7 *Shrink and Swell Properties*

The Pierre Shale has an appreciable amount of smectite clay minerals (Table 3-1) that can swell when subjected to moisture increases and can shrink when dried. A swelling and shrinking relationship, described in Liu et al. (2011), was programmed using **FISH** to model this behavior as:

$$\Delta\sigma'_{sw} = 3K \cdot \Delta s \cdot \beta_{sw} \tag{5-15}$$

where:

$$\Delta\sigma'_{sw} = \text{volumetric swelling stress}$$

$$\beta_{sw} = \text{moisture swelling coefficient.}$$

A series of tests measuring the swelling pressure of the Pierre Shale was performed by (Hansen and Vogt, 1987) and is summarized in Table 5-8. Using the average swelling stress, the average change in saturation, and the bulk modulus as previously defined, the moisture swelling coefficient, $\beta_{sw}$, was determined to be 0.001.

**Table 5-8. Swelling Pressure of the Pierre Shale (Hansen and Vogt, 1987)**

| Property | Best Estimate | Minimum | Maximum |
|---|---|---|---|
| Swelling stress, $\Delta\sigma'_{sw}$ (MPa) | 0.24 | 0.17 | 0.42 |
| Saturation change, $\Delta s$ (%) | 19.2 | 9.0 | 43.9 |

Before excavation, in situ Pierre Shale is expected to be completely saturated. Desaturation and shrinkage is expected to occur after the excavation is dewatered. If the change in saturation is great enough, desiccation cracks may form. The development of desiccation cracks is related to tensile strength (Puppala et al., 2012), and when the shrinkage stress exceeds the tensile strength, cracking develops. These fractures are expected to transmit water orders-of-magnitude quicker than the intact rock. This expected behavior was accounted for by assigning increased bulk permeability to regions where desiccation cracking was predicted. The resulting bulk permeability value was modeled as an average of the permeability of the intact rock and the permeability of the fracture by using the following relationships:

$$
\begin{aligned}
&\text{if } \Delta\sigma'_{sw} > \sigma^t, \text{ then} \\
&\varepsilon_{frac} = \Delta s \cdot \beta_{sw} \\
&k_f^{frac} = \frac{{\varepsilon_{frac}}^2}{12\rho_f g\mu} \\
&k_f^{bulk} = k_f^{rock}\left(1-\varepsilon_{frac}\right) + k_f^{frac}\cdot\varepsilon_{frac}
\end{aligned}
\tag{5-16}
$$

where:

$\varepsilon_{frac}$ = swelling strain, fracture aperture

$k_f^{frac}$ = **FLAC$^{3D}$** permeability coefficient, fracture

$k_f^{rock}$ = **FLAC$^{3D}$** permeability coefficient, intact rock

$k_f^{bulk}$ = bulk **FLAC$^{3D}$** permeability coefficient, fracture, and intact rock.

### 5.2.8 *Radionuclide Transport Properties*

A simplified advection-dispersion equation that included sorption and decay was used to evaluate radionuclide transport through clay and shale. The solution was based on an initial concentration of zero at all locations outside of the constant concentration source (i.e., the source is not depleted). The analytical solution for this system, described in Hansen et al. (2010), was:

$$
C(z,t) = \frac{C_o}{2} e^{\left(\frac{zv_z}{2D_z}(1-\Omega)\right)} erfc\left(\frac{z - \frac{v_z}{R_f}t\Omega}{2\sqrt{\frac{D_z t}{R_f}}}\right) + e^{\left(\frac{zv_z}{2D_z}(1+\Omega)\right)} erfc\left(\frac{z + \frac{v_z}{R_f}t\Omega}{2\sqrt{\frac{D_z t}{R_f}}}\right)
\tag{5-17}
$$

where:

$C$ = concentration

$C_o$ = constant source concentration

$z$ = vertical distance

$t$ = time

$v_z$ = groundwater pore velocity

$$v_z = \frac{\mathrm{K}^H}{\phi_e} i_z$$

$\phi_e$ = effective transport porosity, estimated 0.05

$i_z$ = vertical hydraulic gradient, estimated 0.01 m/m

$$\Omega = \sqrt{\frac{4\lambda D_z R_f}{{\upsilon_z}^2}}$$

$D_z$ = coefficient of hydrodynamic dispersion

$$D_z = \alpha_z \upsilon_z + \tau D_m$$

$\alpha_z$ = longitudinal dispersivity, estimated 1 m

$\tau$ = tortuosity, estimated 0.5

$D_m$ = molecular diffusion coefficient

$$D_m = \frac{D_e}{\tau \phi_e}$$

$D_e$ = effective diffusion coefficient

$$D_e = D_a \left(\phi_e + \rho_b k_d\right)$$

$D_a$ = apparent diffusion coefficient

$k_d$ = distribution coefficient

$R_f$ = retardation factor

$$R_f = 1 + \frac{\rho_b k_d}{\phi_e}.$$

The estimated variables provided in Equation 5-16 were based on Hansen et al. (2010), except for the upward hydraulic gradient, which was an order-of-magnitude greater than was used by Hansen et al. Some of the variables were specific to individual radionuclides (e.g., $\lambda, k_d, D_e$), and other variables were changed based on the repository depth (e.g., $\rho_b, K^H$). These variables are defined in Section 5.3.5.

### 5.2.9 *In Situ Stress and Geothermal Conditions*

Nichols and Collins (1986) performed pressuremeter tests in boreholes drilled into the Pierre Shale in central South Dakota. These tests measured the effective vertical stresses and indicated that the state of stress at the site was essentially lithostatic (i.e., the horizontal stresses were equal to the weight of the overburden). Therefore, lithostatic stress conditions were used in the modeling.

A geothermal gradient was determined for use in the analysis of a repository design by using a calculated geothermal gradient of 67.7 °C/km obtained from boreholes in the Pierre

Shale located in central South Dakota (Sass and Galanis, 1983) Figure 5-5 displays the geothermal gradient measured in the Pierre Shale and includes temperatures at potential repository depths.

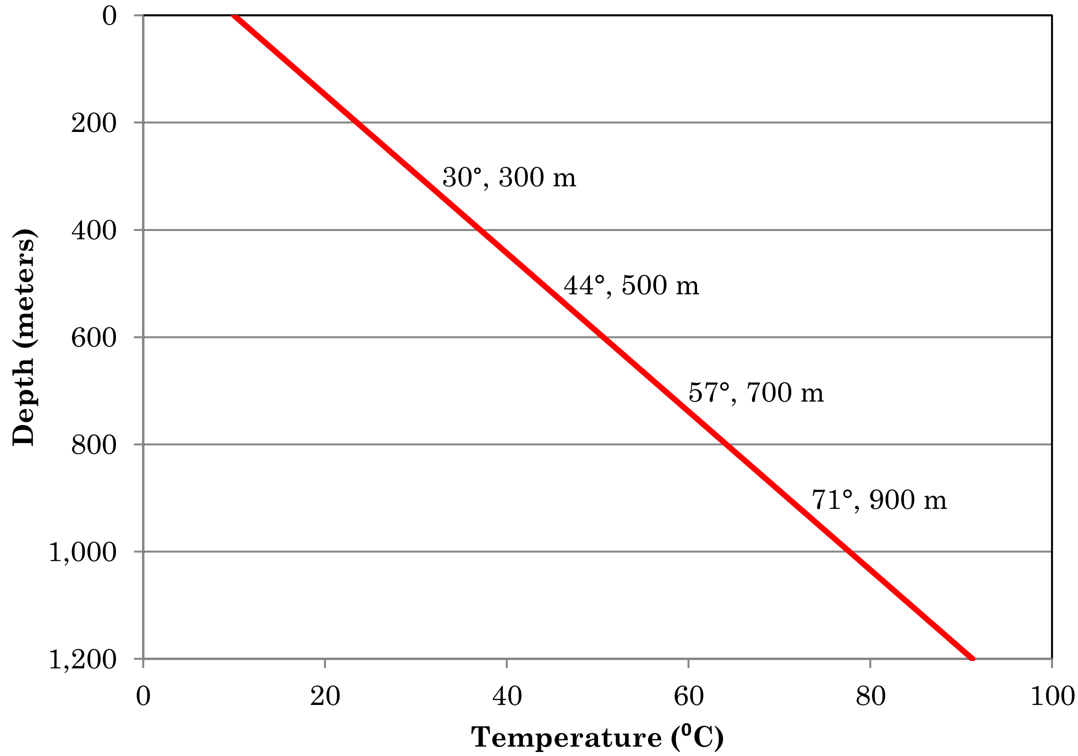


**Figure 5-5.** Geothermal Gradient in the Pierre Shale (Line) From Sass and Galanis (1983) Including Temperatures Within Likely Repository Depths Between 300 and 900 Meters.

## 5.3 Analysis and Results

Defined parameters are used to evaluate the Pierre Shale's suitability for hosting a potential waste repository. The parameters include temperature limitations within the host rock, deviatoric and effective mean stresses and their changes over time, the potential for plastic failure, and estimated radionuclide transport times. The following sections provide additional information on the evaluation parameters and the findings of the analysis.

### 5.3.1 *Thermal Constraints and Repository Design*

A defined design for a U.S. repository in fine-grained geological units has not been finalized by the Department of Energy (DOE). Developing a generic repository design for analysis requires a review of existing design concepts from U.S. National Labs and European URLs. The general design for a U.S. nuclear repository in fine-grained geological units will likely be based on existing European concepts. France, Switzerland, and Belgium have developed proposed concepts (Hardin et al., 2011) that are based on a series of horizontal, bored excavations connected by a main access tunnel. Figure 5-6 shows a proposed example for a nuclear waste repository based on the French model. Nuclear waste canisters are disposed in the horizontal borings, which are surrounded by bentonite, and the intersection with the main tunnel is sealed with concrete. The proposed diameter of the waste-storage drifts in the European concepts ranges from 0.7 to 3.0 meters. The Swiss and French concepts are based on self-supporting rock, which requires only intermittent ground support (e.g., rock bolts). The Belgium URL is located in a low-strength, unconsolidated clay, which requires continuous support in the form of a 0.66-m-thick concrete liner surrounding the borehole.

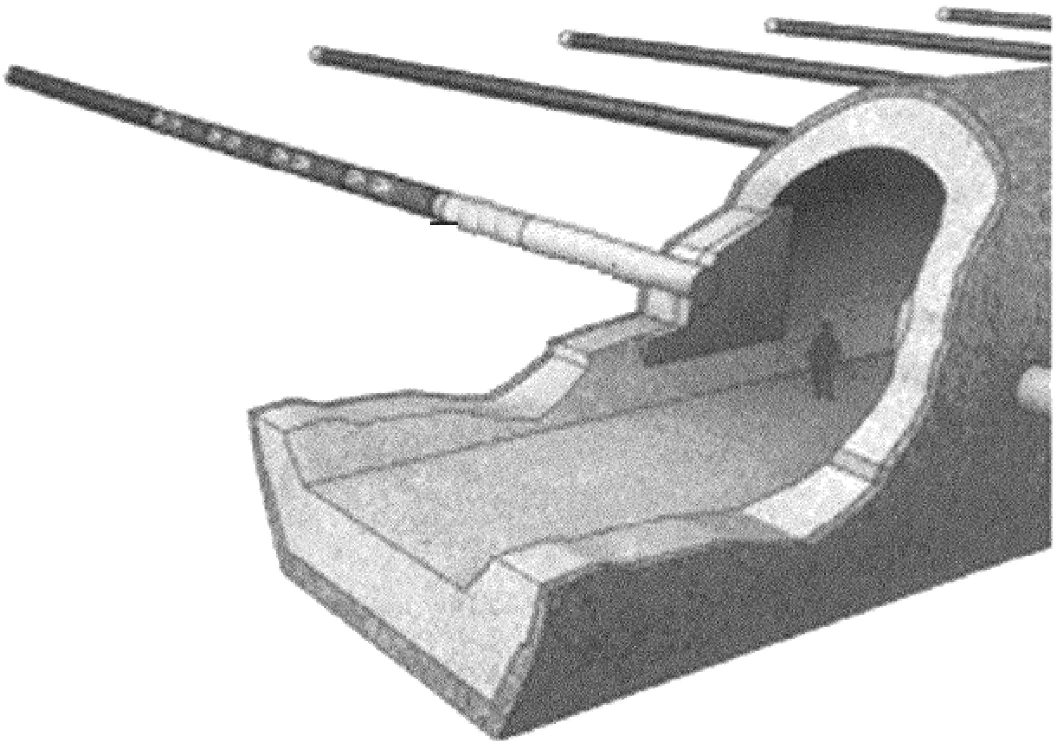

**Figure 5-6.** General Repository Design Based on French Concept Consisting of a Series of Horizontal Waste Repository Boreholes Connected by a Main Access Tunnel (Delage et al., 2010).

A common design requirement for the repositories is to ensure that peak temperatures in the host rock do not exceed 100°C. Maintaining the peak temperature of the host rock below 100°C is desired to prevent issues that may alter conditions in the host rock. Altered conditions can include the boiling of pore water, desaturation and its associated shrinkage, and the mineralogical alteration of the host rock. Although groundwater at depths of over 300 m has the capability to be superheated (i.e., the boiling point is greater than 100°C because of increased pressure), the pressure in rock surrounding the excavated area will likely be much less than the premining pressure. These thermal considerations will mostly determine the horizontal distance between drifts and the borehole diameter.

The initial design considerations used in the thermal evaluation are based on the characteristics of the nuclear waste for the Yucca Mountain project reported by the (U.S. Nuclear Waste Technical Review Board, 2008). The 21-assembly pressurized water reactor (PWR) UNF is the hotter waste type considered by the U.S. Nuclear Waste Technical Review Board (2008) and, therefore, is used in the analysis. Typical properties for a 21-PWR UNF are listed in Table 5-9. The power and decay constants are based on the burnup of 48 Gigawatt-days per ton (GWd/ton), which is indicated as the average PWR burnup by the U.S. Nuclear Waste Technical Review Board (2008). Nuclear waste is composed of radioactive materials that decay at different rates. A sum of three decaying exponentials is used to provide a more accurate representation of the power decay of each assembly:

$$Q(t) = Q_1 e^{-\lambda_1 t} + Q_2 e^{-\lambda_2 t} + Q_3 e^{-\lambda_3 t} \tag{5-18}$$

where:

$Q$ = power

$t$ = time

$Q_1, Q_2, Q_3, \lambda_1, \lambda_2, \lambda_3$ = power ($Q$) and decay ($\lambda$) constants determined by UNF type and burnup.

**Table 5-9. Thermal and Design Properties for 21-Assembly PWR UNF at Yucca Mountain (U.S. Nuclear Waste Technical Review Board, 2008)**

| UNF Type | | PWR |
|---|---|---|
| Number of assemblies | | 21 |
| Waste package length (m) | | 5.85 |
| Waste package spacing (m) | | 0.70 |
| Waste package diameter (m) | | 1.88 |
| Burnup (GWd/ton) | | 48 |
| Power constants (W) | $Q_1$ | 2,114.44 |
| | $Q_2$ | 688.19 |
| | $Q_3$ | 154.47 |
| Decay constants (years$^{-1}$) | $\lambda_1$ | 0.35243 |
| | $\lambda_2$ | 0.024561 |
| | $\lambda_3$ | 0.002473 |
| Age at emplacement (years) | | 16 |
| Line load at emplacement (W/m) | | 1,990 |

The power and decay of each assembly is converted to an infinite line load by using the following equation:

$$Q(t) = \frac{N_A Q_1 e^{-\lambda_1 t}}{WP_l + WP_s} + \frac{N_A Q_2 e^{-\lambda_2 t}}{WP_l + WP_s} + \frac{N_A Q_3 e^{-\lambda_3 t}}{WP_l + WP_s} \quad (5\text{-}19)$$

where:

$N_A$ = number of assemblies

$WP_l$ = waste package length

$WP_s$ = waste package spacing.

A graphical representation of the power decay for the 21-PWR UNF with the waste package length and package spacing proposed for Yucca Mountain is displayed in Figure 5-7. A 4-PWR design based on the French concept for storage in fine-grained geological units (Agence nationale pour la gestion des dechets radio, 2005b) is also displayed in Figure 5-7.

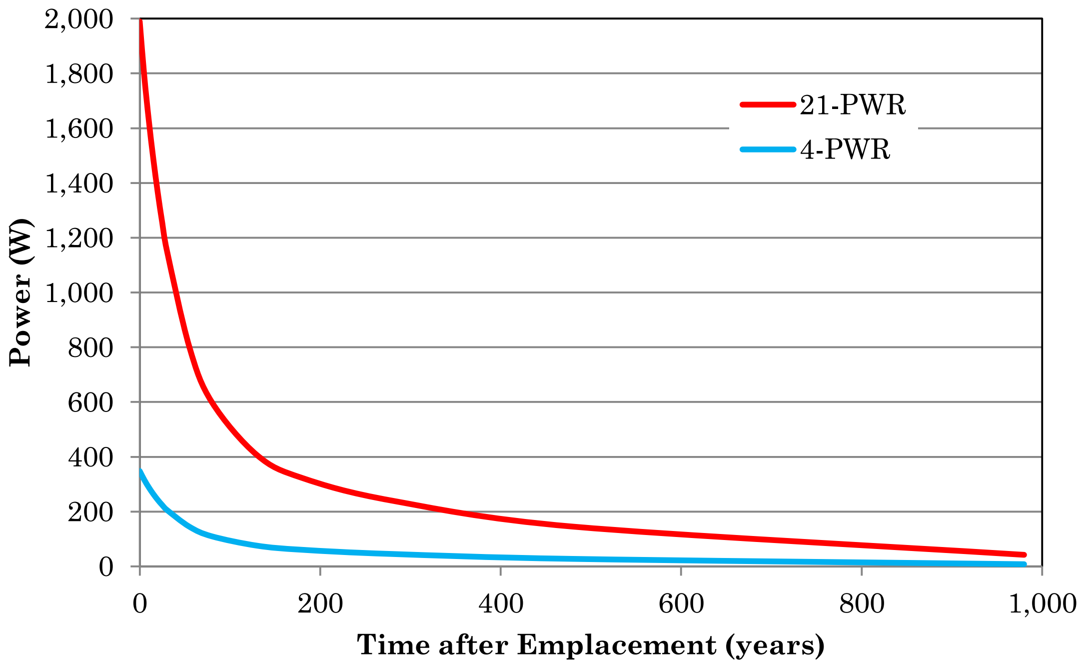


**Figure 5-7.** Power Decay of Line Load for 21-PWR and 4-PWR Assemblies With 5.85-Meter Waste Package, 0.7-Meter Package Spacing, and Emplacement After 16 and 20 Years of Decay, Respectively.

The thermal characteristics of the Pierre Shale, provided in Table 5-3, are used to evaluate thermal limitations. Based on the thermal properties and typical density, the thermal diffusivity is estimated to be $3.01 \times 10^{-7}$ m²/s. A one-dimensional model of an infinite line decaying heat source is used to calculate the increase in temperature at radial distances away from the UNF line load at various times using **SPECTROM-41**. Figure 5-8 displays the increase in temperature of the Pierre Shale at radial distances away from the UNF at various times. Values from within the waste package (a radius of 0.94 m) are omitted, because the results are considered inaccurate. The inaccuracy is related to the simplified, analytical method that converts multiple waste assemblies into a single line power source, which results in unrealistically high temperature predictions within the waste package. Note the temperature increase exceeds 100°C to a maximum distance of 25 m from the UNF in Figure 5-8. The host rock within 5 m of the UNF is predicted to experience a temperature increase of 100°C for a period of 500 years.

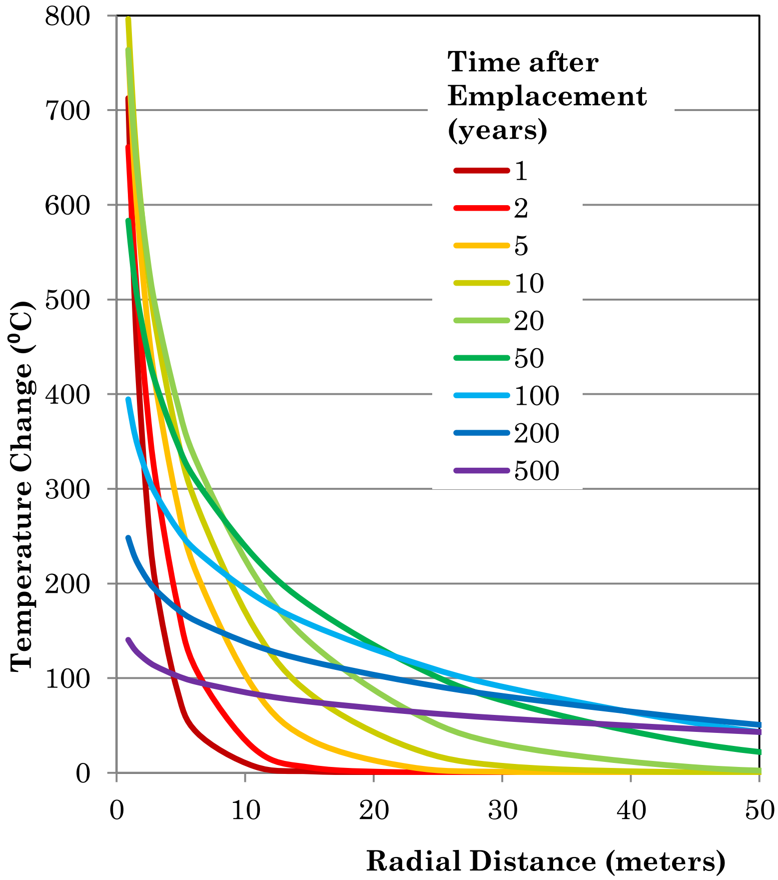


**Figure 5-8.** The Temperature Increase in the Pierre Shale at Radial Distances Away From an Isolated Drift Containing 21-PWR UNF at Various Times After Emplacement.

The 21-PWR design proposed for use at Yucca Mountain is clearly unsuitable for use in the Pierre Shale. The unacceptable design is derived from thermal conductivity of the Pierre Shale (0.96 W/m·K), which is lower than that of the tuff at Yucca Mountain (1.83 W/m·K). In addition, the unique design concept of Yucca Mountain included open drifts and decades of ongoing ventilation that cooled the drifts.

A second thermal analysis is performed using the same waste package length and package spacing, but with a 4-PWR instead of a 21-PWR. The waste age at the time of emplacement is also increased to 20 years to allow additional radioactive decay, which decreases the initial power. Increasing the waste age at emplacement requires longer temporary storage in surface facilities before long-term storage emplacement. Table 5-10 summarizes the design properties that are changed from those previously listed in Table 5-9. The power decay of the 4-PWR assembly line load is shown in Figure 5-7.

**Table 5-10. Changes to the Design Properties to Reduce the Line Load at Emplacement**

| | |
|---|---|
| Number of assemblies | 4 |
| Waste package diameter (m) | 1.25 |
| Age at emplacement (years) | 20 |
| Line load at emplacement (W/m) | 348 |

The 4-PWR configuration resulted in a thermal prediction that is reasonable for the design constraints of shale. The results from the thermal prediction of the 4-PWR assembly are used to model multiple drifts by summation of the temperature increases. Figure 5-9 shows the temperatures at different radial distances from the UNF line load for various times. In Figure 5-9 an initial temperature of 44°C (equivalent to a depth of 500 m from Figure 5-5) and a drift spacing of 40 m is used. The temperatures in Figure 5-9 are near or below 100°C in most locations. The 40-m drift spacing is considered an acceptable design; minor adjustments to variables such as the waste package spacing and the age of waste at emplacement can be made to maintain the temperature below 100°C.

Based on the results of the thermal analysis, a drift diameter of 3 m and a drift spacing of 40 m is selected for this study. An observation from the thermal analysis is how hot the temperature is predicted to be near the waste package when compared to other geological options. A limitation of the shale repository is that the footprint of the excavated waste repository must be over 5 times greater than that proposed at Yucca Mountain.

### 5.3.2 *Numerical Model Description*

A **FLAC$^{3D}$** finite difference model is created based on the proposed repository design derived from the thermal analysis of Section 5.3.1. A two-dimensional plane strain model of a circular drift that is 3 m in diameter is created for the analysis. Kinematic boundary conditions on the vertical boundaries of the models impose zero-normal displacements on the four vertical planes and zero-vertical displacement on the bottom plane. The upper surfaces of the models are allowed to move freely in the vertical direction. The grid mesh created for the numerical model and dimensions of the model are shown in Figure 5-10. The mesh size along the drift walls is approximately 0.1 m by 0.1 m. The boundary conditions applied on the model simulate an array of infinitely long drifts spaced 40 m on center. The dimensions in Figure 5-10 include an example of a concrete liner, which is listed as 0.25 m thick. The presence and thickness of the liner needed for support depends on the depth of the repository, which is described in Section 5.3.3.

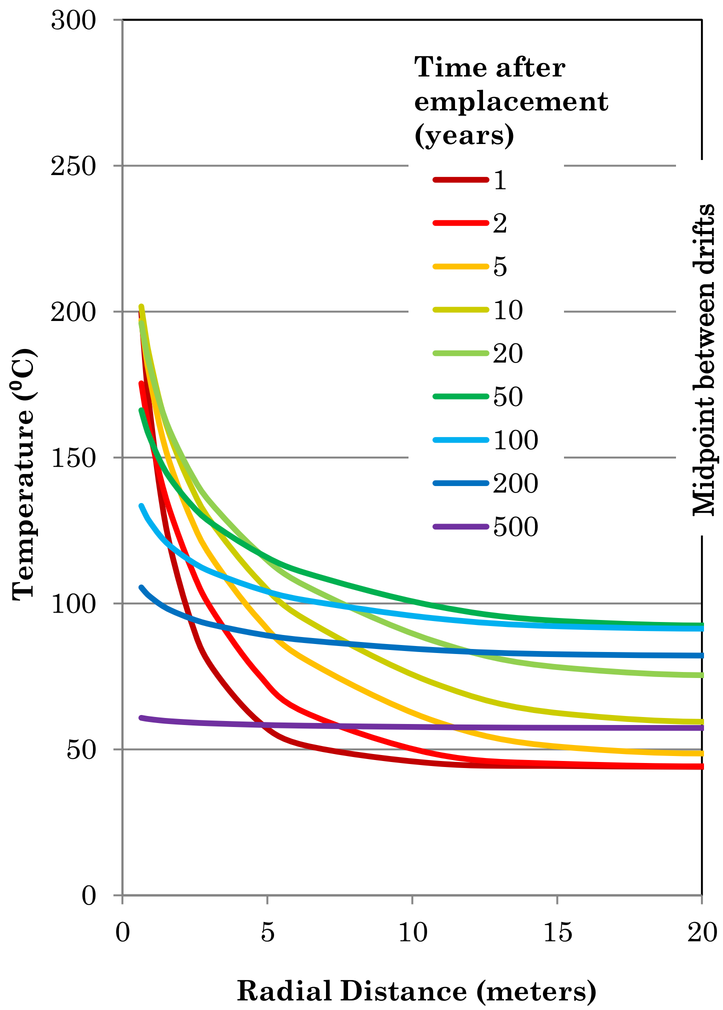


**Figure 5-9.** The Temperature in the Pierre Shale at Radial Distances Away From a Drift Containing 4-PWR UNF at Various Times After Emplacement. Drift spacing is 40 meters on center and repository depth is 500 meters.

Numerical evaluation of the repository is performed at three depths to assess the effect of depth on the evaluation measures. The three depths modeled are at 300 m, 500 m, and 700 m below the surface. The same model dimensions shown in Figure 5-10 (which has a vertical height of 200 m) is used in each instance. A surface traction is applied at the top of the model that is equivalent to the stress applied by the weight of the equivalent overburden of each depth modeled. A pore pressure is also applied to the top of the model that is equivalent to a fully saturated thickness of overburden. Before simulating an excavation, each model is solved for gravity loading conditions where the initial conditions of variables dependent on means stress (i.e., density, porosity, and permeability) are established. Pore pressures are fixed along the model boundaries to simulate the steady recharge of water.

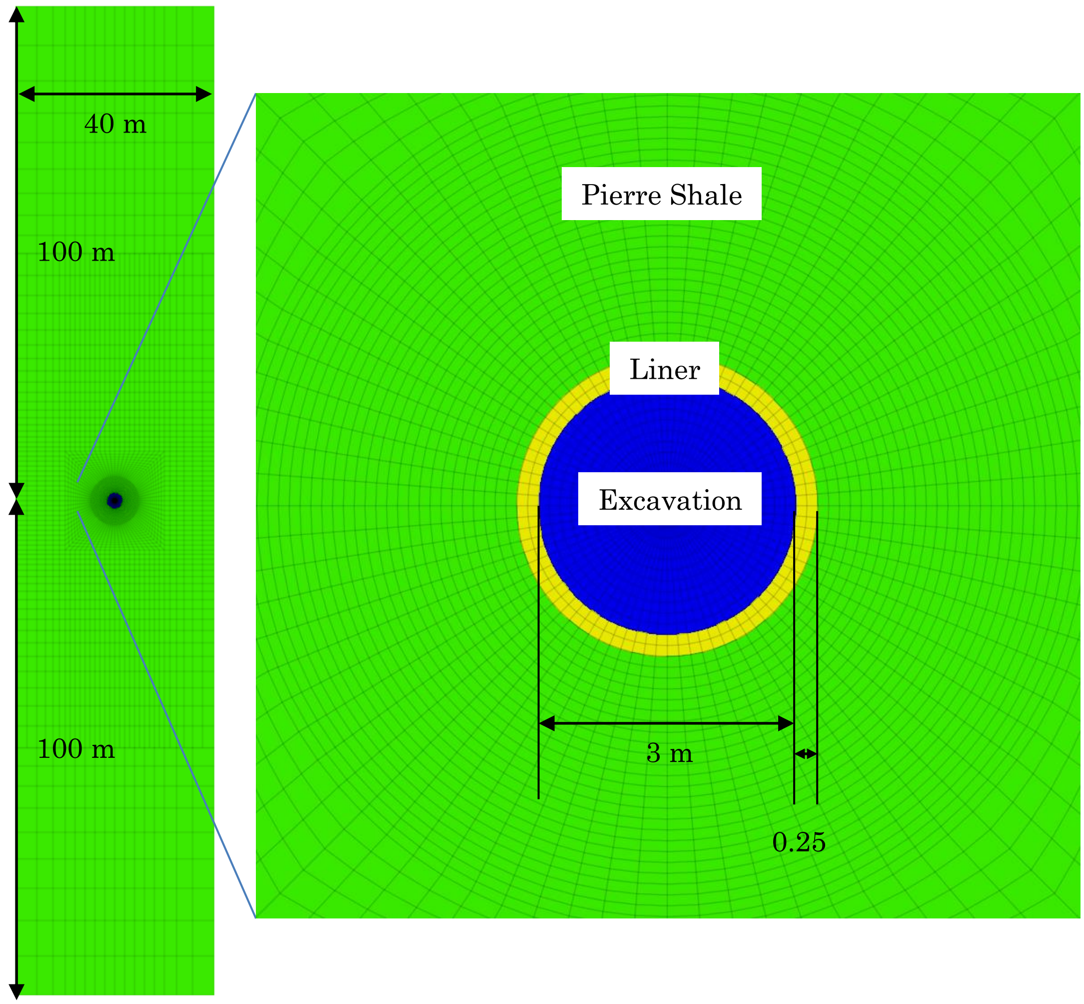


**Figure 5-10.** Numerical Model Dimensions and Grid Mesh.

The material within the 3-m-diameter drift is converted into a mechanical and hydrological “null” material to simulate excavation. Mechanically “null” elements do not support any stress, and hydrologic “null’ elements are considered impermeable. A discharge that is greater than the permeability of the materials is applied along the wall of the drift to simulate the removal of water that enters the excavation. Groundwater is allowed to adjust in the model while solving the elastic solution (time is near 0). Because the host rock has low permeability and the simulation time required to analyze flow in transient conditions is excessive, the fluid model was turned off after the elastic solution occurred. This simplification is considered conservative because pore pressure will not decrease further over time. As pore pressure decreases, the effective mean stress increases, which results in a greater confining pressure and lower permeability. One of the limitations of this approach is that the desaturation front and associated shrinkage pressures do not advance into the host rock.

The numerical models at 300 m, 500 m, and 700 m are all evaluated over simulation times of 20 years, and intermediate simulation times of 1, 2, 5, and 10 years are also recorded for further analyses.

### 5.3.3 *Potential for Plastic Failure and Expected Support*

The Pierre Shale is not as strong as the indurated shale units proposed for repository storage in Europe (i.e., Opalinus and Callovo-Oxfordian Formations). A Mohr-Coulomb failure criterion is used to evaluate the potential for shear failure in the stratigraphy at the site. Factor-of-safety values are used to quantify the competency of the modeled layers against shear failure. The Mohr-Coulomb factor of safety (FS) is defined as the ratio between the strength of the material ($S^f$) and the developed internal deviatoric stress ($S'$) and may be written as:

$$\mathrm{FS} = \frac{S^f}{S'} = \frac{\left( c_o \cos\varphi + \dfrac{\sigma_1' + \sigma_3'}{2} \sin\varphi \right)}{\sqrt{J_2}\cos\psi} \tag{5-20}$$

where:

$$J_2 = \frac{1}{6}\left[ \left(\sigma_1' - \sigma_2'\right)^2 + \left(\sigma_2' - \sigma_3'\right)^2 + \left(\sigma_3' - \sigma_1'\right)^2 \right]$$

$$\psi = \tan^{-1}\left[ \frac{\sigma_1' - 2\sigma_2' + \sigma_3'}{\sqrt{3}\left(\sigma_1' - \sigma_3'\right)} \right] \text{ (Lode angle)}$$

$\sigma_1', \sigma_2', \sigma_3'$ = effective principal stress components ($\sigma_1' \geq \sigma_2' \geq \sigma_3'$, compression positive)

$\sigma' = \sigma - \alpha p$

$c_o$ = cohesion

$\varphi$ = angle of internal friction.

In this equation, compression is positive and tension is negative. Strength increases as principal stresses increase (i.e., increasing confinement). The Lode angle describes the relative magnitudes of the principal stresses. An FS of less than 1.2 is used as a means of indicating the potential for fracturing in the EDZ of the Pierre Shale.

#### 5.3.3.1 Unsupported Excavation

At the shallowest depth analyzed in this study (300 m), the Pierre Shale is not predicted to be capable of supporting a 3-m-diameter circular excavation. Deviatoric stresses are great enough to induce plastic failure around the excavation. The region surrounding the excavation is predicted to strain plastically, and the excavation is predicted to collapse; the numerical solution does not converge. An example of the deformed mesh of an unsupported excavation is shown in Figure 5-11, which displays a series of shear planes developing where shear strain is substantial. All zones with shear strain contours greater than 0.05 have strength values reduced to residual values (i.e., zero cohesion and a friction angle of 8°) and factors of safety of less than 1. This includes all of the shear zones shown in Figure 5-11. Because collapse is predicted at the 300-m-deep excavation, the 500-m- and 700-m-deep repositories (where stresses are greater) are also expected to collapse.

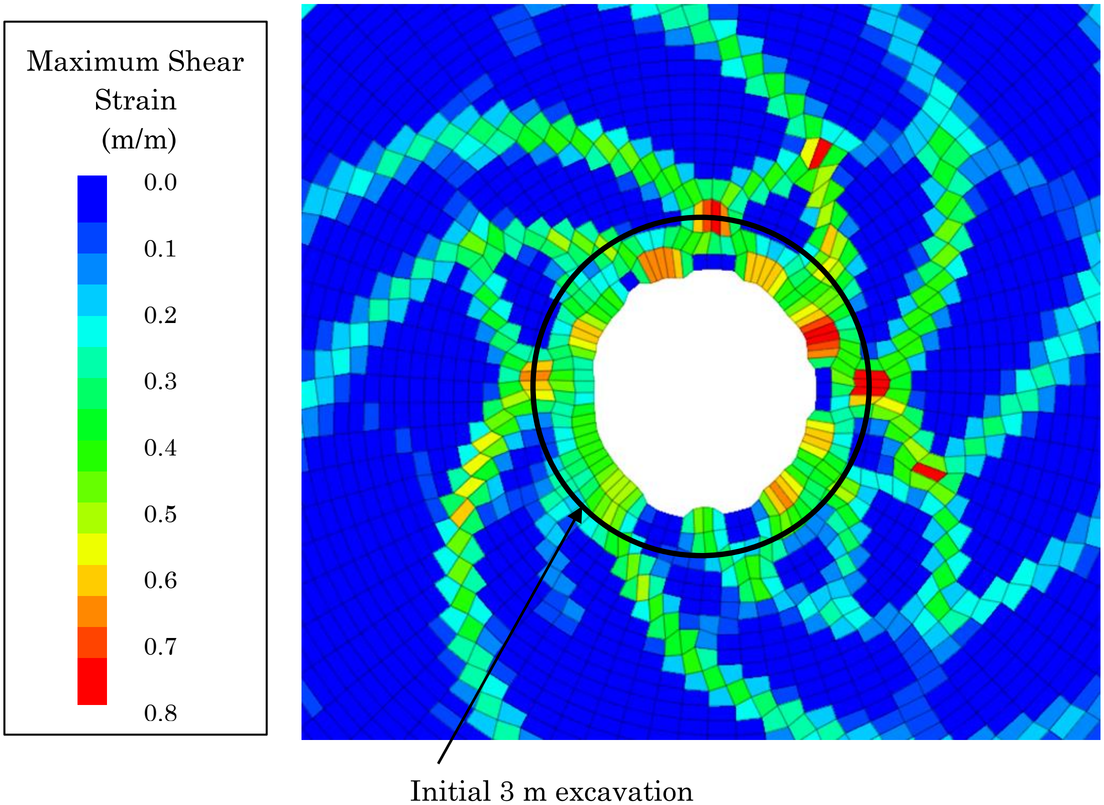


**Figure 5-11.** Deformed Mesh and Maximum Shear Strain of Unsupported Excavation at 300 Meters.

Ground support is expected to be necessary for excavations in the Pierre Shale at depths at or below 300 m. The numerical modeling predicts immediate failure after excavation (i.e., during the elastic solution), which suggests that the drift will not remain open long enough for installing rock bolts and/or shotcrete and that more aggressive support is required.

#### 5.3.3.2 Ground-Support Design

The proposed method used to provide support to the excavations is similar to that of the Mol Facility in Belgium where concrete liners are installed immediately behind a tunnel-boring machine. A shield supported by hydraulic jacks protects the construction operation from the yielding clay as segments of the concrete liner are poured. Other techniques could be considered, such as installing forepoles and steel sets (Hoek, 2001), but these techniques are not explicitly analyzed in this study.

The installation of concrete liners is simulated by allowing the rock to respond elastically and then by installing concrete liners into the model before the rock is allowed to fail plastically. The concrete is modeled as a Mohr-Coulomb material with strain softening. Material properties for the concrete are obtained from sources that include concrete as part of the repository design (Bastiaens and Demarche, 2003; Agence nationale pour la gestion des dechets radio, 2005b). The FS is determined using Equation 5-19. High-strength concrete is required to provide long-term support at the proposed repository depths. A summary of the concrete material properties is provided in Table 5-11.

**Table 5-11. Material Properties of the Concrete Liner (Bastiaens and Demarche, 2003; Agence nationale pour la gestion des dechets radio, 2005b)**

| Property | Value |
|---|---|
| Young's modulus, $E$ (GPa) | 36.7 |
| Poisson's ratio, v | 0.20 |
| Bulk modulus, $K$ (GPa) | 20.3 |
| Shear modulus, $G$ (GPa) | 15.2 |
| Compressive strength, $\sigma^c$ (MPa) | 60 |
| Internal friction angle, $\varphi$ (°) | 37 |
| Cohesion, $c_o$ (MPa) | 15 |
| Tensile strength , $\sigma^t$ (MPa) | 5 |
| Porosity, $\phi$ | 0.1 |
| Permeability, $k$ ($m^2$) | $10^{-18}$ |
| Initial saturation, s | 0.11 |
| Density, $\rho_{con}$ ($kg/m^3$) | 2,300 |

Even though the permeability of intact concrete is comparable to the Pierre Shale, the concrete liner is not considered a true hydrological barrier. This is caused by the construction joints that exist between the blocks of the concrete liner. Joints with an aperture as thin as 1 μm still have a hydraulic conductivity that is orders-of-magnitude greater than intact concrete. In the numerical modeling a permeability of $5.0 \times 10^{-15}$ $m^2$ is used for the concrete to account for flow through construction joints.

The thickness of the concrete liner that is required to support the drift is dependent on the excavation depth. Table 5-12 lists the thickness of concrete liner that is used at each repository depth. A concrete with a stronger compressive strength could be used to reduce the liner thickness, but is not considered as part of this study.

#### 5.3.3.3 Ground-Support Performance

One of the findings of the numerical modeling is that viscoplasticity transfers deviatoric stress from the Pierre Shale to the concrete liner over time. Figure 5-12 displays the deviatoric stress in the concrete liner at various simulation times for the 500-m repository depth. As shown in Figure 5-12, the greatest change of deviatoric stresses in the concrete liner is predicted to occur in the first 2 years. The maximum deviatoric stress of approximately 15 MPa at the elastic solution increases to approximately 30 MPa after 2 years of simulation time. Subsequent increases in deviatoric stress are more gradual. This implies that the concrete liner design must consider the anticipated duration that the drift will remain open. The concrete liner thicknesses used in the design are determined by performing a series of numerical simulations on different liner thicknesses to determine the minimum thickness that is predicted to remain intact for a simulation period of 20 years. The minimum concrete liner thickness determine by this approach is 0.25 m at the 300-m repository depth, 0.50 m at the 500-m depth, and 0.75 m at the 700-m depth.

**Table 5-12. Thickness of the Concrete Liner Used at Each Repository Depth**

| Repository Depth (m) | Concrete Liner Thickness (m) |
|---|---|
| 300 | 0.25 |
| 500 | 0.50 |
| 700 | 0.75 |

Deviatoric stresses for the concrete liner of three repository depths (300 m, 500 m, and 700 m) are displayed in Figure 5-13 at a simulation time of 20 years. Figure 5-13 shows that the deviatoric stress in the concrete liner reaches 40 MPa in all of the repository depths. The FS in the interior of the concrete liner is predicted to drop to approximately 1.2 by 5 years and remain near 1.2 at 20 years. If a higher FS is needed for the concrete liner, the liner thickness would need to be increased. Figure 5-14 illustrates the changes in deviatoric stress in the concrete liner for various simulation times at point "A," as indicated in Figure 5-13. The trend of deviatoric stress evolution displayed in Figure 5-14 is similar for the three repository depths; most of the change in deviatoric stress occurs in the initial 2 to 5 years and is more gradual thereafter.

### 5.3.4 *Extent of Excavation Damage Zone*

The extent of the EDZ (characterized by the presence of fractures in the region surrounding the excavated drift) may differ for different excavation depths. The numerical modeling in this study uses continuum modeling, which does not simulate the development of new fractures (discontinuum). The potential location of fractures is inferred from observed conditions, including the evolution of deviatoric stresses, the plasticity state indicators of the numerical modeling program, and FS.

The finite difference program, **FLAC$^{3D}$**, divides each brick in the mesh into a series of tetrahedra for calculation. If shear failure or tensile failure (as defined by Equations 3-4 and 3-5, respectively) occurs in any of the tetrahedra at any point during the simulation,

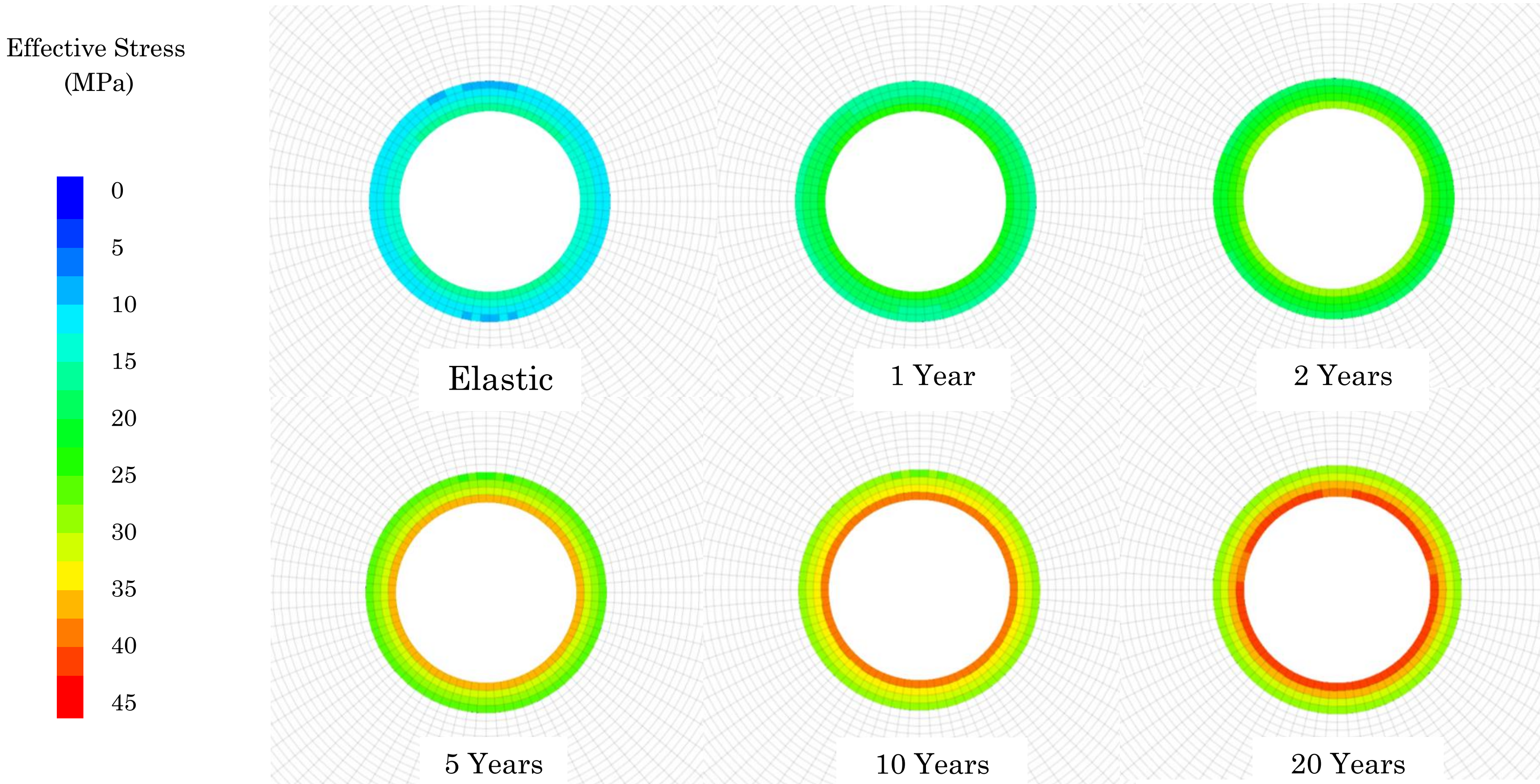


**Figure 5-12.** Deviatoric Stress in the 0.50-Meter-Thick Concrete Liner of the 500-Meter-Deep Repository at the Elastic Solution and After 5, 10, and 20 Years.

the plasticity state is recorded. The region where shear failure is recorded is considered to indicate the likely extent of the EDZ. The recorded shear failures do not occur at the same point in time and are of short duration, because stresses are redistributed as plastic strain occurs. Figure 5-15 displays the radial extent where shear failure is recorded during the simulation for the three repository depths. The limit of the recorded shear failure increases with increasing depth, which indicates that the extent of the EDZ will be greater for deeper repository depths. The radial extent where the FS is less than 1.2 also increases with increasing depth. The radial extent where the FS is less than 1.2 is slightly more extensive than the extent of the recorded shear failure shown in Figure 5-15.

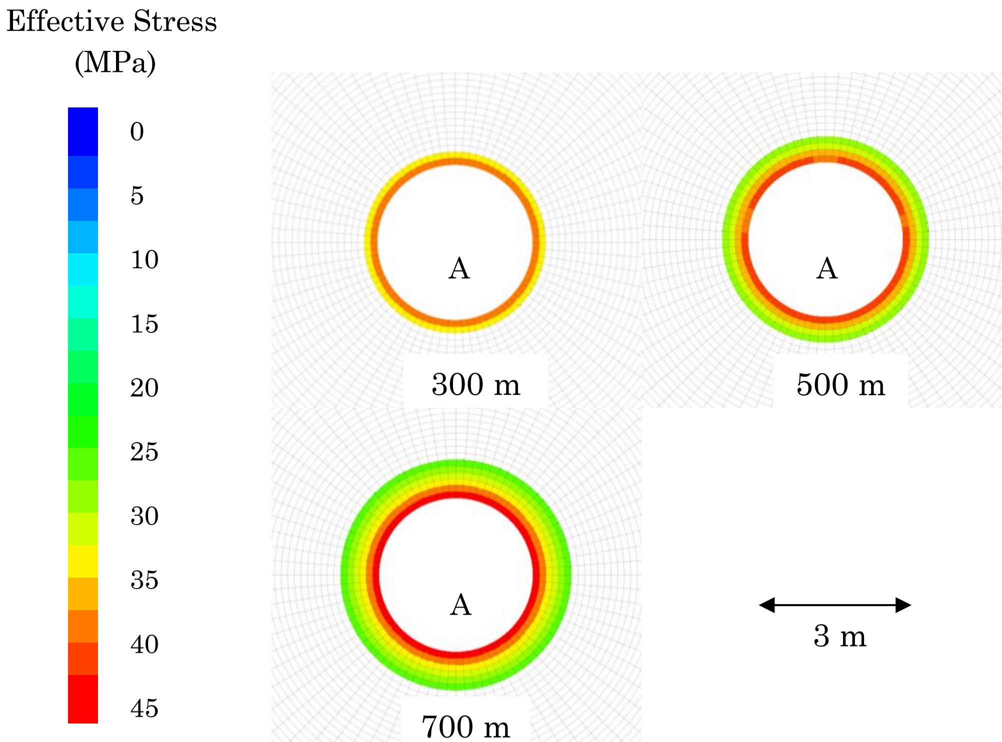


**Figure 5-13.** Deviatoric Stress in the Concrete Liner of the 300-Meter, 500-Meter, and 700-Meter Repository Depths at a Simulation Time of 20 Years. The liner thickness is 0.25 meter at the 300-meter repository depth, 0.50 meter at the 500-meter depth, and 0.75 meter at the 700-m depth.

Deviatoric stresses in the host rock are greatest immediately after the initial excavation (i.e., the elastic solution). Figure 5-16 displays the deviatoric stress in the Pierre Shale for the three repository depths after the initial excavation. Deviatoric stress in the concrete liner is omitted for clarity. The deviatoric stresses increase with increasing depth, which was expected. The region of lower deviatoric stress located directly outside of the concrete liner in the 500-m- and 700-m-deep repository is created by plastic failure and strain, which reduces deviatoric stress.

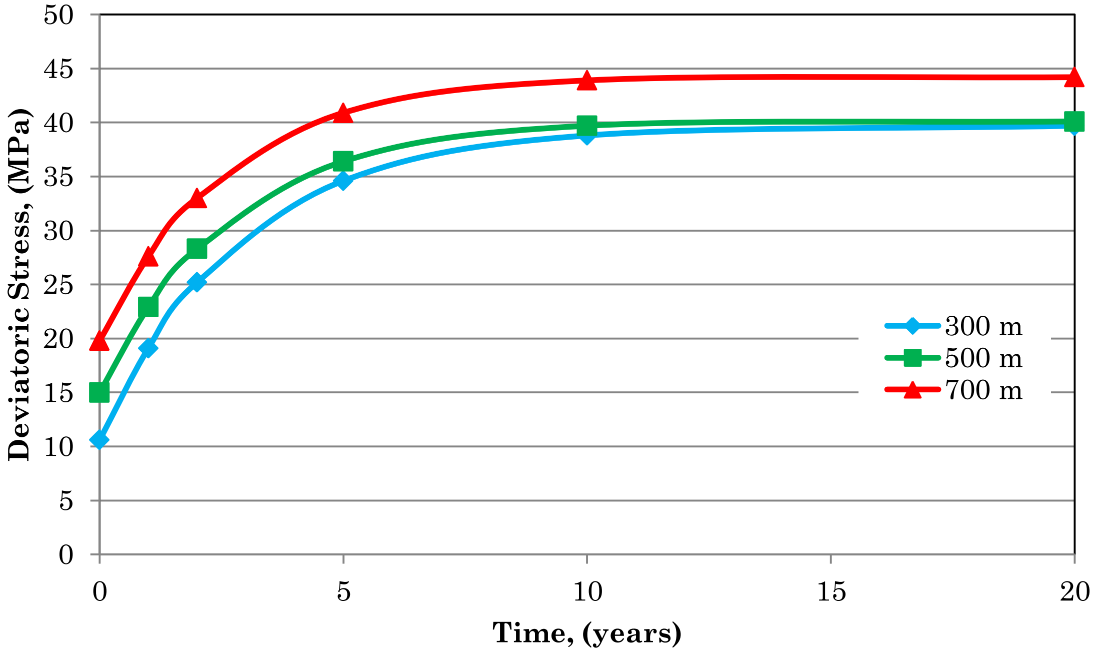


**Figure 5-14.** Deviatoric Stress at Point "A" on the Concrete Liner of the 300-Meter, 500-Meter, and 700-Meter Repository Depths at Various Simulation Times.

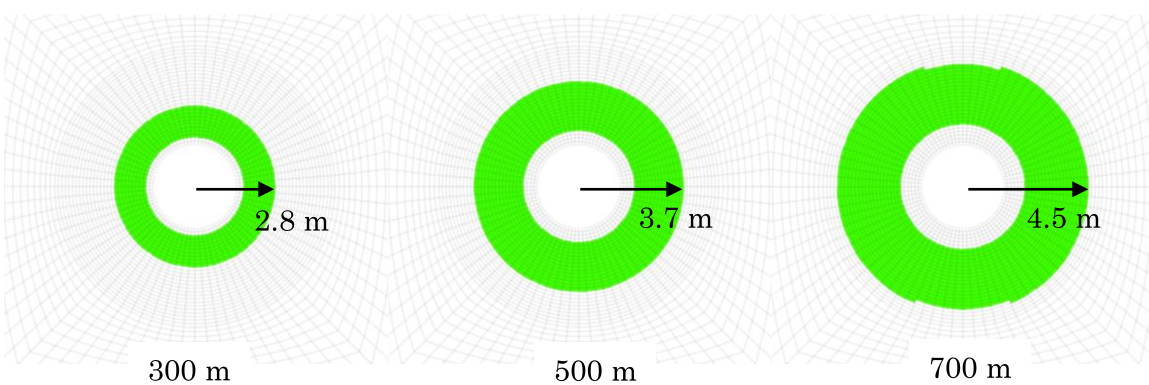


**Figure 5-15.** Radial Extent of Zone Tetrahedra Where Shear Failure Is Recorded at Repository Depths of 300, 500, and 700 Meters.

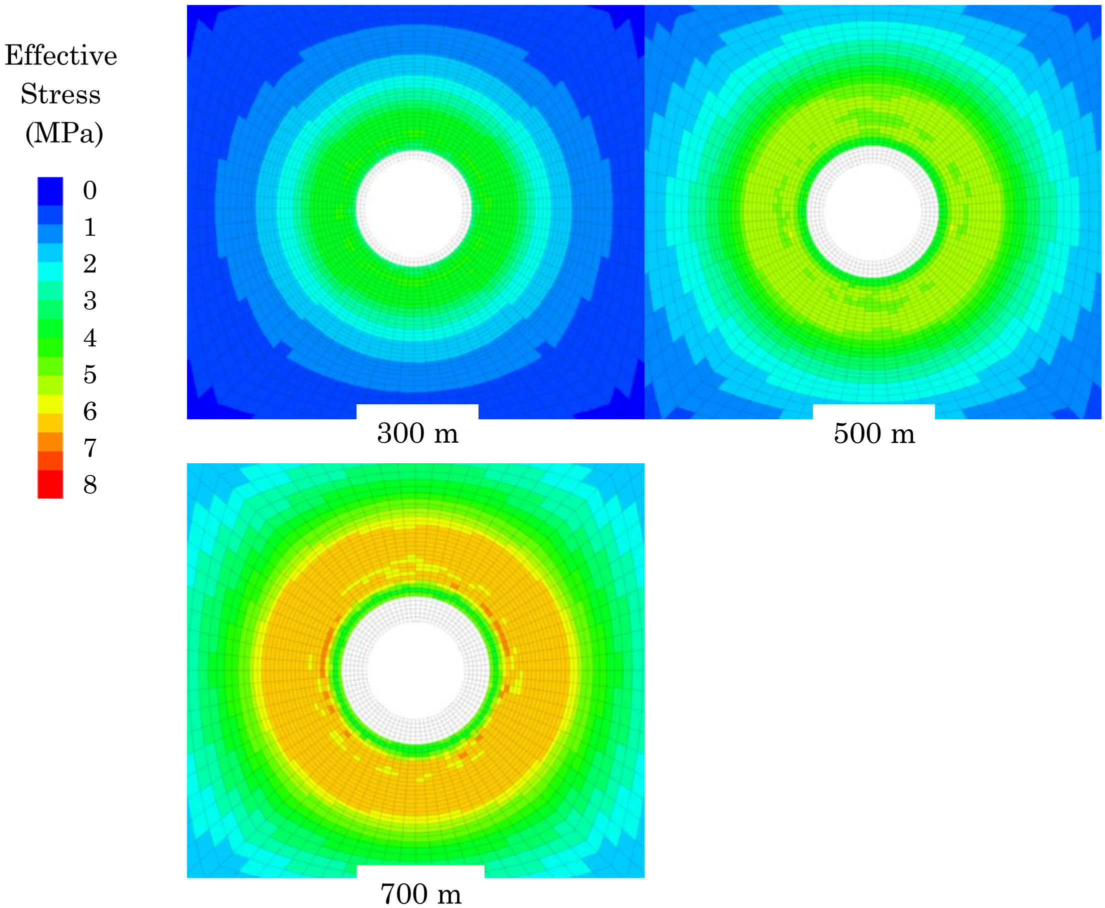


**Figure 5-16.** Deviatoric Stresses in the Pierre Shale of the 300-Meter, 500-Meter, and 700-Meter Repository Depths at the Elastic Solution.

The concrete liner used to support the excavations provides a structural barrier for the plastic and viscoplastic responses of the host rock. Plastic failure and creep allows the transfer of deviatoric stress from the Pierre Shale to the concrete liner. This process is displayed in Figure 5-17, which shows deviatoric stress in the Pierre Shale at various simulation times for the 700-m-deep repository. The decrease in deviatoric stress over time is displayed graphically in Figure 5-18 for all three repository depths. The trends observed in Figure 5-18 show an inverse relationship to the trends in Figure 5-14. The difference between the maximum deviatoric stresses for the different repository depths continues to decrease over time. After 20 years of simulation time, the maximum predicted deviatoric stress for the three repository depths is essentially the same, approximately 0.1 MPa.

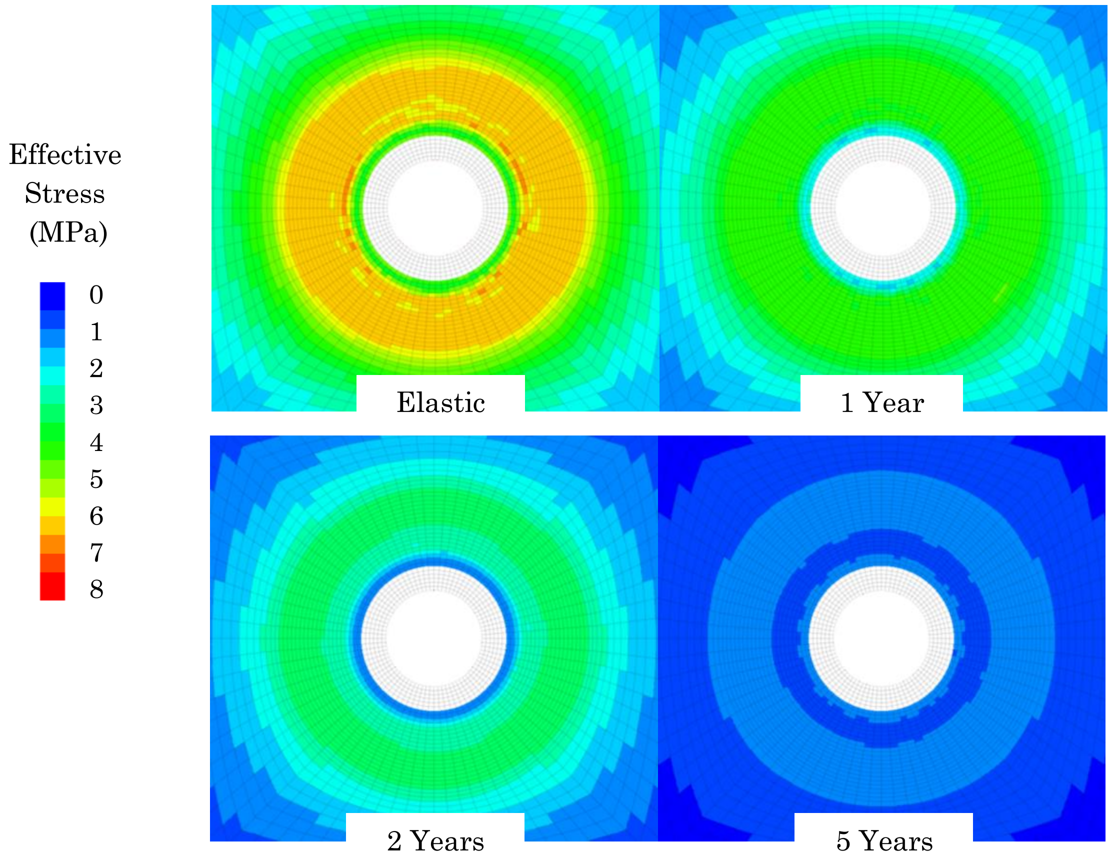


**Figure 5-17.** Deviatoric Stress in the Pierre Shale of the 700-Meter Repository Depth at the Elastic Solution and After 1, 2, and 5 Years.

In a uniform medium, fractures will develop perpendicular to the direction of the least compressive effective principal stress $(\sigma_3')$. In a circular excavation, the direction of $\sigma_3'$ is oriented radially out from the center of the circle. Fractures would, therefore, be expected to develop preferentially as concentric circles surrounding the excavation. The evolution of $\sigma_3'$ is predicted to follow a trend inverse to the deviatoric stresses shown in Figure 5-18; the minimum $\sigma_3'$ in the Pierre Shale is the lowest immediately after excavation and increases with time. After 20 years, the minimum $\sigma_3'$ in the Pierre Shale is predicted to be equal to the preexcavation $\sigma_3'$.

The maximum $\sigma_3'$ after 20 years is greater than the preexcavation $\sigma_3'$. The greater $\sigma_3'$ values in the Pierre Shale are located near the concrete liner. Strain from plastic failure and creep increases stress on the Pierre Shale near the relatively unyielding concrete liner. Figure 5-19 is a schematic that displays the stress changes between the initial excavation and 20 years. Figure 5-19 demonstrates that the increase in stress from plastic failure and creep is great enough that the directions of the most compressive and least compressive principal stresses are reversed from the elastic solution.

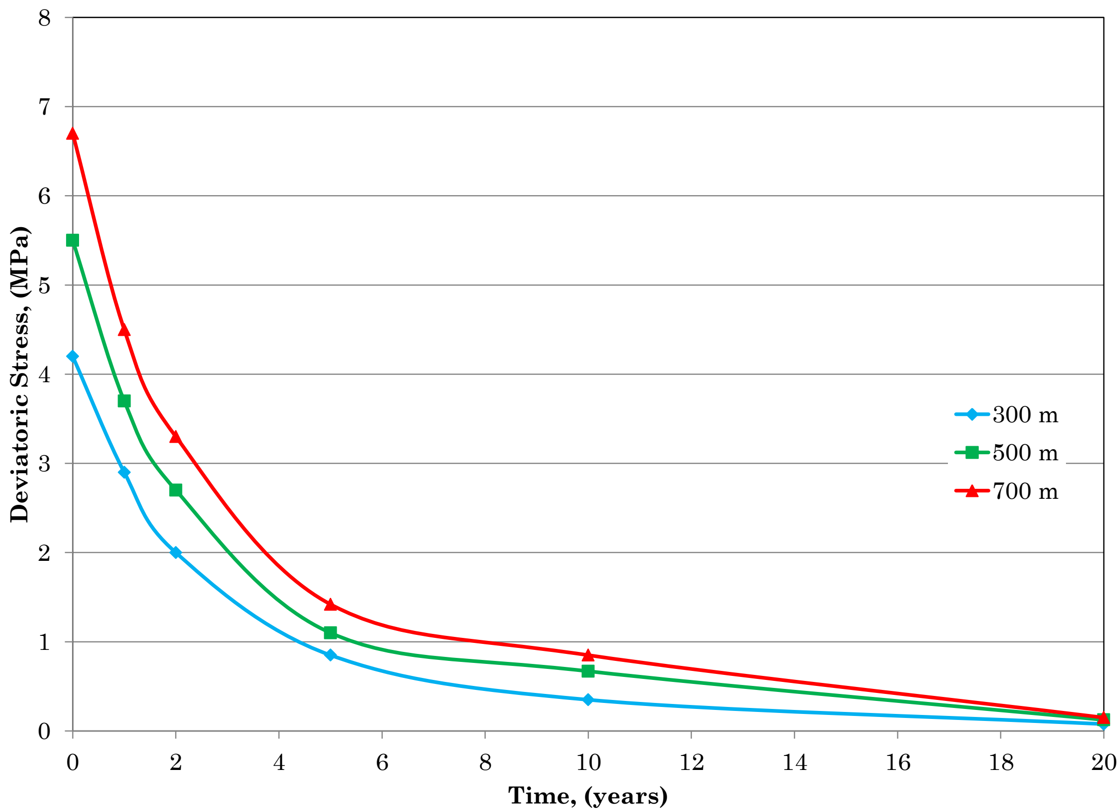


**Figure 5-18.** Maximum Deviatoric Stress in the Pierre Shale for the 300-Meter, 500-Meter, and 700-Meter Repository Depths at Various Simulation Times.

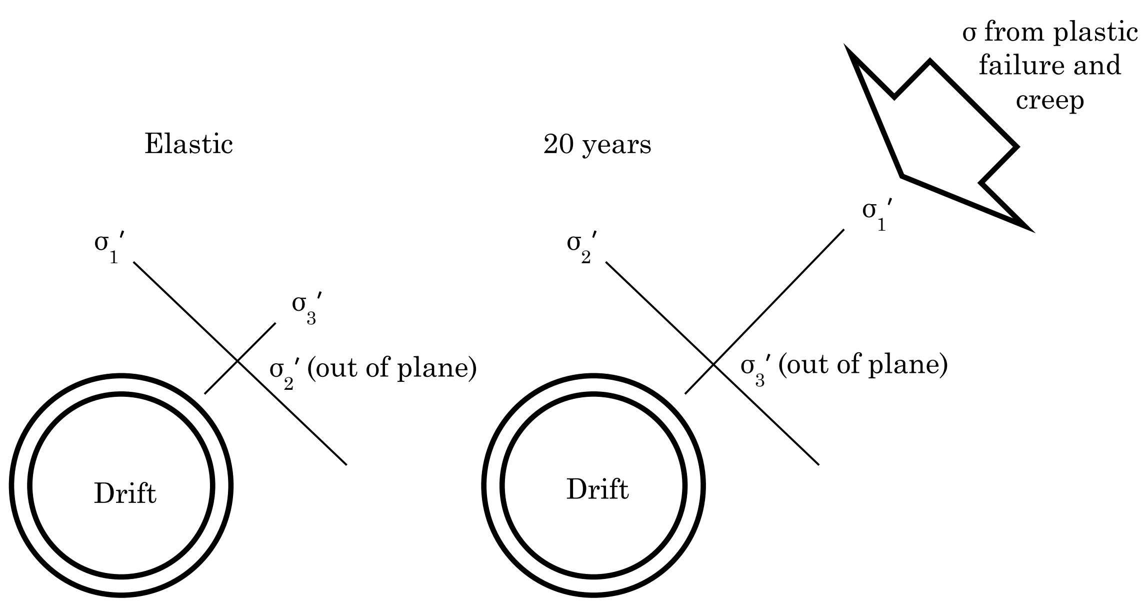


**Figure 5-19.** Schematic of Changes in a Representative Stress Rosette From the Elastic Solution to 20 Years (Length of Line Corresponds to Relative Magnitude).

As time increases, the deviatoric stress decreases and the effective mean stress increases in the Pierre Shale near the concrete liner. At 20 years of simulation time, the deviatoric stress and effective mean stress are at preexcavation magnitudes. The effective mean stress is greater than the preexcavation stress near the concrete liner. This behavior indicates that fractures created during the initial excavation will likely be closed by 20 years.

### 5.3.5 *Hydraulic Conductivity and Radionuclide Transport*

The hydraulic conductivity of the host rock around the drift depends on the repository depth and follows a relationship similar to the permeability in Equation 3-12. The predicted preexcavation hydraulic conductivity at the various repository depths and at 100 m above each repository depth is listed in Table 5-13. The relationship used to describe changes in the hydraulic conductivity is based on changes in the effective mean stress. The presence of the repository drift will change the effective mean stress, because the stress changes are related to the excavation and changes in pore pressure and are caused by dewatering. The numerical modeling predicts that the effective mean stress does not change appreciably after excavation; changes in the principal stresses are largely offset by changes in the pore pressure. The predicted hydraulic conductivity is, therefore, similar before and after excavation.

**Table 5-13. Preexcavation Hydraulic Conductivity (m/s) at Repository Depth and 100 Meters Above the Repository Depth**

| Hydraulic Conductivity at: | Repository Depth (m) | | |
|---|---|---|---|
| | **300** | **500** | **700** |
| Repository depth | $1.7 \times 10^{-12}$ | $6.0 \times 10^{-13}$ | $2.4 \times 10^{-13}$ |
| 100 m above repository depth | $2.8 \times 10^{-12}$ | $9.9 \times 10^{-13}$ | $3.7 \times 10^{-13}$ |

As discussed in Section 5.3.4, new fractures that developed in the EDZ are not explicitly included in the numerical model. The presence of these fractures would enhance the hydraulic conductivity in the EDZ that is not accounted for in the internal calculation. However, the findings in Section 5.3.4 indicate that any fractures that did develop in the EDZ have likely closed by 20 years. The preexcavation hydraulic conductivity values are, therefore, considered reasonable for further analyses.

The hydraulic conductivity and density calculated from the numerical models is used to estimate the transport of radionuclides at the various repository depths. Three of the most mobile radionuclides are selected for this preliminary analysis. Properties for $^{129}$I, $^{238}$U, and $^{135}$Cs are listed in Table 5-14. The distribution coefficients, which are used to account for adsorption of the radionuclides, can vary by orders-of-magnitude depending on the sorbing material and the chemistry (e.g., oxidizing versus reducing environments). The values selected for the analysis are on the low side of the values reported by Hansen et al. (2010).

**Table 5-14. Properties for Selected Radionuclides (Modified From Hansen et al., 2010)**

| Property | Isotope | | |
|---|---|---|---|
| | $^{129}$I | $^{238}$U | $^{135}$Cs |
| Apparent diffusion coefficient, $D_a$ (m$^2$/s) | $1.0 \times 10^{-10}$ | $1.0 \times 10^{-11}$ | $1.0 \times 10^{-11}$ |
| Effective diffusion coefficient, $D_e$ (m$^2$/s) | $5.0 \times 10^{-12}$ | 0.45 | 0.22 |
| Decay constant, $\lambda\left(\text{yr}^{-1}\right)$ | $4.4 \times 10^{-8}$ | $1.6 \times 10^{-10}$ | $3.0 \times 10^{-7}$ |
| Distribution coefficient, $k_d$ (mL/g) | 0 | 20 | 10 |

A distance of 100 m above the repository is selected as a location for comparison. At this location, the percent of the initial radionuclide concentration is calculated at various times for the three repository depths. The predicted percent of the initial radionuclide concentration at a distance of 100 m above the repository is the same for all three of the repository depths and is shown in Figure 5-20. This finding indicates that the hydraulic conductivity is low enough at all depths, and transport is controlled by diffusion and sorbtion.

Radionuclide transport through the intact rock is compared with transport through a continuous fracture with an aperture of 10 $\mu$m. Hydraulic conductivity in the fracture is estimated through the following relationship:

$$K_{fr}^{H} = \frac{b^2}{12\mu} \tag{5-21}$$

where:

$K_{fr}^{H}$ = fracture hydraulic conductivity

$b$ = fracture aperture

$\mu$ = dynamic viscocity, $10^{-3}$ Pa $\cdot$ s.

A fracture aperture of 10 µm predicts a hydraulic conductivity of $8.3 \times 10^{-9}$ m/s. The transport calculation is performed based on the fracture hydraulic conductivity and the effective porosity and tortuosity set to unity. The calculated results are displayed in Figure 5-21, which shows that the sorping radionuclides ($^{238}$U and $^{135}$Cs) are not affected by the increased hydraulic conductivity. The nonsorping radionuclide ($^{129}$I) shows a significant increase in transport time, indicating the dominant process is advection instead of diffusion. The $^{129}$I concentration in the fracture-controlled transport is 99 percent of the initial concentration after 6,000 years, and the $^{129}$I concentration reaches 46 percent of the initial concentration after 1 million years when transport is through intact rock.

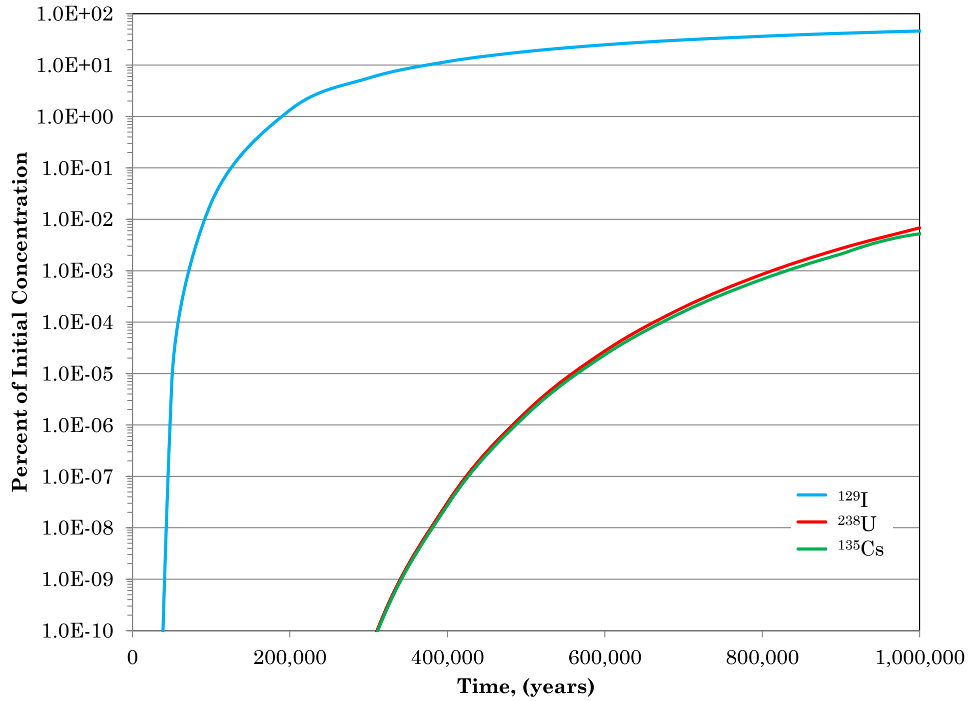


**Figure 5-20.** Percent of the Initial Concentration of Selected Radionuclides at 100 m Above the Repository at Various Times (Transport Through Intact Pierre Shale).

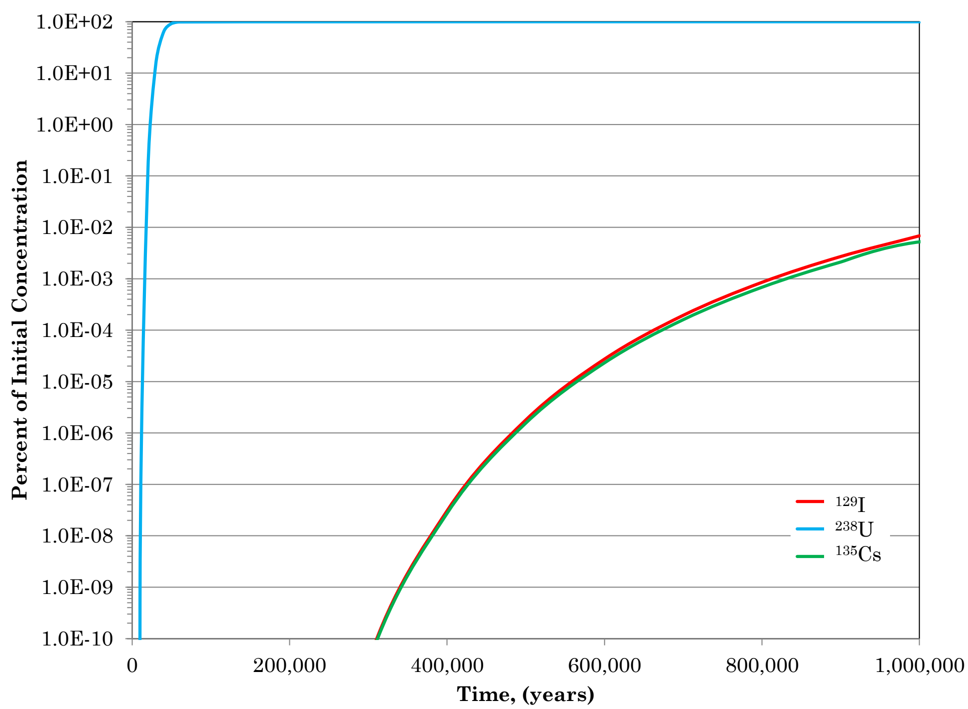


**Figure 5-21.** Percent of the Initial Concentration of Selected Radionuclides at 100 m Above the Repository at Various Times (Transport Through 10 μm Fracture in Pierre Shale).

## 5.4 Conclusions From Modeling

The purpose of this study is to perform a preliminary assessment of the Pierre Shale as a potential nuclear waste repository and to assess potential benefits and limitations of various repository depths. The Pierre Shale was selected because it is a well-defined geological unit with many physical properties that are dissimilar to those units in existing European URLs. The following text provides an evaluation of the Pierre Shale in comparison to other geological media and shale units.

Clays and shales have a lower thermal conductivity than many other geological media. Available information indicates that the Pierre Shale has a lower thermal conductivity than European URLs constructed in clay and shale. A 100°C limit is a common design requirement for potential repositories in shale. The consequence of the low thermal conductivity and the 100°C temperature limit is a low density of waste packages within the repository. The lateral extent of a repository in the Pierre Shale will be much greater than other geological media with a higher thermal conductivity and higher temperature limit (e.g., salt).

The Pierre Shale has low strength properties and the numerical modeling results indicate collapse in unsupported excavations at or below 300 m. Significant ground support is expected to be necessary to safely maintain excavations in the Pierre Shale. A current study evaluated a ground-support program similar to the program used in the Mol Facility in Belgium. This approach uses a tunnel-boring machine with shields to support the excavation while the concrete liner is poured. Other ground-support options could also be considered (e.g., forepoles). The high-level of effort necessary to support the excavation may be considered a limitation, because it will likely result in a slower rate of advancement than using traditional hard-rock mining methods (or the use of a tunnel-boring machine in self-supporting rock).

The thickness of the concrete liner necessary to prevent shear failure needs to be increased as the depth increases. The numerical modeling predicts a concrete liner of 0.25 m is necessary at 300 m, and the liner thickness must be increased 0.125 m per every 100 m of increasing depth.

The extent of the EDZ is predicted to increase with increasing depth. The extent of the EDZ was inferred from the presence of recorded shear failure in the numerical model. This is considered to be a minimum extent of the EDZ. The numerical modeling predicts that the EDZ occupies a radius of at least 2.8 m from the centerline of a 3 m diameter excavation at a depth of 300 m. The radial extent of the EDZ is predicted to increase at least 0.43 m per every 100 m of increasing depth.

Viscoplastic behavior is predicted to transfer deviatoric stress from the Pierre Shale to the concrete liner. Deviatoric stress in the Pierre Shale decreases with time, and the deviatoric stress in the concrete liner increases with time. At 20 years of simulation time, the deviatoric stress in the Pierre Shale is predicted to be near preexcavation levels (approximately 0.1 MPa) at all repository depths. At 20 years of simulation time, effective mean stress is predicted to be at or above preexcavation levels at all repository depths. This observation indicates that any fractures developed from the EDZ have likely closed at 20 years.

The findings indicate that the hydraulic conductivity of the intact Pierre Shale is low enough that radionuclide transport is controlled by diffusion, regardless of the repository depth. The findings also illustrate the importance of understanding advective transport through fractures and absorption. The time required for transport of nonsorbing radionuclides through a fracture's aperture of only 10 μm is predicted to be orders-of-magnitude faster than through intact Pierre Shale.

In summary, the results of this study indicate the Pierre Shale has many characteristics comparable to other shale units considered as potential repository sites. The cost associated with a lower-density waste package placement and high ground-support effort must be weighed against benefits such as diffusion-controlled transport and deformation characteristics that cause the Pierre Shale to strain and close fractures more quickly and effectively than other geological units (or more indurated shale). The knowledge gaps identified through this project are compatible with knowledge gaps identified in other studies.

# 6. Path for a U.S. Shale-Hosted Laboratory

The justification, design, and implementation of a URL in the U.S. in shale must meet a number of major and minor milestones. The first major milestone is the general justification of a need for a U.S. URL, and depends on current knowledge gaps and the ability to fill those knowledge gaps through available means. If available means are considered insufficient and a U.S. URL in shale is considered justified, the second major milestone consists of general siting identification. This effort will define broad areas with qualifying conditions and omit areas with disqualifying conditions. Once broad areas have been defined, the effort of the third major milestone is more specifically classifying and ranking favorable and potentially unfavorable conditions. This more detailed classification includes physical properties, the physical system, and construction considerations. A broad overview of these three major milestones is provided in this section.

## 6.1 Major Milestone 1: Justification for a U.S. Underground Research Laboratory in Shale

The first major milestone of a U.S. URL in shale is identifying a need for such a laboratory. If currently available resources are capable of adequately characterizing the desired attributes, then the cost associated with designing and constructing a new URL is likely unjustified. Considering the following questions will aid in the assessment of a need for a U.S. URL in shale:

*Do Important Knowledge Gaps Exist?*

A point may be reached where the processes controlling the behavior of shale are sufficiently understood that large-scale experiments in URL do not significantly contribute to advancing knowledge. However, the current understanding of important behaviors and mechanisms of shales is insufficient in many regards. Important knowledge gaps were defined in Section 4.0. For fine-grained geological units, the most important knowledge gaps that need to be filled are related to developing and sealing fractures, the transport of radionuclides, and developing coupled THMC constitutive models to describe behavior.

*Are Existing European URLs Sufficient?*

Three existing URLs are currently operating, as described in Chapter 4.0. The large-scale tests performed in these facilities have greatly advanced the understanding of complex, coupled behaviors. The benefits of the collaborative opportunities that European URLs offer should not be underestimated. However, the variability of physical characteristics of fine-grained geological units is considerable. The variety of geological environments and mineralogical compositions demonstrates the need for specific information from additional sites. Limitations still exist regarding the transferability of concepts between dissimilar materials and physical systems. The additional characterization of dissimilar units (beyond the units that host European URLs) is necessary to validate the transferability of certain concepts. Cooperating with the existing European URLs may not accurately reflect the important compositional effects of typical

U.S. shales. One of the more important factors regarding U.S. Midcontinent shales, for instance, may involve their bentonite content.

Ownership and access issues also deserve consideration. The large-scale tests performed in European URLs will be driven by the types of tests approved by the entities that own and manage these facilities. A URL owned and operated by the U.S. will have the control to direct which experiments are performed. However, good cooperation appears to exist between the U.S. and the owners and operators of European URLs.

*Are Small-Scale Laboratory Experiments and Numerical Modeling Sufficient?*

The transferability of concepts cannot be confidently made until the database of tested units is expanded. The detailed and systematic laboratory characterization of multiple, disparate fine-grained geological units will expand the database of information. A larger amount of samples will better allow empirical relationships and constitutive models to be based on the most applicable physical properties.

Although laboratory and bench scale studies are crucial to understanding the behaviors of shales from mechanical and geochemical standpoints, these types of investigations may be difficult to scale up to larger blocks of material. Acquiring access in situ reduces the effects of disturbance caused by the sample acquisition process; however, the existence of an underground laboratory is essential in understanding the development of a damaged zone in the vicinity of free surfaces in the excavations. The effect of pressure on the ductility of shales for both disturbed and undisturbed rock is an important factor that needs to be understood to assess its influence on sealing excavations, the modification of thermal properties, and the promotion of permeability pathways. These types of studies are difficult, if not impossible, to accomplish at the surface by only using sufficiently large volumes of rock. Modeling the effects is cost effective, but those computer models require calibration, which can only be done with actual in situ rock samples. The benefit of a URL is to validate the developed concepts in complex, large-scale environments. This validation is necessary to create confidence in the proposed methods. Validating concepts across dissimilar conditions increases confidence in the concepts.

The ability to demonstrate the capabilities of a shale system is important to ensure the necessary confidence from sufficient knowledge to move forward. It is unlikely that a full-sized facility could or should be constructed without substantial preliminary work to constrain the range of issues that might be experienced. The construction of a URL is a natural step in developing a repository, and finding committed sources of generous funding without this experience is unlikely.

Milestone 1 is completed when a thorough evaluation of these and other considerations have been performed. The outcome of Milestone 1 will be one of the following determinations:

(a) a U.S. URL in shale is justified

(b) a U.S. URL is unwarranted

(c) additional information is required to make an informed judgment.

If the results of Milestone 1 find that a U.S. URL is justified, characterizing further siting information should be initiated. The continuation of this process does not guarantee that a U.S. URL will be constructed; it only documents the justification for a potential U.S. URL in shale. More detailed investigations performed as part of subsequent milestones may determine that construction is cost-prohibitive.

The Milestone 1 findings may indicate that there is not enough information to make an informed judgment regarding the necessity of a U.S. URL in shale. For example, limits on the current understanding of behaviors may not be able to conclusively assess if the combination of European URLs and small-scale testing on a diversity of specimens can fill existing knowledge gaps. In this situation, additional investigations would be needed to define the limits of the existing knowledge gaps. The results of these future investigations will help define the necessity for a new U.S. URL in shale.

## 6.2 Major Milestone 2: General Siting

If the broad justification to investigate the feasibility of a U.S. URL in shale has been established, general siting efforts can be performed to attempt to narrow the search area. The initial general siting will consist of identifying locations with qualifying conditions and omitting sites with disqualifying conditions. A discussion of likely qualifying and disqualifying conditions is provided in the following text.

### 6.2.1 *Qualifying Conditions*

At the most basic level, any potential URL in shale should have conditions that are reasonably similar to conditions that would exist in a repository. If conditions in a URL are not similar to an actual repository location (e.g., the URL is very shallow), the transfer of concepts developed in the URL to a repository may be difficult to justify. The benefit of shale as a repository for nuclear waste rests in its ability to limit the transport of radionuclide to acceptable doses. Radionuclide transport in shale is limited by low hydraulic conductivity, self-sealing of fractures, and favorable adsorption conditions. The majority of fine-grained units will likely meet these broad, quantitative requirements.

### 6.2.2 *Potential Disqualifying Factors*

A number of factors related to the natural system that could potentially disqualify a location as a potential repository site in shale have been identified (Fossum et al., 1985), and many of these factors are applicable to locating a URL. Potential disqualifying factors are those that are not consistent with the benefits of fine-grained geological units and could limit transferability to actual repository conditions. Potential disqualifying factors identified for a URL in a fine-grained geological unit include the following:

- **Hydrology:** The hydraulic conductivity should be low enough that transport in the intact formation is anticipated to be controlled by diffusion instead of advection. This will allow large-scale experiments to focus on the transport methods that are expected to dominate in an actual repository. Sites with a high hydraulic gradient may also be disqualified, because the corresponding increase in transport time could limit transferability to an actual repository.

- **Depth:** The minimum depth of a URL must be deep enough that preexisting structural fractures have been sealed. The depth where preexisting fractures have sealed will depend on the physical properties of the unit and components of the physical system, such as the stress state. Assessing the effects of weathering on the shale is important, because economic tradeoffs between depth are required for a repository, and the need to avoid weathering effects should be determined. It is likely that, in many instances, the geochemical and geomechanical behaviors of shale beneath the weathered horizon may be vastly different from those above. Maximum depths will likely be limited by construction costs and, possibly, decreases in ductile behavior associated with increasing induration.
- **Seismicity:** The URL should not be located in a region where seismic activity could threaten its use. The URL will need to include design considerations that take into account the seismicity of the region where it is located.
- **Structure:** The URL should be located in an area with few existing geological structural features (e.g., faults and fractures) that may limit the effectiveness of the large-scale tests and their interpretations. Experiments from the Mont Terri URL suggest that preexisting fractures created through tectonic activity have sealed. However, an understanding of the self-sealing behavior of fine-grained units is among the current knowledge gaps; transferability of the sealing behavior at Mont Terri to other sites may be premature.
- **Mineral and water resources:** The URL should avoid areas where its presence will limit the future exploitation of mineral and water resources. Regions containing existing boreholes related to mineral and water resources should also be avoided, because these penetrations may have an effect on the physical system.
- **Ground support:** The URL must maintain the safety of personnel during construction and operation with reasonably available technology.
- **Extent:** The available extent of a proposed URL must be adequate to perform proposed large-scale tests in relative isolation and to accommodate growth.

### 6.2.3 *Implementation*

The siting effort will likely rely heavily on the Geographic Information Systems (GIS) mapping being performed by Los Alamos National Laboratories (LANL). LANL is in the process of defining the extents, thicknesses, and depths of major shale units in the U.S. The capabilities of GIS can be used to eliminate those portions of the major shale units that fall within one or more of the disqualifying factors. A few examples of the application of the GIS siting include the following:

- Eliminates those parts of shale formations that are too deep or too shallow
- Buffers from major oil and gas fields
- Buffers from major structural features or areas of high seismicity.

The Milestone 2 siting exercise is intended to reduce the volume of potential sites so that a more detailed characterization and ranking can be performed as part of Milestone 3.

## 6.3 Major Milestone 3: Classification and Ranking

Designing and planning a facility with the size and complexity of a URL in support of a program in shale is a significant undertaking. A broad classification of qualifying and disqualifying factors will be defined as part of Milestone 2. Milestone 3 is concerned with a more detailed classification of the requirements for the facility, which are defined as favorable and potentially adverse conditions. For example, a number of physical characteristics and site conditions would be expected to limit the transport of radionuclides, including low hydraulic conductivity, self-sealing behavior, and radionuclide adsorption. Generally speaking, hydraulic conductivity is expected to decrease as follows:

- Clay content increases
- Porosity decreases
- Transmissive layers (e.g., sandstone beds) are avoided
- The hydraulic gradient decreases
- The in situ fracture density decreases.

The effectiveness of the self-sealing behavior of shale is generally expected to increase as follows:

- Clay content increases
- The degree of induration decreases
- The percentage of swelling clays (e.g., smectite) increases
- Normal stress or mean stress increases

The adsorption capabilities of shale are expected to be more favorable when:

- The cation exchange capacity increases
- Reducing conditions are encountered.

These properties would be included in the classification and ranking of Milestone 3. Once a full list of potentially favorable and adverse conditions have been acquired, a weighted ranking can be developed to compare different sites. Because the present effort is very preliminary, the scope of this section is limited to the functional requirements identified by researchers currently active in the U.S. Requirements based upon polling currently involved U.S. researchers are listed in Table 6-1. The issue is posed as a question and the requirement is either a quantified value or an indication whether or not a requirement exists. The priority rating is based on a preliminary assessment regarding the importance of the requirement placed on it by researchers in the polling. Summarizing the directions requested in Table 6-1 emphasizes the desire for a significant depth requirement, some variability in material properties, and the appeal of a material that would actually be used as a host medium. In general, the polling seemed to indicate that a URL with a vertical access would be acceptable, but horizontal access was available, such as a side gallery from a tunnel, this would also be suitable for many experiments. The probable lower cost of such a horizontal opportunity is attractive, and opportunities for colocation should continue to be sought. Although horizontal access is greatly preferred over vertical access through some sort of shaft because it is convenient and cost effective, this type of access has not been identified yet and will continue to be sought.

Overall, the results of accumulating the requirements for the shale URL are not unusual because they parallel many of the research requirements for other geologic media, including the well-studied case of salt. Figure 6-1 shows the generalized path that the URL process would be expected to take. Timelines are not shown on the diagram because the nature of the study is preliminary, but the overall process would be expected to take between 5 and 10 years.

**Table 6-1. Requirement Matrix: 1–Highest Priority (Page 1 of 2)**

| Issue | Requirement | Reason | Priority |
|---|---|---|---|
| Depth Range – Shallowest/ Deepest | Probably in the range of > several hundred meters | The URL should be in the range of a likely repository, shallower than 50 m would put it in the weathered zone; whereas, a repository is unlikely to be developed deeper than 500 m because of cost | 1 |
| Requirement to be below the water table | Yes | A repository in clay/shale is likely to be below water table so the URL should be similarly located | 1 |
| Requirement for uniformity of the mechanical properties of the shale host material | Possibly | Should be representative of suitable clay/shale environments for hosting a repository, including natural features commonly found (e.g., bedding and faults) | 1 |
| Requirement for the minimum thickness of shales | ~ 100 m | This thickness is similar to some of the European URLs and would probably be required for a repository developed in shale | 1 |
| Determine which important clay mineralogies should be sought | Sorbing and/or swelling clays. | In situ geochemical tests are an important part of the URL work | 1 |
| Ranges of clay mineral content to be considered | Representative of likely clay/shale compositions for a repository | Other international sites considered are either claystones or muds; a URL that has at least 1/3 clay mineral fraction would be appropriate | 1 |
| Preferred type of access for a URL(e.g., horizontal/vertical | Horizontal access preferred | Horizontal access is logistically much easier, but vertical access is acceptable | 2 |
| Multiple depth requirement | Possibly | Both overconsolidated units and normally consolidated units would be desirable | 2 |
| Requirement for a dedicated “walk-in” laboratory | Yes | Required for heater tests and examining EDZ | 2 |
| Background values of U, Th, and K content important | Should represent of suitable clay/shale environments for hosting a repository | The values could be useful for studies of evolution and transport of these elements within the URL formation; background values of the shale should not be high enough to interfere with migration/absorption studies | 2 |

**Table 6-1. Requirement Matrix: 1–Highest Priority (Page 2 of 2)**

| Issue | Requirement | Reason | Priority |
|---|---|---|---|
| Variation in geochemical properties | Should be representative of suitable clay/shale environments for hosting a repository | Pore water chemical conditions (e.g., salinity, oxygen fugacity) could be important. | 2 |
| Variations in induration | Yes | Although a shale-hosted repository will probably be sited in a massive unit with similar mechanical properties, variations in mechanical properties caused by differences in induration and mineral content are likely | 2 |
| Requirement for variability or nonvariability of stratigraphy (i.e., massive versus thinly layered) | Yes | Should not be too thinly layered | 2 |
| Requirement for variations in the mechanical properties of the host rock | No | Should represent suitable clay/shale environments for hosting a repository | 3 |
| Importance of easy access to airport, labor force, transportation | Medium importance | These factors may have a significant impact on costs for a URL | 3 |
| Identifiable fault/discontinuities nearby | Yes | One of the favorable factors for shale-hosted repositories is the ability of the shale to “heal” fractures and faults; transmissivities of natural discontinuities will probably be studied | 3 |
| Arrays of boreholes as opposed to a “walk-in” laboratory | No | Boreholes are useful for characterizing and understanding the natural formation | 4 |

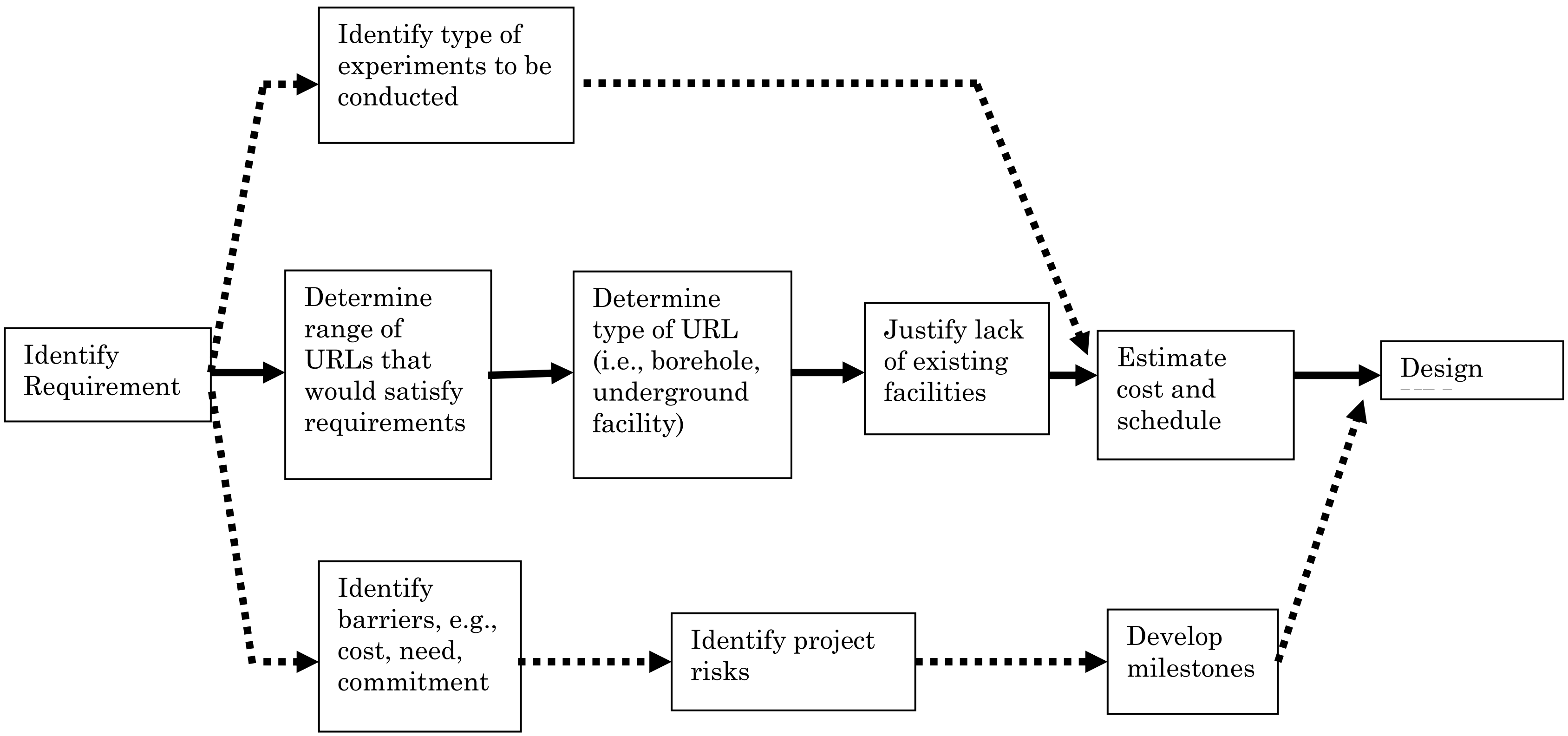


**Figure 6-1.** Critical Path for an Underground Research Laboratory.

THIS PAGE INTENTIONALLY LEFT BLANK

# 7. Conclusions and Recommendations

The process of analyzing the justification, design, and construction of a URL is a necessary step if shale and other fine-grained sedimentary rocks are to be considered as viable waste storage options. European URLs are successfully conducting experiments that provide valuable information. However, knowledge gaps still exist, including understanding the transferability of concepts between shale units with dissimilar properties. The additional investigation into the feasibility of a U.S. shale-hosted URL will aid in filling existing knowledge gaps and is a necessary step in the potential construction of a repository.

To compare results between facilities and experiments, it is important to have a clear definition of the terms for the rock types being used. Descriptions of the various classification schemes for fine-grained sedimentary rocks has been presented in this report. This discussion emphasizes the differences between the classification schemes and also the differences between similar terms that are used for differing purposes, such as geologic descriptions compared to engineering applications. Also apparent is the wide range of materials and material properties that fall under the umbrella term of "shale."

A detailed description of the physical properties that are relevant to nuclear waste disposal has, in recent years, been focused on geological formations that host European URLs. However, the physical properties of these units represent only a small portion of geological materials that classify as shale or fine-grained units. The literature review and preliminary numerical modeling performed in this study accentuated the existing knowledge gaps that include the following:

- Understanding the development and sealing of fractures
- Physical factors affecting radionuclide sorption and solubility
- Relationships describing coupled THMC processes
- Transferability of concepts between dissimilar materials.

These major existing knowledge gaps provide justification for the further investigation into the potential for a U.S.-hosted URL: it is not known if a U.S. URL is warranted or unwarranted because additional information is required to make an informed decision. The detailed characterization of additional shale units is necessary to determine if concepts developed at European URLs are transferable to geological units with dissimilar properties.

This detailed characterization of additional units requires the use of uncommon or novel laboratory tests that can be used to help fill existing knowledge gaps. For example, little work has been done on characterizing creep of shale, and no information is available on the specific viscoplastic behavior of most units. Low-to-moderately indurated units (e.g., the Pierre Shale) may creep faster than other more indurated fine-grained units (e.g., Callovo-Oxfordian and Opalinus Formations). Furthermore, the creep of highly indurated units may be very slow or nonexistent, which would eliminate the benefit of fracture sealing. Creep tests at a variety of different stress differences, and eventually, temperatures, are needed to better understand the viscoplastic behavior of a variety of units. The results of this classification may prove that new or different constitutive models are needed to accurately describe the time-dependent behavior of shale.

Another example of laboratory testing that would help fill existing knowledge gaps is related to hydraulic conductivity of "sealed" fractures. Laboratory tests that measure the hydraulic conductivity of manufactured fractures at different mean stresses could be compared with the hydraulic conductivity results of intact samples. These tests would be used to determine if a minimum mean stress is required to eliminate enhanced conductivity in the fracture. A comparison of these tests on different fine-grained units could indicate which material properties are most important for efficient fracture sealing. Laboratory testing could also be used to characterize the most important properties related to radionuclide transport, which often must be estimated because information is lacking.

The accuracy of the laboratory characterization depends on the quality of the sample used. Because of its mineralogical composition, the mechanical behavior of shale tends to change, if steps are not taken to preserve the sample. Acquiring core from selected U.S. shale units would provide a suite of samples that could be used for detailed characterization by numerous researchers in the Used Fuel Disposition (UFD) program.

Once a suitable array of shale units has been adequately classified, the coupled THMC concepts developed from large-scale tests in European URLs can be used to attempt to model the observed behavior of different shale units. This analysis will evaluate the transferability of these concepts. The effectiveness of transferability will be a major evaluation tool in the necessity of the future development of a U.S. URL.

# 8. Bibliography

**Agence nationale pour la gestion des dechets radio (ANDRA), 2005a.** *Dossier 2005 Argile Tome, Phenomenological Evolution of a Geological Repository,* ANDRA, Chatenay-Malabry, France.

**Agence nationale pour la gestion des dechets radio (ANDRA), 2005b.** *Dossier 2005 Argile Architecture and Management of a Geological Repository*, ANDRA, Chatenay-Malabry, France.

**Al-Bazali, T., J. Zhang, M. E. Chenevert, and M. M. Sharma, 2008.** "Experimental and Numerical Study on the Impact of Strain Rate on Failure Characteristics of Shales," *Journal of Petroleum Science and* Engineering, Vol. 60, No. 3–4, pp. 194–204.

**Argonne National Laboratory, 2011.** *Used Fuel Disposition Campaign Disposal Research and Development Roadmap,* FCR&D-USED-2011-000065, Argonne National Laboratory, Lemont, IL.

**ASTM, 1998.** *Standard Practice for Classification of Soils for Engineering Purposes (Unified Soil Classification System)*, D 2487-98, Annual Book of ASTM Standards, Vol. 14, pp. 238–248.

**Bastiaens, W. and M. Demarche, 2003.** "The Extension of the URF HADES: Realization and Observations,: *Waste Management (WM)'03 Conference,* February 23–27, Tucson, AZ.

**Birkholzer, J., H. Liu, C. Tsang, S. Painter, A. B. Kersting, and M. Simpson, 2011.** *Research & Development Plan for the Used Fuel Disposal Campaign Natural Systems Evaluation and Tool Development,* Fuel Cycle Research & Development.

**Blue Ribbon Commission on America's Nuclear Future, 2011.** *Blue Ribbon Commission on America's Nuclear Future Draft Report to the Secretary of Energy*, U.S. Department of Energy, Washington, DC.

**Bock, H., B. Dehandschutter, C. D. Martin, M. Mazurek, A. de Haller, F. Skoczylas, and C. Davy, 2010.** *Self-Sealing of Fractures in Argillaceous Formations in the Context of Geological Disposal of Radioactive Waste,* NEA No. 6184, Nuclear Energy Agency Organization for Economic Co-Operation and Development, Paris, France.

**Boggs, J. S., 1995.** *Principles of Sedimentology and Stratigraphy,* Prentice Hall, Inc., Upper Saddle River, NJ.

**Boisson, J. Y., 2005.** *Clay Club Catalogue of Characteristics of Argillaceous Rocks,* NEA No. 4436, Nuclear Energy Agency, Organisation for Economic Co-Operation and Development, Paris, France.

**Botts, M. E., 1986.** *The Effects of Slaking on the Behavior of Clay Shales,* University of Colorado, Boulder, CO.

**Delage, P., Y. Cui, and A. Tang, A., 2010.** "Clays in Radioactive Waste Disposal," *Journal of Rock Mechanics and Geotechnical Engineering*, Vol. 2, No. 2, pp. 111–123.

**Delecaut, G., 2004.** *The Geochemical Behaviour of Uranium in the Boom Clay*, Ph.D. Thesis, Université Catholique de Louvain, Les Département de Géologie et de Géographie, Louvain-La-Neuve, Belgium.

**Folk, R., 1974.** *The Petrology of Sedimentary Rocks*, Hemphill Publishing Co., Austin, TX.

**Fossum, A., M. Loken, M., T. Vogt, and K. Johnson, 1985.** *Methodology for Implementing a National Survey of Shales*, ORNL-Sub/85-097343/2, Oak Ridge National Laboratory, Oak Ridge, TN.

**Fracture Systems Ltd., 2011.** *Excavation Damaged Zone Assesment.* NWMO DGR-TR-2011-21, prepared by Fracture Systems, Ltd., St. Ives, United Kingdom.

**Freeze, R. and J. Cherry, 1979.** *Groundwater*, Prentice Hall, Inc., Upper Saddle River, NJ.

**Gilliam, T. M. and I. L. Morgan, 1987.** *Shale: Measurement of Thermal Properties*, ORNL/TM-10499, Oak Ridge National Laboratory, Oak Ridge, TN.

**Gries, J. P. and J. E. Martin, 1985.** "Composite Outcrop Section of The Paleozoic and Mesozoic Strata in the Black Hills and Surrounding Areas," *Geology of the Black Hills, South Dakota and Wyoming: Field Trip Guidebook*, 2nd Edition, Geological Society of America, Rocky Mountain Section, 1981 Annual Meeting, American Geological Institute, Alexandria, VA.

**Hansen, F. D. and T. J. Vogt, 1987.** *Thermomechanical Properties of Selected Shales*, ORNL/Sub/85-97343/2, prepared by RE/SPEC Inc., Rapid City, SD, for Oak Ridge National Laboratory, Oak Ridge, TN.

**Hansen, F. D., E. L. Hardin, R. P. Rechard, G. A. Freeze, D. C. Sassani, and P. V. Brady, 2010.** *Shale Disposal of U.S. High-Level Radioactive Waste*, SAND2010-2843, Sandia National Laboratories, Albuquerque, NM.

**Hardin, E., J. Blink, H. Greenberg, M. Sutton, M. Fratoni, and J. Carter, 2011.** *Generic Repository Design Concepts and Thermal Analysis (FY11)*, SAND2011-6202, and Sandia National Laboratories, Albuquerque, NM.

**Heitzmann, P. and J. P. Tripet, 2003.** *Mont Terri Project–Geology, Paleohydrology, and Stress Field of the Mont Terri Region*, Bundesamt für Wasser und Geologie, Bern, Switzerland.

**Hoek, E., 2001.** "Big Tunnels in Bad Rock," *Journal of Geotechnical and Geoenvironmental Engineering*, Vol. 127, No. 9, pp. 726–740.

**Horseman, S. T., M. G. Winter, and D. C. Entwistle, 1987.** *Geotechnical Characterisation of Boom Clay in Relation to Disposal of Radioactive Waste*, Office for Official Publications of the European Communities, Luxemburg.

**Horseman, S. T., M. G. Winter, and D. C. Entwistle, 1993.** "Triaxial Experiments on Boom Clay," *The Engineering Geology of Weak Rock*, Blkema, Rotterdam.

**Itasca Consulting Group, Inc., 2009.** *FLAC$^{3D}$: Fast Lagrangian Analysis of Continua in 3 Dimensions, 4th Ed. (*FLAC$^{3D}$ *Version 4.0), Minneapolis, MN.*

**Jackson, J. A., 1997.** *Glossary of Geology*, 4th Edition, American Geological Institute, Alexandria, VA.

**Jiang, X. W., X. S. Wang, and L. Wan, 2010.** "Semiemperical Equations for the Systematic Decrease in Permeability With Depth in Porous and Fractured Media," *Hydrogeology Journal*, Vol. 18, No. 4, pp. 839–850.

**Kopp, O. C., 1986.** *A Preliminary Assessment of Mineralogical Criteria on the Utility of Argillaceous Rocks and Minerals of High-Level Radioactive Waste Disposal*, ORNL/TM-9979, Oak Ridge National Laboratory, Oak Ridge, TN.

**Krumbein, W., 1934.** "Size Frequency Distribution of Sediments," *Journal of Sedimentary Petrology*, Vol. 4, No. 2, pp. 65–77.

**Li, X. L., W. Bastiaens, P. Van Marcke, J. Verstricht, G. J. Chen, and E. Weetjens, 2010.** "Design and Development of Large-Scale In-Situ PRACLAY Heater Test and Horizontal High-Level Radioactive Waste Disposal Gallery Seal Test in Belgian HADES," *Journal of Rock Mechanics and Geotechnical Engineering*, Vol. 2, No. 2, pp. 103–110.

**Liu, H.-H., L. Li, L. Zheng, J. Houseworth, and J. Rutqvist, 2011.** *Investigations of Near-Field Thermal-Hydrological-Mechanical-Chemical Models for Radioactive Waste Disposal in Clay/Shale Rock*, Lawrence Berkeley National Laboratory, Earth Sciences Division, Berkely, CA.

**Martin, J. and D. Parris, 2007.** *The Geology and Paleontology of the Late Cretaceous Marine Deposits of the Dakotas*, Special Paper 427, Geological Scociety of America, Boulder, CO.

**Mazurek, M., A. Gautschi, P. Marschall, G. Vigeneron, P. Lebon, and J. Delay, 2008.** "Transferability of Geoscientific Information From Various Sources (Study Sites, Underground Rock Laboratories, Natural Analogues) to Support Safety Cases for Radioactive Waste Repositories in Argillaceous Formations," *Physics and Chemistry of Earth*, Vol. 33 Supplement 1, pp. S95–S105.

**Mitchell, J. K., 1976.** *Fundamentals of Soil Behavior,* John Wiley, New York, NY.

**Nataraj, M. S., 1991.** *Preliminary Geotechnical Evaluation of Deep Borehole Facilities for Nuclear Waste Disposal in Shales*, ORNL/TM-10960, Oak Ridge National Laboratory, Oak Ridge, TN.

**Neuzil, C. E., 1986.** "Groundwater Flow in Low-Permeability Environment," *Water Resources Research*, Vol. 22, No. 8, pp. 1163–1195.

**Neuzil, C. E., 1993.** "Low Fluid Pressure Within the Pierre Shale: a Transient Response to Erosion," *Water Resources Research*, Vol. 29, No. 7, pp. 2007–2020.

**Neuzil, C. E., 1994.** "How Permeable are Clays and Shales?," *Water Resources Research*, Vol. 30, No. 2, pp. 145–150.

**Nichols Jr., T. C. and D. S. Collins, 1986.** "In Situ and Laboratory Geotechnical Tests of the Pierre Shale Near Hayes, South Dakota—A Characterization of Engineering Behavior" *Canadian Geotechnical Journal*, Vol. 23, No. 2, pp. 181–194.

**Nopola, J. R., 2013.** *Preliminary Evaluation of The Pierre Shale As a Nuclear Waste Repository*, Masters Thesis, South Dakota School of Mines and Technology, Rapid City, SD.

**Nopola, J. R. and L. A. Roberts, 2013.** "Viscoplastic Behavior of Fine-Grained Geological Units and its Applicability to Compressed Gas Caverns," ARMA 13-561, *Proceedings, 46th U.S. Rock Mechanics/Geomechanics Symposium*, San Francisco, CA, June 23–26, CD-ROM.

**Norton, F. H., 1929.** *Creep of Steel at High Temperatures*, McGraw-Hill Book Company, New York, NY.

**Poppe, L., V. Paskevich, S. Williams, M. Hastings, J. Kelley, and D. Belknap, 2003.** *Surficial Sediment Data from the Gulf of Maine, Georges Bank, and Vicinity: A GIS Compilation*, U.S. Geological Survey Open-File Report 2003–001, U.S. Geological Survey, Coastal and Marine Geology Program, Woods Hole, MA.

**Potter, P., J. Maynard, and W. Pryor, 1980.** *Sedimentology of Shales*, Springer-Verlag, New York, NY.

**Puppala, A., T. Wejrungsikul, V. Puljan, and T. Manosuthikij, 2012.** "Measurements of Shrinkage Induced Pressure (SIP) in Unsaturated Expansive Clays," *Geotechnical Engineering Journal of the Southease Asian Geotechnical Society (SEAGS) and Association of Geotechnical Societeis in Southeast Asia (AGSSEA)*, Vol. 40, No. 1, pp. 140–147.

**Rocscience Inc., 2013.** *Phase$^2$ 8.0 Manual*, Rocscience Inc., Toronto, Ontario, Canada.

**Rutqvist, J. and C. F. Tsang, 2003.** "TOUGH-FLAC: A Numerical Simulator for Analysis of Coupled Thermal-Hydrological-Mechanical Processess in Fractured and Porous Geological Media Under Multi-Phase Flow Conditions," *Proceedings of the Transport of Unsaturated Groundwater and Heat (TOUGH) Symposium*, Lawrence Berkeley National Laboratory, Berkeley, CA, May 12–14.

**Sass, J. H. and S. P. Galanis, Jr., 1983.** *Temperatures, Thermal Conductivity, and Heat Flow From a Well in Pierre Shale Near Hayes, South Dakota*, USGS Open-File Report 83-25, U.S. Geological Survey, Reston, VA.

**Schlee, J., 1973.** *Atlantic Continental Shelf and Slope of the United States Sediment Texture of the Northeastern Part,* U.S. Geological Survey Professional Paper 529-L, U.S. Geological Survey, Reston, VA.

**Schultz, L. G., H. A. Tourtelot, J. R. Gill, and J. G. Boerngen, 1980.** *Composition and Properties of the Pierre Shale and Equivalent Rocks, Northern Great Plains Region*, USGS Professional Paper 1064-B, U.S. Geolgoical Survey, Reston, VA.

**Shepard, F., 1954.** "Nomenclature Based on Sand-Silt-Clay Ratios," *Journal Sedimentary Petrology*, Vol. 24, No. 3, pp. 151–158.

**Shurr, G. W., 1977.** *The Pierre Shale, Northern Great Plains; A Potential Isolation Medium for Radioactive Waste*, U.S. Geological Survey Open File Report 77-776, U.S. Geological Survey, Reston, VA.

**Stark, T. D., C. Choi, and S. McCone, 2005.** "Drained Shear Strength Parameters for Analysis of Landslides," *Journal of Geotechnical and Geoenvironmental Engineering*, Vol. 131, No. 5, pp. 575–588.

**Svalstad, D. K., 1983.** *User's Manual for SPECTROM-41: A Finite-Element Heat Transfer Program,* ONWI-326, prepared by RE/SPEC Inc., Rapid City, SD, for the Office of Nuclear Waste Isolation, Battelle Memorial Institute, Columbus, OH.

**Tsang, C., J. Barnichon, J. Birkholzer, X. Li, H. Liu, and X. Sillen, 2012.** "Coupled Thermo-Hydro-Mechanical Processes in the Near Field of a High-Level Radioactive Waste Repository in Clay Formations," *International Journal of Rock Mechanics and Mining Sciences*, Vol. 49, January 2012, pp. 31–44.

**U.S. Department of Agriculture, Natural Resources Conservation Service, 2012.** "National Soil Survey Handbook, Title 430-VI," retrieved November 29, 2012, from *http://soils.usda.gov/technical/handbook/*

**U.S. Nuclear Waste Technical Review Board, 2008.** *Thermal-Response Evaluation of Yucca Mountain During the Preclosure and Postclosure Phases*, prepared by the U.S. Nuclear Waste Technical Review Board, Washington, DC.

**Volckaert, G., F. Bernier, X. V. Sillen, J. C. Mayor, I. Gobel, and P. Blumling, 2004.** "Similarities and Differences in the Behaviour of Plastic and Indurated Clays," *Proceedings, The Sixth European Commission Conference on the Management and Disposal of Radioactive Waste: Euradwaste* '04, Luxembourg, March 29–31.

**Wenk, H. R., M. Voltolini, M. Mazurek, L. Van Loon, and A. Vinsot, 2008.** "Preferred Orientations and Anisotropy in Shales: Callovo-Oxfordian Shale (France) and Opalinus Clay (Switzerland)," *Clays and Clay Minerals*, Vol. 56, No. 3, pp. 285–306.

**Wentworth, C., 1922.** "A Scale of Grade and Class Terms for Clastic Sediments," *Journal of Geology*, Vol. 30, No. 5, pp. 377–392.

**Wu, B., C. P. Tan, and T. Aoki, 1997.** "Specially Designed Techniques for Conducting Consolidated Undrained Triaxial Tests on Low Permeability Shales," *International Journal of Rock Mechanics and Mining Sciences*, Vol. 34, No. 3, p. 458.

**Zhang, C. and T. Rothfuchs, 2004.** "Experimental Study of the Hydro-Mechanical Behaviour of the Callovo-Oxfordian Argillite," *Applied Clay Science*, Vol. 26, No. 1–4, pp. 325–336.

FCT Quality Assurance Program Document

# Appendix E
# FCT Document Cover Sheet

| | |
|---|---|
| Name/Title of Deliverable/Milestone | Preliminary planning for development of an underground research laboratory in shale (M3FT-13SN08070813) |
| Work Package Title and Number | UFD Natural Evaluation & Tool Development |
| Work Package WBS Number | FT-13SN080708 |
| Responsible Work Package Manager | Yifeng Wang |
| | (Name/Signature) |

Date Submitted 7/30/2013

| | | | | |
|---|---|---|---|---|
| Quality Rigor Level for Deliverable/Milestone | ☒ QRL-3 | ☐ QRL-2 | ☐ QRL-1<br>☐ Nuclear Data | ☐ N/A* |

This deliverable was prepared in accordance with Sandia National Laboratories

*(Participant/National Laboratory Name)*

QA program which meets the requirements of

☒ DOE Order 414.1 ☐ NQA-1-2000

**This Deliverable was subjected to:**

| | |
|---|---|
| ☐ Technical Review | ☐ Peer Review |
| **Technical Review (TR)** | **Peer Review (PR)** |
| **Review Documentation Provided** | **Review Documentation Provided** |
| ☐ Signed TR Report or, | ☐ Signed PR Report or, |
| ☐ Signed TR Concurrence Sheet or, | ☐ Signed PR Concurrence Sheet or, |
| ☒ Signature of TR Reviewer(s) below | ☐ Signature of PR Reviewer(s) below |

**Name and Signature of Reviewers**

Yifeng Wang [signature]

*Note: In some cases there may be a milestone where an item is being fabricated, maintenance is being performed on a facility, or a document is being issued through a formal document control process where it specifically calls out a formal review of the document. In these cases, documentation (e.g., inspection report, maintenance request, work planning package documentation or the documented review of the issued document through the document control process) of the completion of the activity along with the Document Cover Sheet is sufficient to demonstrate achieving the milestone. QRL for such milestones may be also be marked N/A in the work package provided the work package clearly specifies the requirement to use the Document Cover Sheet and provide supporting documentation.